ALLELE SPECIFIC ALTERATIONS IN GLYCOLIPID BIOSYNTHESIS AND CELL SIGNALING IN GM3 SYNTHASE DEFICIENCY

by

MICHELLE T DOOKWAH-SMITH

(Under the Direction of Michael Tiemeyer and Richard Steet)

ABSTRACT

GM3 Synthase Deficiency (GM3SD) is a rare neurological disorder typically characterized by seizures, severe intellectual disability, choreoathetosis, dysmorphic facial features, and altered skin pigmentation. GM3SD results from variants in the *ST3GAL5* gene that encodes GM3 synthase, a glycosphingolipid (GSL)-specific sialyltransferase. GM3 Synthase (ST3GAL5) adds sialic acid to lactosylceramide (LacCer) to synthesize GM3 ganglioside, which in turn, can be extended by other glycosyltransferases to generate the majority of complex gangliosides. Both ST3GAL5 and gangliosides are highly enriched in neural tissues. Patient fibroblasts from two individuals with different variants in *ST3GAL5* were reprogrammed to pluripotency; one patient line was derived from an African-American cohort (Salt & Pepper Syndrome, SP-ST3) and has a missense variant in the S-motif of the sialyltransferase domain, while the other was derived from an Amish cohort (A-ST3) and has a variant that truncates the polypeptide between the L- and S-motifs of the catalytic domain. The resulting induced pluripotent stem cells (iPSCs) were differentiated to neural crest cells (NCCs) to investigate the impact of loss of GM3 on neural-specific glycosylation and cell signaling during differentiation.

Consistent with our understanding of the variants and with previous research, GM3 and GM3-derived gangliosides are undetectable in iPSCs and NCCs derived from both cohorts. However, GSL profiles exhibited different compensatory responses in relation to how LacCer is utilized and in GSL ceramide composition. Since GSLs are known to be important for membrane organization and cell signaling, we investigated the cell surface proteome and expression levels of receptor tyrosine kinases across NCC differentiation. In SP-ST3 cells, we detected altered relative abundances of signaling receptors, adhesion molecules, and membrane trafficking proteins at the cell surface compared to WT. For both GM3SD variants, we discovered altered ErbB3 and EGFR abundance compared to the differentiation of WT cells. However, the magnitude and timing of altered EGFR and ErbB3 protein expression was different in the two alleles compared to WT. Thus, altered GSL biosynthesis impacts the cell surface proteome and signaling events that accompany differentiation and survival of neural precursors. Additionally, GM3SD cells provide a novel platform to investigate structure/function relationships that connect GSL diversity to cell signaling.

INDEX WORDS: Glycolipid, glycosphingolipid, ganglioside, GM3 synthase, ST3GAL5, glycolipid biosynthesis, gangliosides biosynthesis, GM3 Synthase Deficiency, GM3SD, Salt and Pepper Syndrome, rare disease, induced pluripotent stem cells, neural crest cells

ALLELE SPECIFIC ALTERATIONS IN GLYCOLIPID BIOSYNTHESIS AND CELL SIGNALING IN GM3 SYNTHASE DEFICIENCY

by

MICHELLE T DOOKWAH-SMITH

B.S., Yale University, 2013

A Dissertation Submitted to the Graduate Faculty of The University of Georgia in Partial Fulfillment of the Requirements for the Degree

DOCTOR OF PHILOSOPHY

ATHENS, GEORGIA

2021

ALLELE SPECIFIC ALTERATIONS IN GLYCOLIPID BIOSYNTHESIS AND CELL SIGNALING IN GM3 SYNTHASE DEFICIENCY

by

MICHELLE T DOOKWAH-SMITH

Major Professors:	Michael Tiemeyer
	Richard Steet
Committee:	James Lauderdale
	Stephen Dalton

Electronic Version Approved:

Ron Walcott
Vice Provost for Graduate Education and Dean of the Graduate School
The University of Georgia
May 2021

DEDICATION

Sean Anthony Dookwah

Oct 5, 1972 – April 25, 2016

“But in my heart is a memory, and there you’ll always be”

And

Dr. Dr. Hugh Denroy Dookwah

August 24, 1949 – July 23, 2020

I’m honored to be even half the doctor you ever were.

Thank you for all of your support and love.

I’ll always be your little pumpkin.

ACKNOWLEDGEMENTS

I have had so much support throughout this journey, and I am so grateful for each and every person who has helped me get to this point.

I would like to thank my committee Richard Steet, Stephen Dalton, James Lauderdale, and Michael Tiemeyer. I'd like to give a special thanks to Mike, I truly appreciated your guidance, support, patience, and compassion for all of these years. A quick thanks to some of the other scientific mentors I've had along the way: Stella Guerrero, MaryAnn Moran, Robert Gogal, Joanne Weidhaas, and Dave Salzman – your labs and training led the way here.

An abundance of gratitude to my mom, Joycelyn A. Dookwah. I can honestly never thank you enough for all of your love and sacrifice, and for raising me in the most supportive environment. You were never afraid to let me leave the nest, and it gave me the confidence to pursue my dreams. To my sister, Jeanette Amanda Dookwah, my biggest cheerleader. Thank you for your faith that I'd have the strength to accomplish this, and your unwavering support for when I felt that I couldn't. Thank you also for flying across the country in a pandemic to be with me on my defense day. So many things about this day weren't able to occur as I had envisioned for so many years, but I always pictured you right by my side to support me and celebrate with me. I'll always be grateful that you made sure that happened. To my aunt, Arlene Dookwah, I will never forget that you took me to my first day of college and made sure that I felt safe and supported. Thank you for being such an amazing female role model in my life and for your unending wisdom and support throughout my education.

Special thanks to my husband, Dr. Peter James Smith. I'm so glad that we've gone through this journey together. This past year, I've learned that finishing a Ph.D. is a lot like learning to ski. I appreciate that you always go down a new run for me first to let me know how challenging they are. You did the same with graduating a year before me, and you warned me that it could be difficult and steep at times. But you promised you'd be right by my side the whole way down, and that you were confident I could do this – no matter how slowly I went or how long it would take. Thank you, I love you.

I have to thank the amazing supportive friends and colleagues I've gained on this journey. A very special thanks to Dr. Stephanie Halmo, one of the elite few to have read and edit my dissertation in full. Thank you so much for all of your help and support, I honestly could not have done this without you. Special thanks also to all of my lab mates, past and present - especially Kate Rosenbalm for sharing the joy of stem cell culture with me, Kazuhiro Aoki and Mayumi Ishihara Aoki for the training and technical expertise, and Sarah Baas Robinson for her unending advice and guidance.

I consider myself so fortunate to have too many amazing friends to thank individually. From my college roommates who listened to me complain about lab work and would wait for me to get back from lab on the medical campus to go get dinner, to all of my Athens friends from before and during graduate school. One of the best decisions I ever made was coming back home for graduate school, and all of you made life outside of my Ph.D. truly amazing.

TABLE OF CONTENTS

Page

LIST OF TABLES

Page

LIST OF FIGURES

Page

CHAPTER 1

INTRODUCTION AND LITERATURE REVIEW

This dissertation informs our understanding of the cell-type-specific molecular phenotypes resulting from the loss of GM3 synthase function. It is well established that glycosylation is essential for life, and that glycolipids are indispensable for many cellular functions (Ajit Varki, 2016). Through the study of a rare disorder in ganglioside biosynthesis, nature gives us the unique opportunity to see how loss of a specific subset of glycosphingolipids affects development and molecular processes.

This chapter will give an overview of glycosphingolipid (GSL) biosynthesis, the role of GSLs in lipid rafts and cell signaling, the function of GSLs in the brain, current knowledge on GM3 Synthase Deficiency (GM3SD) in humans, animal models of GM3SD, using induced pluripotent stem cells (iPSCs) to model disease, and a brief introduction to the neural crest. This review sets the stage for Chapter 2, which will present findings from patient-derived iPSCs, and how glycolipid and cell signaling molecular changes occur during neural crest differentiation in two different allelic backgrounds for GM3SD. Finally, Chapter 3 will provide conclusive remarks that will summarize our major findings, discuss future directions using the knowledge gained from this project, and elaborate on how the information from this project can be applied to the study of other diseases in order to gain a better understanding of the role glycolipids play in cell signaling and neurodevelopment.

Glycosphingolipid Biosynthesis

In higher organisms, the majority of glycosylated lipids, or glycolipids, are glycosphingolipids (GSLs), which are defined as a glycolipid comprised of a glycan attached to the primary hydroxyl group of a ceramide group. The ceramide component consists of an amino alcohol in an amide linkage to a fatty acyl chain (A. Varki et al., 2015). The length, hydroxylation, and saturation of these components can vary in GSLs with the same glycan head group, which is believed to affect the functionality of these groups (D'Angelo, Capasso, Sticco, & Russo, 2013). Glycosphingolipids comprise over 80% of the glycoconjugates found in the vertebrate brain (Schnaar, 2016). While many studies have been conducted to understand the effects of altered GSL catabolism and the rare disorders that arise from defects in this process, there are fewer examples of studies that address the effects of improper GSL biosynthesis – as these disorders are even more rare (Bejaoui et al., 2001; Boccuto et al., 2013; Bowser et al., 2019; Anthony H. Futerman & van Meer, 2004; Gordon-Lipkin et al., 2018; Harlalka et al., 2013; Indellicato et al., 2019; Lee et al., 2016; Simpson et al., 2004).

Glycosphingolipid biosynthesis (**Figure 1.1**) occurs in a stepwise manner, with the ceramide receiving either a galactose or glucose residue, then subsequent sugars are added by glycosyltransferases from nucleotide sugars. The composition of various GSLs in a given tissue or cell type is determined by the expression and intracellular distribution of the biosynthetic enzymes that extend the glycan portion of the GSL. These enzymes can compete for the same precursor molecule for extension, but each branch (a-series vs. b-series, c-series) is a committed pathway. There are also neutral, or non-sialylated, pathways that LacCer can be utilized for – the globo- and neolacto-

series of GSLs. Lastly, LacCer could be used to make GA2, which is the first GSL in the o-series. Within this series, another sialyltransferase, ST3GAL2, can make GM1b, and subsequently GD1c – two gangliosides that can be produced without GM3 Synthase activity. This biosynthetic process means that expression and competition between two enzymes at a key branch point determines the relative abundance of the final GSL products (D'Angelo et al., 2013). For example, GM3 Synthase (ST3GAL5) and A4GALT are both competing for LacCer as a precursor to make gangliosides or globosides, respectively. The levels of the nucleotide sugar donors available for use by the glycosyltransferases in the Golgi lumen are what affects the ultimate structure of glycans. The donor nucleotide sugars are regulated by synthetic enzymes in the cytoplasm or nucleus and the nucleotide sugar transporters in the Golgi membrane (A. Varki et al., 2015).

GSLs containing one or more sialic acid residues are generally referred to as gangliosides, although this term should more appropriately be reserved for sialylated GSLs that posess the ganglio-series neutral backbone structure as well (Galβ3GalNAcβ4Galβ4Glcb-). The enzyme ST3GAL5, or GM3 Synthase, generates the simplest ganglioside, GM3 (sialyl-lactosylceramide), from lactosylceramide (**Figure 1.1**). GM3 can be used as a substrate for further extension and branching reactions that produce almost all of the major complex gangliosides in the a-, b-, and c-series (Yu, Tsai, Ariga, & Yanagisawa, 2011).

Mammalian glycolipid biosynthesis starts with the synthesis of the ceramide component at the membrane of the endoplasmic reticulum (ER). Ceramide, which can technically be considered a class of molecules due to the possible variation in structure,

is formed by the acylation of sphingosine with one of several possible acyl CoA molecules by the action of specific ceramide synthases (Gault, Obeid, & Hannun, 2010). These ceramide synthase enzymes are localized on the cytosolic leaflet of the ER membrane (Mandon, Ehses, Rother, van Echten, & Sandhoff, 1992; Michel et al., 1997).

Ceramide is the precursor molecule for sphingomyelin and GSLs. Sphingomyelin, a phospholipid composed of a phosphocholine headgroup attached to sphingosine and a fatty acid (ceramide), is produced in the luminal part of the Golgi membranes (A. H. Futerman, Stieger, Hubbard, & Pagano, 1990). Most GSLs are derived from lactosyceramide (LacCer). First, glucosylceramide (GlcCer) is formed when a glucose residue is β-glycosidically linked to the 1-position of the ceramide tail by glucosylceramide synthase (UGCG), which is located on the cytosolic leaflet of the Golgi apparatus. GlcCer can then be transported to the plasma membrane, or be further glycosylated in the Golgi apparatus (Sandhoff & Kolter, 2003). LacCer is generated by the addition of galactose to from UDP-Gal to GlcCer. This process is catalyzed by the β-1,4-galactosyltransferase, also called LacCer synthase, encoded by *B4GALT6*. LacCer formation and subsequent glycosylation to form other GSLs and gangliosides take place in the luminal leaflet of Golgi membranes, where they are then transported to the plasma membrane by exocytotic membrane flow (Daniotti & Iglesias-Bartolomé, 2011; Lannert, Gorgas, Meissner, Wieland, & Jeckel, 1998).

Glycosphingolipids Function in Lipid Rafts and Cell Signaling

Glycosphingolipids are highly enriched at the cell surface, and primarily reside on the outer leaflet of the cell surface (S. Hakomori, 1981). However, GSLs are not

uniformly distributed within the plasma membrane (D. A. Brown & London, 1998). Rather, they can be found within small, 10-200nm, micro-domains known as lipid rafts (Pike, 2009). The detection and comprehensive characterization of lipid rafts have proven to be a major challenge in the field since their first discovery, and this has even led to some controversies over their existence and biological relevance (Levental, Levental, & Heberle, 2020).

Sphingolipid enriched domains were originally identified by their insolubility to non-ionic detergents, which led to them being called detergent-resistant membrane domains or DRMs. However, it was questioned for years whether or not these DRMs actually existed in membranes or were simply a detergent-induced artifact (D. A. Brown & London, 1997). Model membranes were developed to try to prove their existence, and as advanced and more complex model membranes came about, better evidence arose for the existence of lipid rafts. These models include giant plasma membrane vesicles (GPMVs), or intact, isolated plasma membrane blebs that retain lipid diversity and protein content of living membranes (Sezgin et al., 2012). Lack of direct visualization of lipid raft domains still left many skeptics of their existence. Microscopy efforts using fluorophores attached to putative lipid raft-residing proteins or GSLs provided some indirect visual evidence of clustering and partitioning on the cell surface, but the technological advancement of super-resolution microscopy seems to be a major driving force for finally being able to more directly visualize lipid raft domains in living cells (Levental et al., 2020; Stone, Shelby, Núñez, Wisser, & Veatch, 2017; Stone & Veatch, 2015).

As mentioned, lipid rafts exist as a part of the plasma membrane, and laterally partition the membrane through the physicochemical properties of their components (Almeida, 2009). These rafts are believed to contain a high concentration of cholesterol (30-40%) and sphingolipids (10-30%) (Van Meer, Voelker, & Feigenson, 2008). Sphingolipids are a class of lipid composed of a sphingosine base attached to a fatty acid, with a variable polar head group. Types of sphingolipids include sphingomyelin, spingosine-1-phosphate, and glycosphingolipids. The propensity of the sphingolipids to partition together is due to their long, saturated carbon chains. Cholesterol is believed to promote phase separation of lipid rafts from the rest of the plasma membrane due to favorable packing interactions between the sterol and the saturated chains in the sphingolipids, including glycosphingolipids. Depletion of cholesterol can disrupt rafts and affect raft function (Deborah A. Brown & London, 2000).

These lipid raft microdomains also contain particular proteins, including glycosylphosphatidylinositol-anchored proteins (GPI-anchored proteins or GPI-APs) and signaling proteins like Receptor Tyrosine Kinases (D. A. Brown & Rose, 1992; Mineo, James, Smart, & Anderson, 1996; Sargiacomo, Sudol, Tang, & Lisanti, 1993; Schnitzer, McIntosh, Dvorak, Liu, & Oh, 1995). Gangliosides have been demonstrated to be modulators of cell growth, alter membrane affinity to growth factor binding, and change receptor phosphorylation (E. G. Bremer, Hakomori, Bowen-Pope, Raines, & Ross, 1984; Eric G Bremer, Schlessinger, & Hakomori, 1986; Keenan, Schmid, Franke, & Wiegandt, 1975; Laine & Hakomori, 1973; R. Li, Liu, & Ladisch, 2001; Liu, Li, & Ladisch, 2004). GSLs were shown to be facilitating these functions within microdomains at the cell surface, often within lipid rafts (S.-i. Hakomori, Handa, Iwabuchi, Yamamura, &

Prinetti, 1998; S.-I. HAKOMORI, YAMAMURA, & HANDA, 1998; Simons & Ikonen, 1997). The GSLs in lipid rafts modulate cell signaling indirectly through the clustering of these domains that enables signaling molecules, like RTKs and GPI-APs, to come into contact range with each other (Simons & Ikonen, 1997).

Beyond the indirect method of modulating cell signaling through spatial orientation within the plasma membrane, gangliosides have also been found to directly modulate signaling through carbohydrate-protein or carbohydrate-carbohydrate interactions(E. G. Bremer et al., 1984; Eric G Bremer et al., 1986; Kawashima, Yoon, Itoh, & Nakayama, 2009; Miljan et al., 2002). Extensive research by E.G. Bremer, S. Hakomori and others have shown that gangliosides, such as GM3 and GM1, modulate RTK signaling, notably that addition of exogenous GM3 or GM1 diminishes EGFR and platelet-derived growth factor (PDGF) autophosphorylation (E. G. Bremer et al., 1984; Eric G Bremer et al., 1986; Laine & Hakomori, 1973). Alternatively, work from the Ladisch group found that ganglioside GD1a enhances EGFR autophosphorylation (R. Li et al., 2001; Liu et al., 2004). It has since been determined that many of the RTK responses to ganglioside exposure are the result of direct interactions through carbohydrate-carbohydrate interactions. For example, GM3 has been shown to inhibit EGFR autophosphorylation through an interaction of GM3 with GlcNAc-terminated N-glycan on EGFR and this inhibition is abolished when the sialic acid on GM3 is removed or EGFR glycosylation is disrupted(Coskun, Grzybek, Drechsel, & Simons, 2011; Kawashima et al., 2009; X.-Q. Wang, Sun, O'Gorman, Tai, & Paller, 2001).

The example with GM3 inhibition of EGFR through a carbohydrate binding motif on the RTK is an example of a *cis* mechanism of interaction, where gangliosides

interact laterally with proteins on the same cell surface. Another mechanism of direct interaction is a *trans* interaction, where gangliosides bind on one cell surface to complementary carbohydrate binding proteins on an opposing cell – facilitating intracellular communication (Hakomori Si, 2002; Regina Todeschini & Hakomori, 2008). Therefore, alterations in ganglioside biosynthesis may have a great impact on proper cell signaling.

Ganglioside Function in the Brain

Glycosphingolipids, and especially gangliosides, are highly expressed in neural tissue. In fact, they constitute 10-12% of the lipid content of the brain (Kracun et al., 1992). Furthermore, GSL represent ~80% of total glycan mass in the brain, and gangliosides account for ~75% of sialic acid content in the brain (Schnaar, Gerardy-Schahn, & Hildebrandt, 2014). It is well established that gangliosides play a critical role in neuronal development and brain function (Palmano, Rowan, Guillermo, Guan, & McJarrow, 2015). Four complex ganglioside structures - GM1, GD1a, GD1b, and GT1b - comprise greater than 90% of gangliosides in the brain in all mammals (Tettamanti, Bonali, Marchesini, & Zambotti, 1973). The shift in GSL expression from neutral GSLs, such as globo- and lacto-series structure, to complex gangliosides has been shown to be a key driver in neural differentiation (Russo et al., 2018). Gangliosides primarily function on neural cell surfaces in a similar fashion to how they function on any cells surface – through direct (*cis* and *trans)* and indirect interactions with other cell surface molecules.

There are numerous examples of vital cell signaling events involving gangliosides that occur within the nervous system. One such example of a critical *trans*

interaction involved in the binding of myelin-associated glycoprotein (MAG), also known as siglec-4, with the gangliosides GD1a and GT1b – the most abundant gangliosides in axonal membranes and both GM3-derived (DeVries & Zmachinski, 1980). However, the o-series gangliosides GM1b and GD1α have been shown to be able to bind MAG with high affinity and is believed to compensate for loss of a- and b-series gangliosides in *st3gal5*-null mouse models (Collins et al., 1999).

Additionally, gangliosides have been shown to bind with low affinity to many neurotransmitter receptors. An example being GTb1 and GM1 binding to GluR2-containing AMPA receptors, a major excitatory neurotransmitter receptor in the brain. Decrease of sialoglycans on hippocampal neurons with sialidase treatment, which removed sialic acid, resulted in altered distribution on the GluR2-containing AMPA receptors on the cell surface (Prendergast et al., 2014).

Secondary accumulation of the gangliosides GM2 and GM3 is a common phenotype that occurs in several lysosomal storage disorders – a group of rare, inherited metabolic diseases caused by lysosomal dysfunction. The accumulation of gangliosides is associated with neuropathology in Niemann-Pick diseases (Types A and C) and mucopolysaccharidoses, among others (Brunngraber, Berra, & Zambotti, 1973; Constantopoulos & Dekaban, 1978; Cumings, 1962; Elleder, 1989; Vanier, 1999; Walkley & Vanier, 2009). GM2 and GM3 are typically minor components in developed neural tissues, with GM1, GD1a, GD1b, and GT1b constituting 90% of the gangliosides in the brain (Russo et al., 2018; Tettamanti et al., 1973).

Lastly, gangliosides play a role in neurodegenerative disorders in the brain. Amyloid beta (Aβ) isolated from Alzheimer brain extract was discovered to be

associated with the ganglioside GM1, and recent work suggests that GM1- Aβ may be prerequisite for Aβ toxicity (Kakio, Nishimoto, Yanagisawa, Kozutsumi, & Matsuzaki, 2002; Matsuzaki, Kato, & Yanagisawa, 2010; Yanagisawa, Odaka, Suzuki, & Ihara, 1995). GM1 is also a molecule of interest for Parkinson's research. GM1 was found to bind to α-synuclein and inhibit fibril formation in vitro, and that *B4galnt1*-null mice, which lack the majority of complex gangliosides aside from GM3, acquire characteristic symptoms of Parkinson's including motor impairment, depletion of striatal dopamine, and aggregation of α-synuclein (Martinez, Zhu, Han, & Fink, 2007; Wu, Lu, Kulkarni, & Ledeen, 2012).

With GSLs, and more specifically gangliosides playing such an important role in neurodevelopment and brain function, it's not surprising that mutations in a biosynthetic enzyme for gangliosides would result in severe neurological phenotypes. Such is the case for GM3 Synthase Deficiency (GM3SD).

Recessive GM3 Synthase Deficiency

GM3SD is a rare disorder of glycosphingolipid biosynthesis, caused by a mutation in a key enzyme that lies very early in the GSL biosynthetic pathway. This enzyme is required to make the majority of a subset of GSLs, which are important for proper neural development and brain function. GM3SD is caused by variants in *ST3GAL5,* which encodes the protein GM3 Synthase (ST3 beta-galactoside alpha-2,3-sialyltransferase 5; ST3GAL5; also previously referred to as SIAT9). There have been three allelic combinations identified in several cohorts around the world. These cohorts and their disease-causing variants are outlined in **Table 1.1**, and depicted in **Figure 1.2**, but a detailed description of the patient cohorts can be found below, titled using the

colloquial name for the disease as described in the literature when available, or the country of origin for the patients.

Two of the original “hallmark” phenotypes that were identified in the first cohorts of GM3SD patients were seizure activity and skin pigment changes, which lend their names to the first two cohorts of patients – Amish Infantile Epilepsy Syndrome and Salt and Pepper Syndrome. However, several other severe cognitive, psychomotor, and general growth phenotypes were also present, and they seem to be fairly consistent across cohorts of patients. These symptoms include severe intellectual disability (ID), choreoathetosis, failure to thrive, hearing impairments, and microcephaly. Gastrointestinal issues appear in several cohorts, along with sleep disturbances, and patients are often non-verbal and non-ambulatory. The skin phenotype originally identified in Salt and Pepper Syndrome patients is seen in about 70% of identified cases (**Table 1.1**).

Amish Infantile Epilepsy Syndrome

The most widely prevalent GM3SD-causing variant is the c.862C > T, p.Arg288X mutation, The p.Arg288X variant lies between the L-sialylmotif and the S-sialylmotif, which are two conserved protein motifs in the luminal catalytic domain of GM3 synthase (ST3Gal5) (Boccuto et al., 2013). This variant results in the truncation of the protein after the L-sialylmotif, or L-motif. The L-motif, which is larger, has been shown to be necessary for binding of the donor sugar nucleotide (CMP-NeuAc). The S-motif, however, has been shown to participate in binding of the donor nucleotide sugar and the acceptor – for GM3 Synthase, this would be lactosylceramide (Audry et al., 2011; Datta & Paulson, 1995; Datta, Sinha, & Paulson, 1998).

The amish variant was first identified by Simpson et al. (2004) in eight children from two families (**Figure 1.3**) that shared a fifth-generation common ancestor within the Amish population of the Northeastern United States (Simpson et al., 2004). Due to the founder effect within these closed communities, it is believed that the carrier frequency within this population is about 5-6%, which translates to approximately one per 1,200 births. However, the carrier frequency does vary by region, with higher concentrations within certain groups in Ohio, Pennsylvania, and Indiana (Bowser et al., 2019). The resulting disorder, known as Amish Infantile Epilepsy Syndrome, is among several other rare genetic diseases that are prevalent within these communities. This collection of rare genetic diseases is being studied and treated by community clinics that specialize in working with members of Amish and Mennonite communities.

H. Wang, Bright, Xin, Bockoven, and Paller (2013) presents data from 42 patients, including the eight from the aforementioned Simpson et al. (2004), from Amish settlements in Indiana, Kentucky, Michigan, Ohio, and Pennsylvania that were all diagnosed with genetically confirmed GM3SD. Four of the 42 patients were deceased, but of the remaining 38 patients, the Wang group describe hyperpigmented macules that looked like large freckles in 20 of the patients. The macules ranged in size from 2-5mm, and they were typically found on both hands and feet, with occasional sites on hips, face, chest wall, and back. Interestingly, the frequency of their appearance was found to correlate with increasing age – they were found in 86% of the patients six years or older and 93% of the patients 11 years or older. However, they were not found on children three years or younger. Seven of the 20 patients with hyperpigmentation, were also described to have patches of depigmentation as well. These patches were also 2-

5mm in size, and typically appeared after the onset of the hyperpigmented macules. Two siblings developed the depigmented patches perineally, and later on their face, extremities, neck and back, but the other five patients had the lesions only on their extremities. It was reported that in at least three cases, the hyperpigmented freckles almost disappeared, after being present for years. Additionally two of the seven cases with depigmentation also reported that those patches became significantly more or less visible over time (H. Wang et al., 2013).

A consortium of specialized clinics from Pennsylvania, Ohio, Wisconsin, Indiana and Kentucky has been formed, and Bowser et al. (2019) presented data from consortium patients discussing the natural history and biochemical features associated with the c.862C > T, p.Arg288X variant in the Amish population. From this study, they determined that the majority of these GM3SD babies were born with normal weight, length, and head circumference, but exhibited poor somatic growth within a few months of life. Common symptoms during infancy included developmental delay, slow weight gain, visual detachment, changes in muscle tone, gastrointestinal issues, involuntary movements, agitation, and irritability. Skin dyspigmentation was reported in some older patients. The patients also exhibited auditory issues and eyesight problems. Neurological defects presented after birth, and signs of dysmylenation and atrophy developed with advancing age. Lastly, the patients also exhibited varying types of seizures.

Bowser et al. (2019) presents a thorough assessment of patient biochemical analysis associated with GM3SD patient plasma with the c.862C > T, p.Arg288X variant. They found that GM3, GD3, and their downstream derivatives were

undetectable by mass spectrometry analysis. They found that the precursor to GM3, Lactosylceramide (LacCer) was elevated 2-fold in the patient samples, and they detected excess o-series gangliosides and globosides, a subset of neutral GSLs, relative to wildtype controls. They also looked at *ST3GAL5* c.862C > T heterozygotes and found that they had normal levels of GM3 and GD3, but the precursors LacCer and glycosylceramide (GlcCer) were elevated (Bowser et al., 2019).

Salt and Pepper Syndrome

Salt and Pepper Syndrome (S&PS or SP-ST3) was first reported in three siblings in South Carolina, two brothers and one sister (**Figure 1.4**). The patients were described to have delayed psychomotor development in infancy. Pigmentary changes, hyper- and hypo-pigmentation of the skin, developed by two years of age. These were described as 'salt and pepper' macules that ranged from 1-5mm in diameter and lend to the disorder's naming. Other symptoms included severe intellectual disability, dysmorphic cranio-facial features, including mid-face hypoplasia, microcephaly, hypotonicity, scoliosis, seizures, and abnormal EKG. According to the family pedigree, the affected sister had a female child reported to have severe intellectual disability and cerebral palsy, but no skin pigment changes (Boccuto et al., 2013; Saul, Wilkes, & Stevenson, 1983).

Whole-exome sequencing was performed on one of the male patients (III-5 in Boccuto et al. 2013), and this led to the identification of a homozygous variant, c.1063G>A, in exon 7 of the *ST3GAL5* gene, which translates to a missense alteration (p.E355K). Sanger sequencing of exon 7 of *ST3GAL5* in the patient (III-5) and their affected sister (III-4) confirmed the homozygous mutation in both patients. The p.E355K

mutation lies within the S-sialylmotif, or S-motif, which has been shown to participate in binding of the donor and the acceptor (Audry et al., 2011; Datta & Paulson, 1995; Datta et al., 1998). The alteration was modeled onto porcine ST3GAL1 (Rao et al., 2009), and predicted to cause instability, and even partially unfolding, of the resulting enzyme (Boccuto et al., 2013).

Analysis of glycosphingolipids isolated from fibroblasts harvested from patient III-5 by thin-layer chromatography and mass spectrometry showed no GM3 or GM3-derivatives in the GM3-deficient patient (Boccuto et al., 2013). Additionally, the ceremide profiles for the globosides Gb3 and Gb4 were shifted towards longer forms in the Salt and Pepper patient relative to wildtype. The patient fibroblasts did have a small amount of GM1b, which is synthesized by ST3GAL2. Lastly, the patient profiles showed no increase in the level of the GM3-precursor molecule lactosylceramide (LacCer) levels relative to wildtype. Glycoprotein analysis of the Salt and Pepper fibroblasts by mass spectrometry analysis found that O-linked glycans shifted towards more highly sialylated forms, with a reduction in precursor structures, relative to wildtype. The patient profiles also showed an increase in abundance of complex, sialylated N-linked structures, and a decrease of the high-mannose precursors (Boccuto et al., 2013), indicating secondary effects on other glycan structures.

French GM3SD Cohort

Fragaki et al. (2013) describes two siblings of French descent with GM3 Synthase Deficiency (**Figure 1.5**). The children were born to consanguineous parents, and they presented with early-onset epilepsy, with seizures beginning by two months and nine months of age. Other symptoms include psychomotor delay, failure to thrive,

blindness, and deafness. Skin pigment issues were not described. Exome sequencing revealed the same homozygous nonsense variant, c.862C > T, p.Arg288X, that results in GM3SD within the Amish community (Fragaki et al., 2013). Glycolipid analysis of patient fibroblasts by mass spectrometry analysis showed an increase of the globoseries glycosphingolipids Gb3 and Gb4, which was also upregulated in the Salt and Pepper fibroblasts (Boccuto et al., 2013; Fragaki et al., 2013).

Another phenotype that was identified in this patient cohort, but was not investigated in other cohorts, is a decrease in mitochondrial membrane potential. The researchers used flow cytometry experiments with DiOC6(3) fluorescent dye to show that patient fibroblasts had a significant decrease of mitochondrial membrane potential compared with their control cells. Additionally, the French cohort patient fibroblasts exhibited an increase in apoptosis, a phenotype that is seen in the zebrafish disease model of GM3SD (discussed below in *GM3SD Disease Modeling* section), by AnnexinV. They also saw increased sensitivity to an apoptosis inducer, rotenone, which is a strong inhibitor of complex I of the mitochondrial respiratory chain (Fragaki et al., 2013). Our studies, discussed in Chapter 2 of this work, also found that GM3SD cells exhibit increased sensitivity to an apoptosis inducer.

Pakistani GM3SD Cohort

Gordon-Lipkin et al. (2018) describes three siblings of Pakistani descent with GM3SD (**Figure 1.6**) caused by the c.862C > T, p.Arg288X nonsense variant, which was identified by whole exome sequencing. The children were born to non-consanguineous parents. However, the parents noted they may be distantly related and that their family history includes a distant cousin who was reported to have growth

failure and intellectual disability resulting from an undiagnosed “enzyme deficiency”. All three siblings presented with developmental delays by nine months of age, with one sibling as early as three months. Their other symptoms include failure to thrive, profound developmental delays and intellectual disability, cerebral palsy, severe gastrointestinal problems, atopic dermatitis, and abnormal EEGs; however, their EEGs did not show seizure activity. The siblings did exhibit some phenotypic differences from each other. The older brother and sister had skin pigment phenotypes, ichthyosis vulgaris, and require feeding tubes, while the younger brother has normal skin pigmentation and is able to self-feed. The two males both have hearing and vision impairments. The sister and younger brother both display severe self-injurious behaviors (SIB), including breath-holding spells, sleep disturbances and head-banging episodes. It’s interesting to note that none the siblings have facial dysmorphic features.

The authors note that an alternative diagnosis of Sjogren-Larsson syndrome was considered given their symptoms of ichthyosis, cerebral palsy, and intellectual disability, but that their fatty acid dehydrogenase enzyme activity was normal for the older brother’s fibroblasts.

The study concludes that in patients exhibiting cerebral palsy and severe intellectual disability, an analysis of their GSL profile or genetic analysis may point to GM3SD, even without the symptoms of epilepsy and skin pigment phenotypes. They also add that their patients provide additional symptoms to be aware of as possibly more GM3SD cases are discovered – severe atopic dermatitis/ichthyosis and self-injurious behaviors (SIB) (Gordon-Lipkin et al., 2018).

Korean GM3SD Cohort

Lee et al. (2016) describes two, Korean sisters who displayed symptoms originally described as Rett-like phenotypes (**Figure 1.7**). Rett syndrome is a rare genetic neurological disorder that typically affects female children. It is caused by variants in MECP2 (methyl CpG binding protein 2), which binds CpG dinucleotides in the mammalian genome and acts as a transcriptional repressor (Amir et al., 1999). Rett-like phenotypes are often found in patients with encephalopathies, and other symptoms can include infantile-onset seizures, loss of hand skills and impaired ability to walk, gait abnormalities, loss of spoken language, abnormal muscle tone, impaired sleep pattern, abnormal muscle tone, and growth retardation (Allou et al., 2017).

The two sisters, born of non-consanguineous parents, did exhibit many of these symptoms over time, with the younger sister presenting psychomotor regression at 4 months of age – the older sister didn't have developmental delay until 2 years and 5 months. Both are nonverbal and experience severe irritability and impaired sleep. Neither have seizure activity or major vision problems (the younger had surgically corrected strabismus). Additionally, the researchers reported that neither sister presented with poor feeding or other gastrointestinal issues nor deafness – symptoms that were rather consistent across other cohorts of GM3SD patients (Boccuto et al., 2013; Bowser et al., 2019; Saul et al., 1983; Simpson et al., 2004; H. Wang et al., 2013). However, the older sister does show hyper-pigmentation on both hands and feet and failure to thrive.

Exome sequencing of the younger sister and her unaffected parents showed novel, compound heterozygous missense variants in *ST3GAL5*. These variants were identified as c.584G>C, p.Cys195Ser, and c.601G>A, p.Gly201Arg., and were validated

by Sanger sequencing in the older sister. Unaffected parents were confirmed to be heterozygous carriers of each variant. Both mutations lie in the conserved L-sialylmotif of the GM3 Synthase enzyme, which has been shown to be necessary for binding of the donor nucleotide sugar (CMP-NeuAc) (Datta & Paulson, 1995). This is the first report of a GM3SD variant in this part of the enzyme (**Figure 1.2**), as the other variants lie either in the S-motif or between the L- and S-motif and result in a truncated protein.

Ganglioside analysis by Multiple Reaction Monitoring mass spectrometry found that plasma GM3 and GD3 were barely detectible – 0.35, 0.66ug/ml and 0.20, 0.22ug/ml respectively - compared to healthy controls (10.2+/-4.2ug/ml and 5.9+/-1.8ug/ml respectively). They did not measure enzyme activity *in vitro*. The researchers conclude that their work highlights the need to consider *ST3GAL5* in the cause of atypical Rett syndrome or Rett-like phenotype. They propose that the patient's attenuated and atypical phenotypes might be due to the location and/or type of the variants in these cases, and that this work expands the phenotypic and genetic spectrum of GM3SD (Datta & Paulson, 1995).

Italian Cohort

Indellicato et al. (2019) identified a novel homozygous variant that results in GM3SD in a single female patient of Italian heritage (**Figure 1.8**). The patient is the only child of healthy parents, who are both from a village of approximately 5000 inhabitants. The paper did not discuss if the parents were related or distantly related. Between 4 and 12 months of age, severe bilateral hearing loss was reported. Soon after, she developed failure to thrive and severe psychomotor delay. She also had strabismus and could not follow objects with her eyes. She experienced gastroesophageal reflux and

recurrent vomiting. By 18 months, she had an abnormal EEG and sleep disturbances, but no clinical seizures. However, she soon developed epilepsy after 18 months. She was diagnosed with sickle-cell anemia at age 3. By age 8, she exhibited nonvoluntary movements. The patient was described as having dysmorphic facial features that became progressively more evident over time. She developed freckle-like hyper-pigmentation on her feet beginning around age 9. At 10 years old, exome sequencing was performed and determined that the patient has a homozygous variant in *ST3GAL5,* c.1024G>A, that results in a missense change (p.Gly342Ser) in GM3 Synthase.

This novel GM3SD disease-causing variant lies in the S-motif, similarly to the Salt and Pepper cohort in South Carolina, USA. The authors measured GM3 Synthase activity using HEK-293T cells transiently transfected with mutant cDNA for ST3GAL5. They utilized LacCer as the acceptor substrate. They performed this analysis for all 5 of the known ST3GAL5 variants including the p.Gly342Ser (Italian cohort), p.Arg288X (Amish, French, Pakistani cohorts), p.E355K (Salt and Pepper/South Carolina cohort), p.Cys195Ser (Korean cohort – heterozygous variant), and p.Gly201Arg (Korean cohort – other heterozygous variant). They showed that none of the variants resulted in GM3 Synthase activity, and this result was also reported for the two heterozygous mutations expressed independently. They did not perform glycolipid analysis on patient cells or plasma, so the repertoire of GSLs and gangliosides is unknown for this particular variant (Indellicato et al., 2019).

GM3SD Disease Modeling

Across the literature GM3SD is described as a rare, autosomal recessive neurological or neurocutaneous disorder. Therefore, it would be beneficial to be able to

investigate the disease in neural tissues – such as the brain or peripheral nervous system (sensory and enteric neurons especially). As it is challenging to obtain human neural tissue to study, even in more common disorders, much less in a disease that has currently been identified in <100 patients worldwide, researchers must turn to disease models to further elucidate the effect of loss of complex gangliosides.

GM3SD has been studied in animal models – namely the mouse and zebrafish. While both animal models have contributed to studies of the possible physiological changes that occur due to loss of GM3 Synthase function, the mouse model does not phenocopy many aspects of the human disease pathology and there is currently only one zebrafish study where researchers looked at transient knock-down of *st3gal5* (Boccuto et al., 2013).

The *St3gal5*-null mouse

An *St3gal5*-null mouse was engineered by Yamashita et al. (2003) to investigate the loss of GM3 Synthase (Yamashita et al., 2003). Overall, the mice were viable and did not appear to show major abnormalities. Biochemical analysis of the brain gangliosides in *St3gal5*-null mice shows a loss of GM3 and all GM3-derived gangliosides. The major brain gangliosides present in wild-type mice are GM1a, GD1a, GD1b, and GT1b, which all require GM3 Synthase activity. The knockout mice instead exhibited GM1b and GD1α gangliosides, which belong to the o-series of gangliosides and do not require GM3 Synthase activity (**Figure 1.1**). It appears that these gangliosides are able to compensate for the majority of ganglioside function in mouse brains when GM3 synthase activity is lost. However, the researchers did discover an interesting phenotype in these mice when they decided to investigate the role of GM3 in

insulin cell signaling. Their study found that mice without GM3 Synthase activity exhibit enhanced phosphorylation of insulin receptor after ligand binding, and that the mutant mice were protected from high-fat diet-induced insulin resistance. They concluded that GM3 ganglioside plays an important role in regulating insulin sensitivity (Yamashita et al., 2003).

Another group, (Yoshikawa et al., 2009), engineered a different *St3gal5*-null mouse in order to investigate ganglioside function in hearing. They determined that in normal mice, GM3 is highly expressed in the inner ear, compared to the brain; however, the knockout mice lacked GM3 in the inner ear. The researchers studied the general behavior of the mice by testing their motor function, learning and memory, and sensory function. However, it was discovered that they did not exhibit a startle response to acoustic stimulants even though they responded normally to a physical stimulus of air puffs administered to their backs. They determined that the mice were hearing impaired due to the degeneration of the organ of Corti in the inner ear (Yoshikawa et al., 2009). They later published work using the same model to establish that normal spatial and temporal expression of the ganglioside GM3 is essential to the structural integrity and function of auditory hair cells (Yoshikawa et al., 2015). Their work provides evidence that the loss of GM3 synthase function in mice results in hearing loss and suggests a possible basis for the deaf phenotype seen in many GM3SD human patients.

Using the same *St3gal5*-null mouse model as the hearing studies, Hiraoka et al. (2019) investigated visual function in mice lacking GM3 Synthase activity. Glycosphingolipid analysis of the mice retinas was performed using high performance thin-layer chromatography and the researchers found that the knockout mice retinas did

not express any GM3 but had high levels of o-series gangliosides (GM1b and GD1α) as well as a high content of LacCer. The researchers looked at the morphology of the optic nerves and retinas by hematoxylin-eosin staining and immunohistochemical staining with GFAP antibody but found no significant differences between wild-type and mutant mice. They also conducted electrophysiological analysis but found no major changes. They concluded that the loss of GM3 has no influence on the retina or optic nerve function in mice (Hiraoka et al., 2019). These findings are in contrast to what is seen with human GM3SD patients, where blindness is reported as a phenotype in several patients (Bowser et al., 2019; Fragaki et al., 2013; Gordon-Lipkin et al., 2018).

In an attempt to investigate the seizure phenotype exhibited by many GM3SD human patients, Tang, Wang, Itokazu, and Yu (2020), used the same mouse model from the aforementioned hearing and vision studies and subjected them to chemoconvulsants to induce seizure activity. They showed that the GM3-deficient mice were more sensitive to the chemoconvulsant injections than wild-type and concluded that they had a decreased threshold to seizures. They also reported in their studies that the mice exhibited significantly lower body weight after postnatal day 28 comparted to wild-type littermates, and that the mutant mice displayed hyperactivity compared to the wild-type littermates. These data do lend support to the seizure activity and growth deficiencies seen in GM3-deficient human patients.

Lastly, it's important to point out a mouse model of another congenital disorder of ganglioside biosynthesis called GM2/GD2 Synthase Deficiency. It is caused by variants in B4GALNT1, which adds a N-acetylgalactosamine, or GalNAc, onto GM3/GD3 in a β-1,4 linkage to generate GM2/GD2. The human form of this disorder will be discussed

further in Chapter 3 of this work. Defects in the nervous system of this mouse model were noted, but the abnormal phenotypes were milder than expected (Takamiya et al., 1996). The phenotypes were later shown to be very similar to patients with a form of Hereditary spastic paraplegia, caused by GM2/GD2 synthase deficiency – namely age-dependent neurodegeneration, disordered gait, tremors, and ataxia (Bhuiyan et al., 2019).

Double knockout mouse models were generated to try to counter the ganglioside compensation mechanisms believed to be make the mouse less susceptible to the severe phenotypes seen in human ganglioside-deficient patients (T. A. Li & Schnaar, 2018). A *B4galnt1* and *St8sia1* double knockout mouse lacks all major brain gangliosides aside from GM3. This is because ST8Sia1 is responsible for generating GD3, which is subsequently needed for GT3 formation as well (**Figure 1.1**). The resulting mouse builds up excess levels of GM3, as it can't be further processed, and experienced >80% mortality in the first 6 months, primarily as a result of audiogenic seizures (Kawai et al., 2001). They also demonstrate reduced motor and sensory functions, as well as degeneration of peripheral nerves (Inoue et al., 2002; Tajima et al., 2009). The *B4galnt1* and *St3gal5* double knockout mouse, which has its entire ganglio-series pathway abolished, did exhibit greatly reduced total brain gangliosides and significant neurodegenerative disease. The mice did have small levels of sialylated GSLs in the brain on a neolactoseries GSL core, showing an attempt at compensation still (Yamashita et al., 2005). However, the combinations of knockout mutations appear to lead to a better phenocopy of the human disease in mice and could still prove to be a

valuable tool for studying ganglioside deficiencies, especially when investigating possible therapeutics.

ST3GAL5 Knock-down in Zebrafish

Boccuto et al. (2013) used translation-blocking antisense morpholinos (MO) that targeted *st3gal5* mRNA in order to study whether or not reduced *st3gal5* expression impacts embryonic development. They injected the MOs into one-cell stage zebrafish embryos and analyzed the gross morphology of wild-type and morphant embryos at 3 days post-fertilization (dpf). At this timepoint, there didn't appear to be any notable phenotypes aside from slight developmental delay, which the researchers attributed to a typical response to the morpholino injection itself. Acridine orange staining was performed in WT and morphant embryos to assess cell death within the brain. Increased acridine orange staining was seen in the mid to hindbrain region of the morphant fish, and TUNEL staining confirmed that the cell death was the result of apoptosis. This experiment also revealed increased cell death among neural crest cells in the *st3gal5* knock down zebrafish embryos. These findings were validated by overexpressing *st3gal5* mRNA in the morphant zebrafish to show that these phenotypes were not the result of off-target MO effects (Boccuto et al., 2013).

Induced-Pluripotent Stem Cells

Much of the research investigating GM3SD in human samples has been done using patient fibroblasts or patient plasma, which has provided valuable knowledge on GSL biosynthesis in the absence of a functioning GM3 Synthase enzyme. However, there appears to be some cell-type specificity associated with some of the GSL and ganglioside changes identified. Therefore, the ability to analyze the glycolipid profile in

specific disease-relevant cells types would prove invaluable. To achieve this, we turned to induced-pluripotent stem cells since they have the ability to differentiate to other cell types in the body, including neural lineages.

When studying neurological diseases, patient brain tissue would seem like the gold-standard to utilize. However, there are many challenges to using patient brain samples and several caveats to why it may not be the ideal tool to study all neurological diseases. One of the most obvious challenges is access to samples, which is especially a challenge with rare diseases. Another caveat is that postmortem brain tissue is often representative of end-of-stage for the disease - this can be especially problematic for neurodevelopmental disorders. Furthermore, there's also the fact that for many neurological diseases, phenotypic cell-type specificity is a concern, and access to sufficient quantities of specific cell types from patient tissue samples poses an even greater challenge.

The use of patient-derived induced-pluripotent stem cells (iPSCs) helps to address at least some of the aforementioned challenges associated with patient brain tissue use. iPSCs were first successfully generated through reprogramming adult somatic cells with four key transcription factors – Oct4, Sox2, Klf4, and c-Myc – in 2006 by Yamanaka and colleagues (Takahashi & Yamanaka, 2006). The resulting iPSCs can then be differentiated to all three germ layers or even whole organisms and have the ability to self-renew (Takahashi & Yamanaka, 2006). The therapeutic potential of iPSCs is vast, but they are also a valuable as a tool for disease modeling. Because iPSCs are derived from the somatic tissues of patients, they allow for the investigation of cellular and molecular disease mechanisms within the patient's genetic background. The ability

for iPSCs to be differentiated into cell types from all three germ layers allow them to be used to investigate disease mechanisms in a cell-type specific manner and their capacity for proliferation allows unlimited expansion, which is particularly helpful for rare and difficult to obtain samples. The ability to utilize genome-editing technologies, such as CRISPR-Cas9, on iPSCs provides opportunities to establish the direct impact of a patient's genetic profile on disease pathology and potentially correct the disorder in vitro (Berger, Dookwah, Steet, & Dalton, 2016). Lastly, as is demonstrated with the differentiation time course experiments in Chapter 2 of this work, the ability to collect samples throughout the differentiation process may shed light on molecular or mechanistic changes that occur during differentiation, and possibly development, that may be missed using fully differentiated or end-point samples.

The caveats related to iPSC disease modeling are similar to the challenges faced by many cell culture models. Experiments have to be interpreted within the context of a “disease in a dish” and may lack environmental components or cues that are obtained with animal models for instance. Cell migration or gross structural tissue changes may also be more challenging within the confines of a tissue culture dish. However, cancer researchers have developed useful assays and tools to study cell adhesion and motility (Hulkower & Herber, 2011). And the development of tissue organoid models from iPSCs is taking the field of iPSC disease modeling into a whole new dimension and could help uncover more complex mechanistic understanding for some diseases (Marton & Pașca, 2020). These benefits make iPSC technology a valuable tool for researching human diseases, including those that are caused by defects in the biosynthesis glycolipids (Berger et al., 2016)

The Neural Crest

For this project, we decided to differentiate iPSCs to neural crest cells due to the fact that several of the patient phenotypes appear to be in neural crest-derived lineages – namely, cranio-facial defects, possible enteric innervation defects, peripheral nerve defects, and skin pigmentation issues.

As can be seen by the aforementioned list of lineage-relevant phenotypes, the neural crest is a highly migratory and multipotent cell type. Neural crest cells are unique to vertebrates, and they're derived from the neural tube during early neurogenesis and are one of two cell populations that give rise to the peripheral nervous system – the other being the ectodermal placodes (Crane & Trainor, 2006). Neural crest cells are induced at the dorsal most portion of the neural tube and require contact-mediated tissue interactions with the dorsal surface ectoderm (Moury & Jacobson, 1990; Rollhäuser-ter Horst, 1977).

Notch, BMP, FGF, and WNT signaling pathways have been shown to be used in a reiterative fashion during neural crest cell patterning. Neural crest studies have been performed in classical embryogenesis models such as frog, fish, chick, and of course mouse. It should be noted that none of the *Wnt, Fgf,* or *Notch* pathway mutants that have been generated thus far have demonstrated complete absences of neural crest cell formation. Therefore, it appears that BMP is the crucial morphogen needed for neural crest induction; however, the intersection of BMP, FGF, Notch and WNT signaling may be required for subsequent further differentiation of neural crest cells (Crane & Trainor, 2006).

During induction, the activation of BMP and upregulation of the Wnt pathway promotes neuroepithelial cells to undergo an epithelial-to-mesenchymal transition, which involves a downregulation of the E-cadherin adhesion molecule and promotes delamination and allows the neural crest cells to be migratory (Ahlstrom & Erickson, 2009). The neural crest cells do not migrate randomly from the neural tube though, rather they emerge in a wave that spreads rostrocaudally, or from head-to-tail, along almost the entire neuroaxis. This wave-patterning is facilitated by E-cadherin repression and activation of neural crest patterning genes (Kulesa, Bailey, Kasemeier-Kulesa, & McLennan, 2010).

The neural crest is subdivided into at least four distinct populations of cells along the axis – cranial, cardiac, vagal, and trunk. These populations migrate along specific pathways and differentiate into different cell and tissue types throughout the body. Cranial NC differentiate into cartilage and bone, as well as connective tissue, pigment cells, and sensory and parasympathetic ganglia. Cardiac NC cells result in aortic arch smooth muscle and parasympathetic cardiac ganglia (Kirby, Gale, & Stewart, 1983). Vagal NC cells generate the majority of the neuronal cells and glia that make up the enteric nervous system (Yntema & Hammond, 1954). Lastly, the trunk NC cells give rise to neurons and glia of the peripheral nervous system, sympatho-adrenal cells, and pigment cells in the skin (Burns & Douarin, 1998).

Diseases caused by abnormalities in neural crest development and differentiation during embryogenesis are known as Neurocristopathies (NCPs). There are believed to be over 50 NCPs currently identified. Because the neural crest differentiates into so many different cell types throughout the body, phenotypes can range from craniofacial

abnormalities, to cardiac, gastrointestinal, dermatologic, or other complications with the peripheral nervous system. These disorders are very challenging to diagnose. Researchers are currently developing new ways to categorize sub-types of NCPs in order to aid in discovering and diagnosing this class of diseases (Sato et al., 2019; Vega-Lopez, Cerrizuela, Tribulo, & Aybar, 2018).

Purpose of Study

The next chapter of this dissertation presents findings from our investigations into glycolipid and cell signaling molecular changes that occur due to the loss of GM3 Synthase in neural crest cells differentiated from patient-derived induced-pluripotent stem cells. Glycosylation is cell-type specific, and therefore, the impact of loss of function of a specific glycosyltransferase may have a variable impact on different cell types (A. Varki et al., 2015). At the time of writing this dissertation, there are no current publications reporting on the biochemical or molecular analysis of GM3SD in neural cell types. This work utilized the pluripotent capacity of patient-derived iPSCs to address this need, as access to neural tissues for study is limited. We sought to characterize the glycolipid profiles in iPSCs and neural crest cells for two of the five currently identified GM3SD-causing variants. Knowing that glycolipids play a critical role in cell signaling at the cell surface, we investigated the cell surface proteome and RTK expression in GM3-deficient iPSCs and neural crest cells. An additional benefit of iPSC disease modeling that this project took advantage of was the ability to collect cells throughout the differentiation process, which would allow us to assess RTK expression over the time course of differentiation. Through the data presented in Chapter 2 of this work, we hope to demonstrate that cell signaling molecules and cell surface proteins are altered as a

result of changes in glycolipid expression during neural crest differentiation due to genetic variants in GM3 synthase.

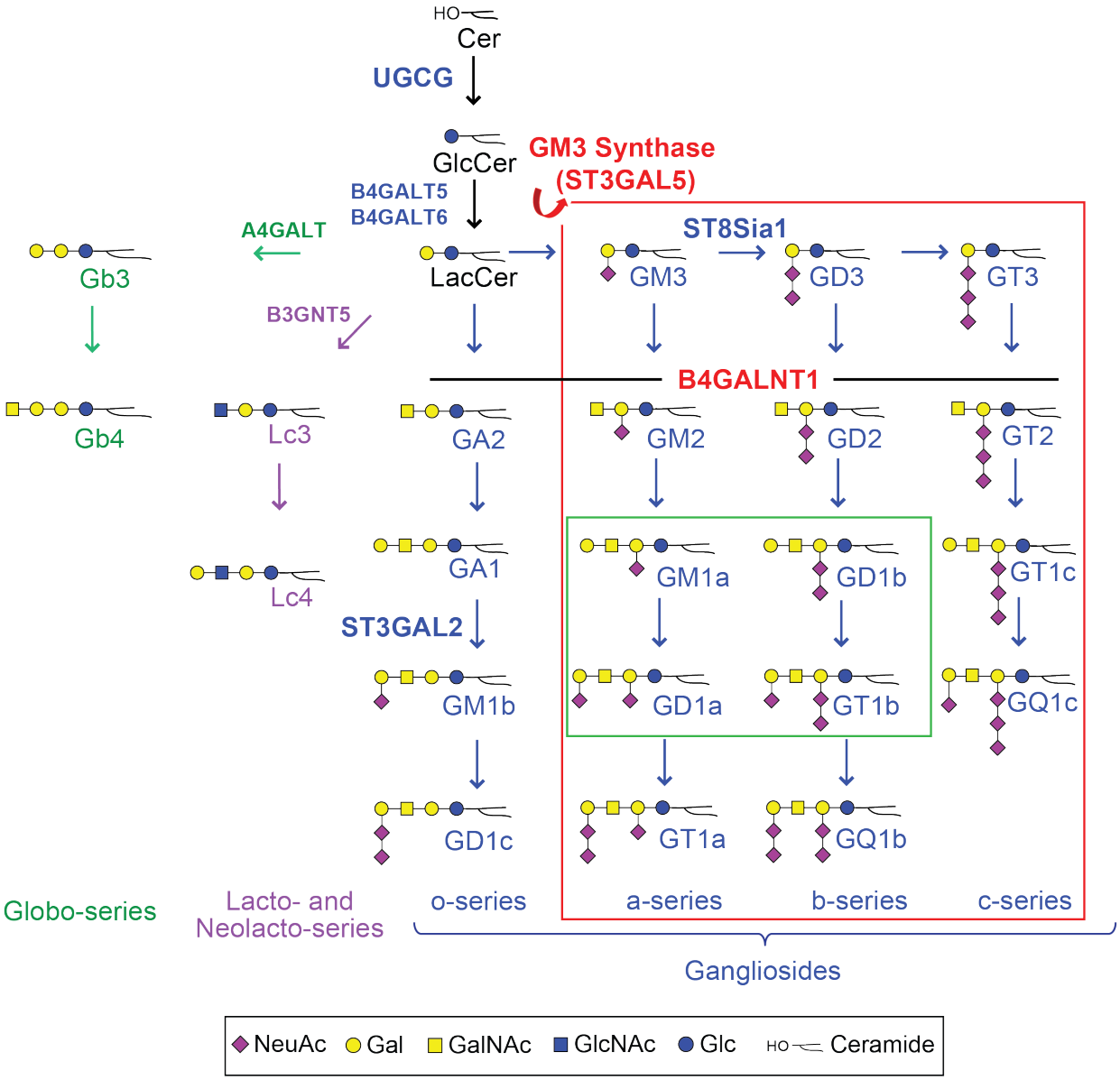

Figure 1.1. Glycosphingolipid Biosynthetic Pathway. GSL biosynthesis in mammals begins with the formation of Glucosyl Ceramide (GlcCer) by the glucosylation of ceramide. GlcCer is then further elongated to form LacCer by the addition of a galactose residue. LacCer is the substrate for GM3 Synthase, which forms GM3 by catalyzing the addition of sialic acid to LacCer. GM3 can then be further extended via the catalysis of other glycosyltransferase enzymes to form all of the ganglioside within the RED BOX. The gangliosides in the GREEN BOX are the 4 gangliosides most highly expressed in neural tissues. LacCer can also be used as the substrate for the o-series and the Lacto-, Neolacto- and Globoseries GSLs. Patients with GM3SD cannot produce any of the gangliosides within the RED BOX.

Table 1.1. GM3SD Patient Cohorts Genotype and Phenotypes

	Old Order Amish	Salt and Pepper	French	Pakistani	Korean	Italian	Total (N)	Total (%)
Report	Simpson Wang Bowser	Boccuto	Fragaki	Gordon-Lipkin	Lee	Indellicato		
Genotype	c.862C>T p.R288X Homozygous	c.1063G>A p.E355K Homozygous	c.862C>T p.R288X Homozygous	c.862C>T p.R288X Homozygous	c.584G>C p.C195S c.601G>A p.G201R Compound Het	c.1024G>A p.G342S Homozygous	-	-
Cognitive								
Intellectual Disability	38/38	3/3	2/2	3/3	2/2	NR	48/48	100
Neurodevelopmental deterioration	8/8	1/3	2/2	0/3	1/2	0/1	12/19	63
Verbal	0/8	0/3	0/2	0/3	0/2	0/1	0	0
Motor								
Choreoathetosis	8/8	3/3	2/2	3/3	2/2	1/1	49/49	100
Tone	Low	spastic	low	mixed	-	low		
Ambulates	0/8	0/3	0/2	1/3	0/2	NR	1/18	6
Seizures								
Epilepsy	8/8	1/3	2/2	0/3	0/2	1/1	12/19	63
Abnormal EEG	8/8	NR	2/2	3/3	NR	1/1	14/14	100
Sensory								
Hearing impairment	8/8	NR	2/2	3/3	NR	1/1	14/14	100
Vision impairment	8/8	0/3	2/2	3/3	1/2	1/1	15/19	79
Growth								
Microcephaly	NR	3/3	NR	3/3	1/2	1/1	8/9	89
Failure to thrive	38/38	3/3	2/2	3/3	1/2	1/1	48/49	98
Gastrostomy tube	6/8	NR	2/2	2/3	NR	NR	10/13	77
Feeds by mouth	NR	NR	2/2	2/3	NR	1/1	5/6	83
Skin Phenotype								
Pigment changes	27/38	3/3	NR	2/3	1/2	1/1	34/49	69
Severe atopic dermatitis/Ichthyosis	NR	NR	NR	2/3	NR	0/1	2/4	50
Behavior								
Sleep disturbance	8/8	NR	NR	2/3	2/2	NR	12/13	92
Self-injurious behavior	NR	NR	NR	3/3	NR	NR	3/3	100
History								
Normal prenatal, birth history	8/8	3/3	2/2	3/3	2/2	1/1	19/19	100
Normal birth parameters	8/8	3/3	2/2	3/3	2/2	1/1	19/19	100

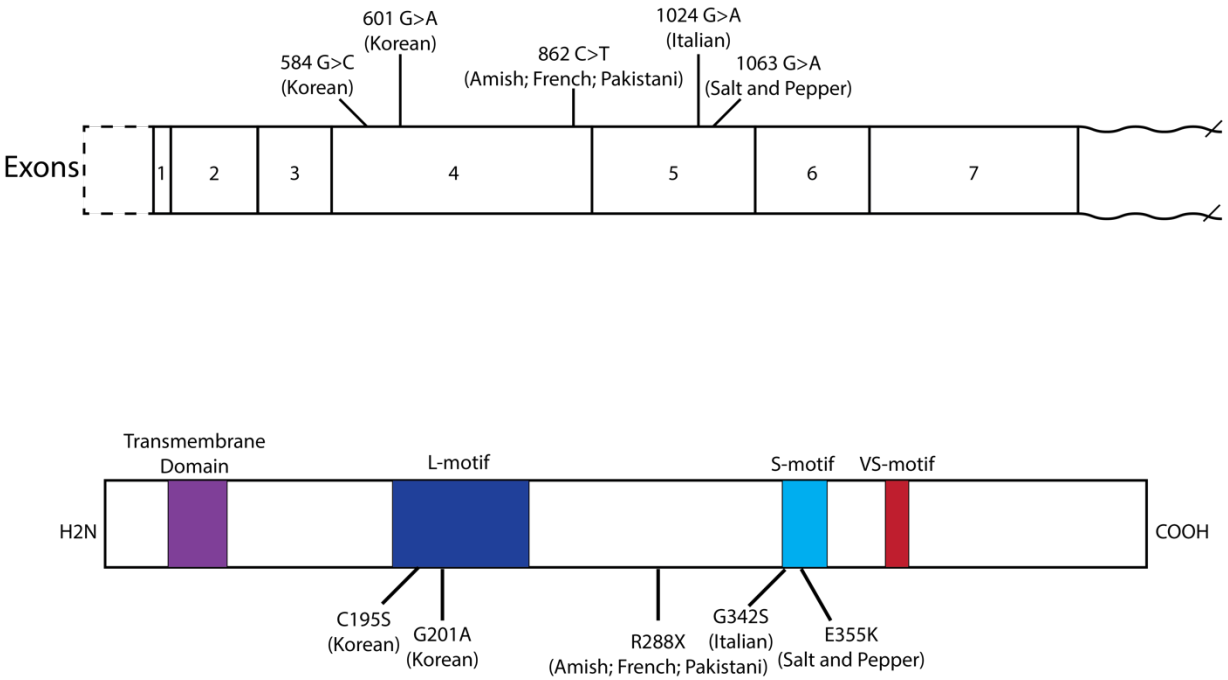

Figure 1.2. Location of GM3SD-variants in *ST3GAL5* Exons and on Protein.
Schematic representation of ST3GAL5 (GM3 Synthase) variants in cDNA and the protein structure. Protein structure includes color representations of conserved sequences in ST3GAL5. Patient cohorts are labeled with respective variant. The most prevalent variant is the p.R288X mutation seen in the Amish, French, and Pakistani cohorts. It results in a truncated protein that lacks the S-motif, motif 3, and the VS-motif. The p.G342S and p.E355K variants, the Italian and Salt and Pepper cohorts, respectively, lie in the S-motif, known to be responsible for binding the LacCer acceptor molecule. Lastly, the p.C195S and p.G201A compound heterozygous variants identifies in the Korean cohort lie in the L-motif, which is responsible for binding CMP-Neu5Ac along with the S-motif.
Adapted from Indellicato et al. (2019).

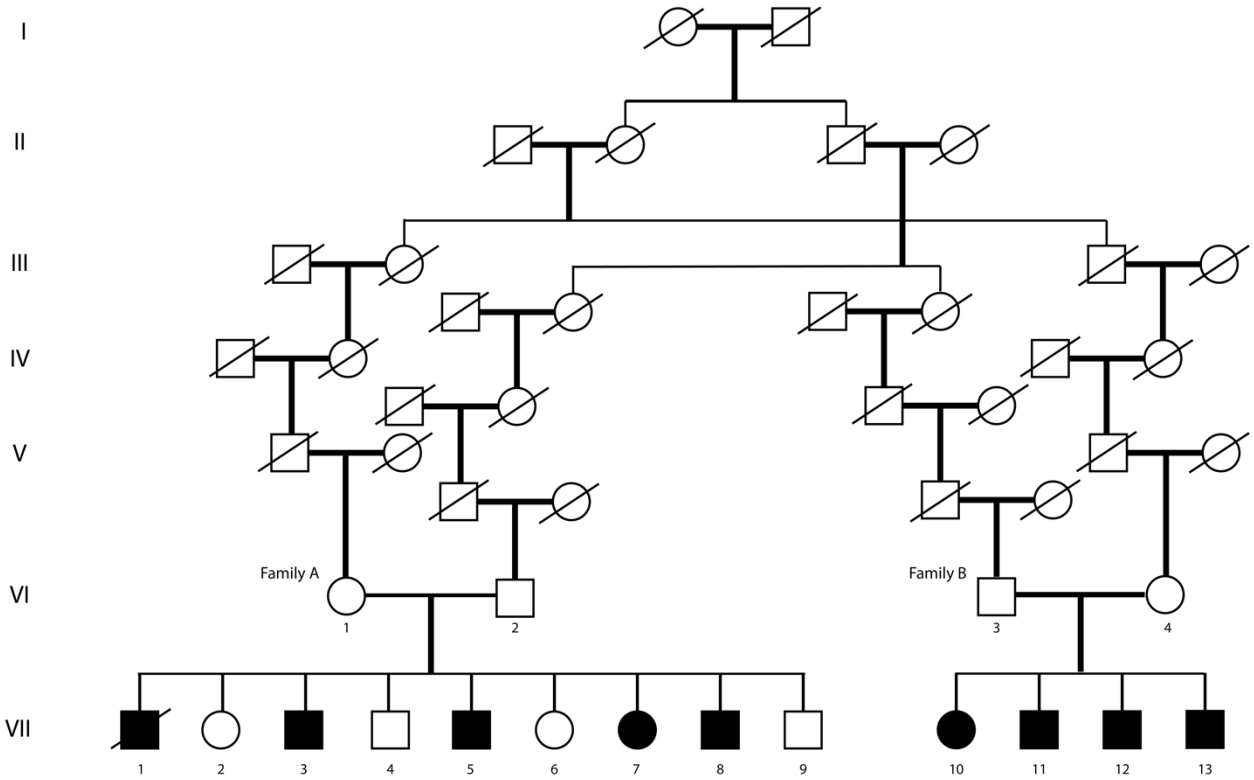

Figure 1.3 Pedigree for Amish Cohort in Simpson et al. (2004).
A family pedigree for the Amish cohort (c.862C > T; p.Arg288X) shows two sets of siblings belonging to two families with a shared relative from five generations prior. Family A had four affected males (VII-1, VII-3, VII-5, and VII8), one of whom (VII-1) was deceased, and one female (VII-7) who was affected. Family B had four children, three males (VII-11, VII-12, and VII-13) and one female (VII-10), all of whom were affected. Adapted from Simpson et al. (2004).

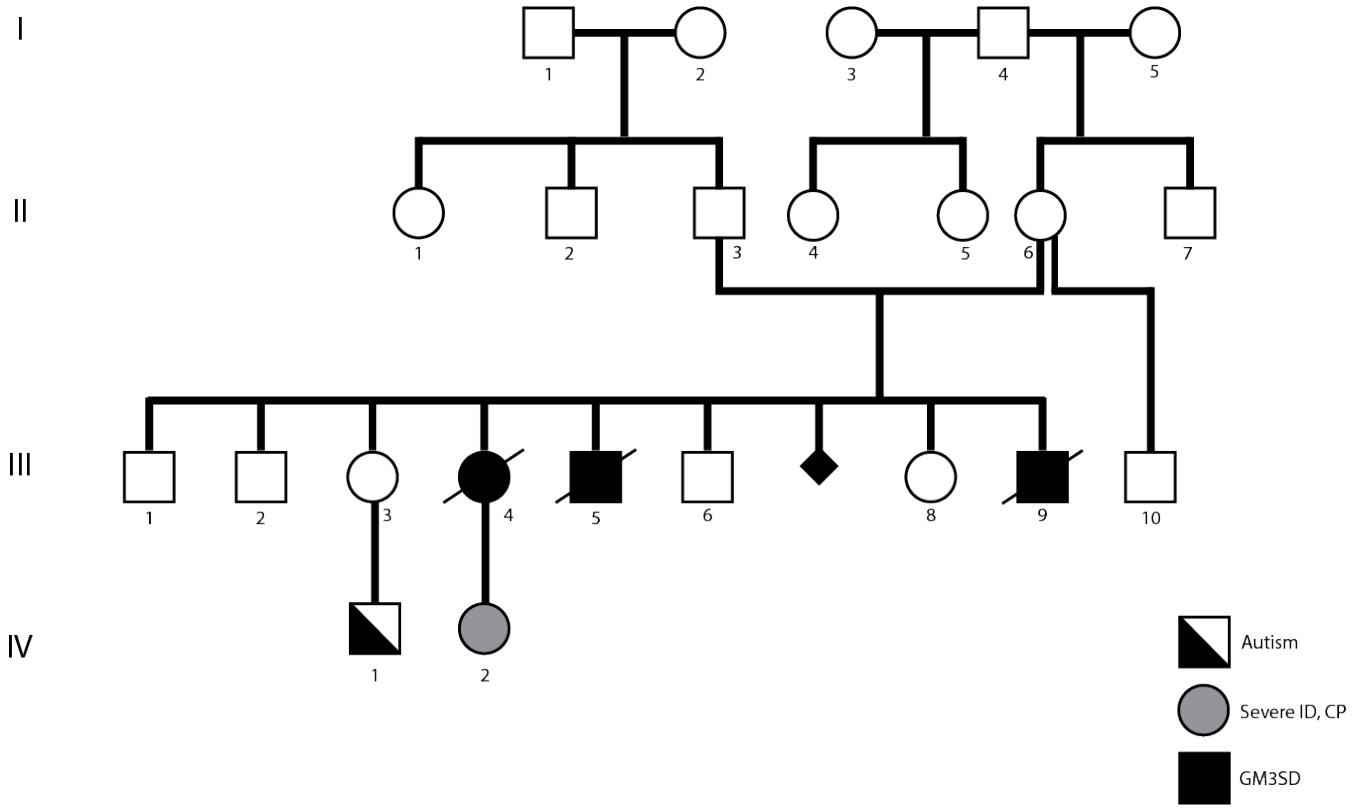

Figure 1.4. Pedigree for Salt and Pepper Cohort.
A family pedigree for the Salt and Pepper cohort (c.1063G>A; p.Glu355Lys) shows the three siblings, two males (III-5 and III-9) and one female (III-4), affected with GM3SD. The cell line used for our studies is from proband III-5. The key to the left indicated affected individuals with GM3SD as well individuals within the family that exhibited other neurological disorders. An unaffected sibling (III-3) has a male child (IV-1) with autism and the GM3SD affected female patient (III-4) had a female child (IV-2) with severe intellectual disability (ID) and cerebral palsy (CP). The small diamond represents a miscarriage. The three GM3SD patients are no longer living.
Adapted from (Boccuto et al., 2013).

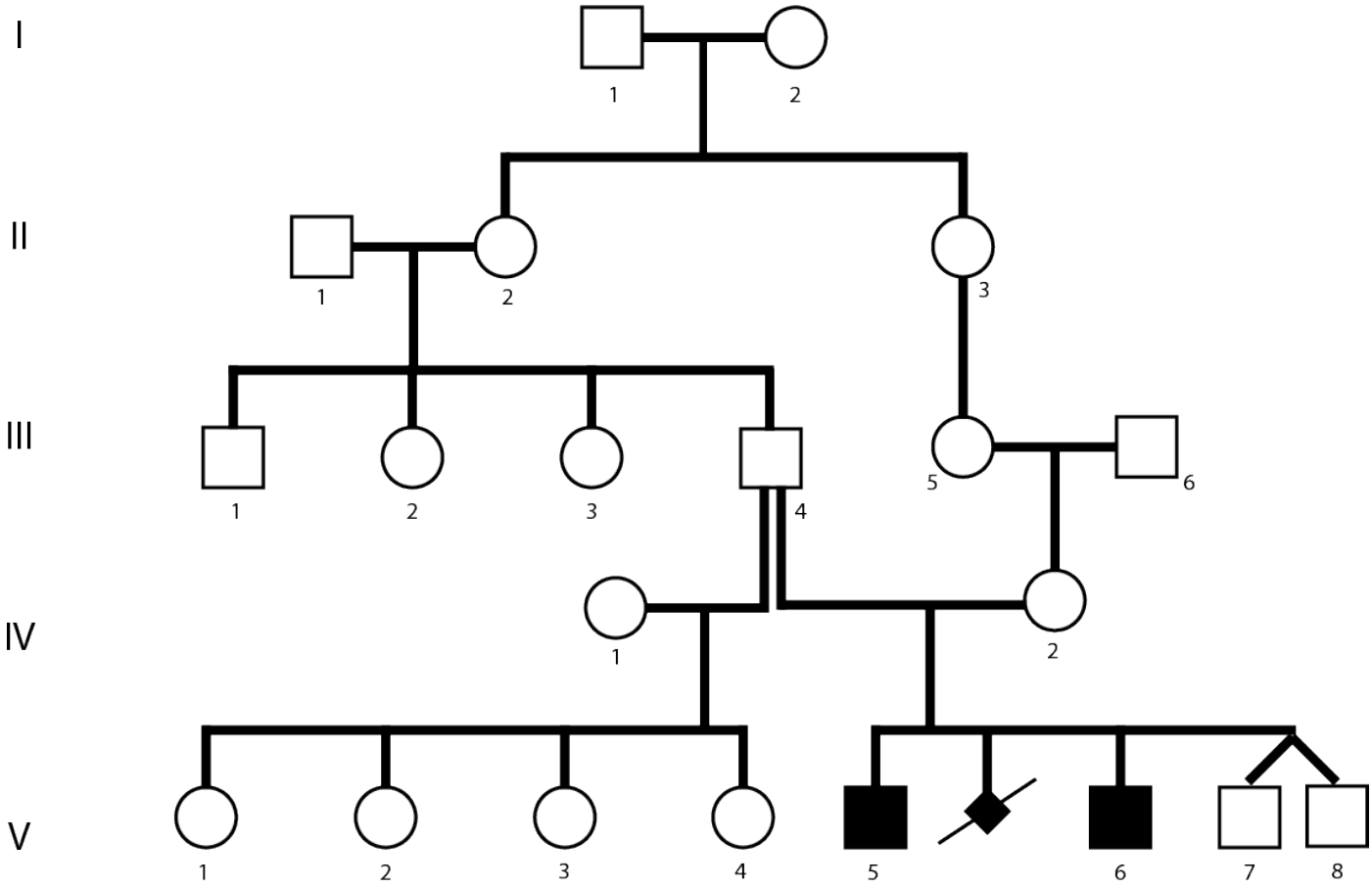

Figure 1.5. Pedigree for French Cohort.
A family pedigree for the French cohort (c.862C > T; p.Arg288X) shows the two male siblings affected with GM3SD (V-5 and V-6). They were born of consanguineous parents. The small diamond represents a miscarriage.
Adapted from Fragaki et al. (2013).

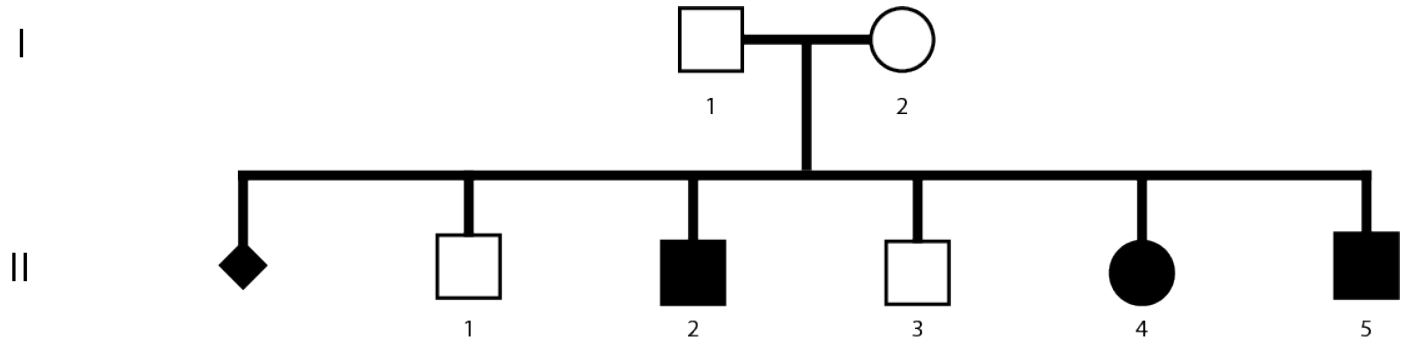

Figure 1.6. Pedigree for Pakistani Cohort.
A family pedigree for the Pakistani cohort (c.862C > T; p.Arg288X) shows the three siblings, two males (II-2 and II-5) and one female (II-4) affected with GM3SD. The small diamond represents a miscarriage. The parents provided information that there was also a distant cousin with an “unknown enzyme deficiency”, but this information could not be mapped onto the pedigree.
Adapted from Gordon-Lipkin et al. (2018).

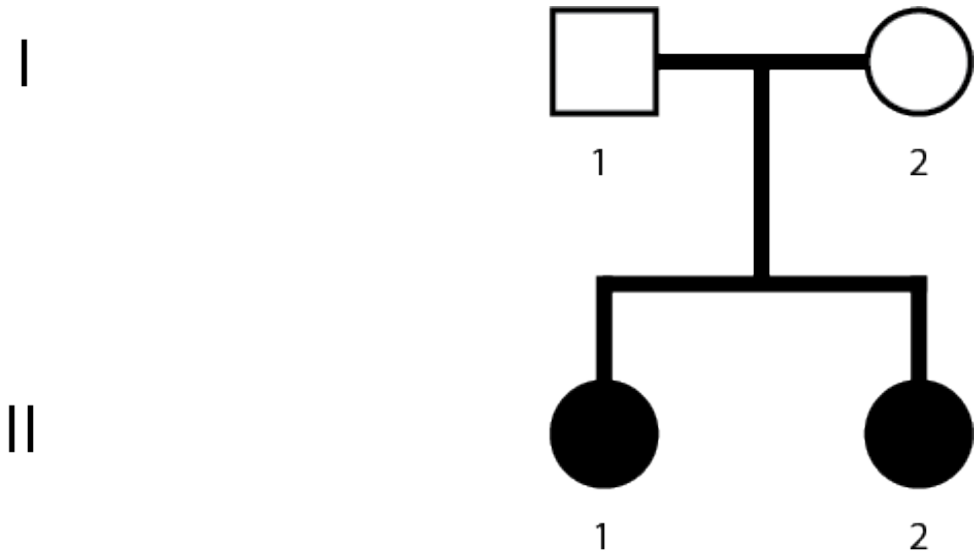

Figure 1.7. Pedigree for Korean Cohort.
A family pedigree for the Korean cohort (c.584G>C; p.Cys195Ser, and c.601G>A; p.Gly201Arg) shows the two female (II-1 and II-2) siblings affected with GM3SD. The parents had no other children.
Adapted from Lee et al. (2016).

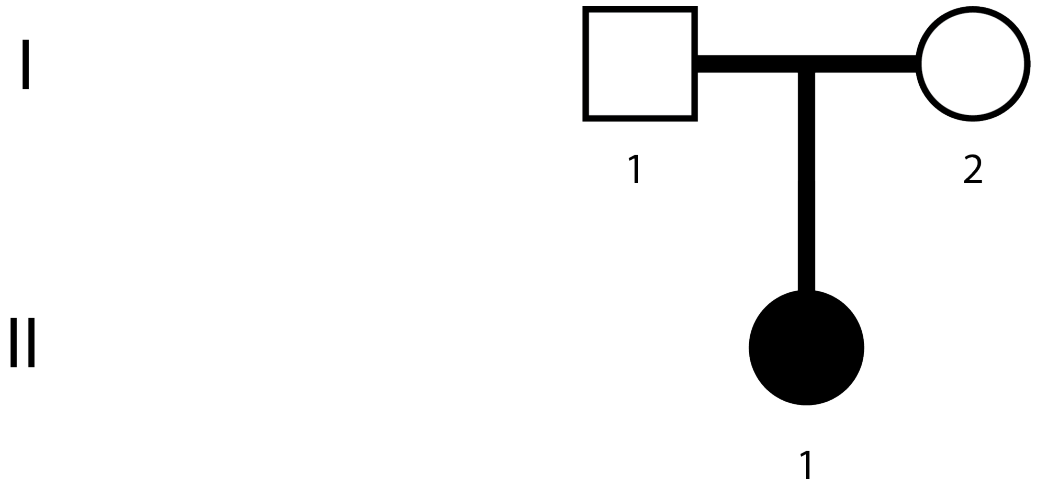

Figure 1.8. Pedigree for Italian Cohort.
A family pedigree for the Italian cohort (c.1024G>A; p. Gly342Ser) shows the female child (II-1) affected with GM3SD. The parents had no other children.
Adapted from Indellicato et al. (2019).

References

Ahlstrom, J. D., & Erickson, C. A. (2009). The neural crest epithelial-mesenchymal transition in 4D: a 'tail' of multiple non-obligatory cellular mechanisms. *Development, 136*(11), 1801-1812. doi:10.1242/dev.034785

Allou, L., Julia, S., Amsallem, D., El Chehadeh, S., Lambert, L., Thevenon, J., . . . Philippe, C. (2017). Rett-like phenotypes: expanding the genetic heterogeneity to the KCNA2 gene and first familial case of CDKL5-related disease. *Clin Genet, 91*(3), 431-440. doi:10.1111/cge.12784

Almeida, P. F. (2009). Thermodynamics of lipid interactions in complex bilayers. *Biochimica et Biophysica Acta (BBA)-Biomembranes, 1788*(1), 72-85.

Amir, R. E., Van den Veyver, I. B., Wan, M., Tran, C. Q., Francke, U., & Zoghbi, H. Y. (1999). Rett syndrome is caused by mutations in X-linked MECP2, encoding methyl-CpG-binding protein 2. *Nature Genetics, 23*(2), 185-188.

Audry, M., Jeanneau, C., Imberty, A., Harduin-Lepers, A., Delannoy, P., & Breton, C. (2011). Current trends in the structure-activity relationships of sialyltransferases. *Glycobiology, 21*(6), 716-726. doi:10.1093/glycob/cwq189

Bejaoui, K., Wu, C., Scheffler, M. D., Haan, G., Ashby, P., Wu, L., . . . Brown, R. H., Jr. (2001). SPTLC1 is mutated in hereditary sensory neuropathy, type 1. *Nat Genet, 27*(3), 261-262. doi:10.1038/85817

Berger, R. P., Dookwah, M., Steet, R., & Dalton, S. (2016). Glycosylation and stem cells: Regulatory roles and application of iPSCs in the study of glycosylation-related disorders. *BioEssays, 38*(12), 1255-1265. doi:https://doi.org/10.1002/bies.201600138

Bhuiyan, R. H., Ohmi, Y., Ohkawa, Y., Zhang, P., Takano, M., Hashimoto, N., . . . Furukawa, K. (2019). Loss of Enzyme Activity in Mutated B4GALNT1 Gene Products in Patients with Hereditary Spastic Paraplegia Results in Relatively Mild Neurological Disorders: Similarity with Phenotypes of B4galnt1 Knockout Mice. *Neuroscience, 397*, 94-106. doi:https://doi.org/10.1016/j.neuroscience.2018.11.034

Boccuto, L., Aoki, K., Flanagan-Steet, H., Chen, C.-F., Fan, X., Bartel, F., . . . Schwartz, C. E. (2013). A mutation in a ganglioside biosynthetic enzyme, ST3GAL5, results in salt & pepper syndrome, a neurocutaneous disorder with altered glycolipid and glycoprotein glycosylation. *Human Molecular Genetics, 23*(2), 418-433. doi:10.1093/hmg/ddt434

Bowser, L. E., Young, M., Wenger, O. K., Ammous, Z., Brigatti, K. W., Carson, V. J., . . . Strauss, K. A. (2019). Recessive GM3 synthase deficiency: Natural history, biochemistry, and therapeutic frontier. *Mol Genet Metab, 126*(4), 475-488. doi:10.1016/j.ymgme.2019.01.013

Bremer, E. G., Hakomori, S., Bowen-Pope, D. F., Raines, E., & Ross, R. (1984). Ganglioside-mediated modulation of cell growth, growth factor binding, and receptor phosphorylation. *J Biol Chem, 259*(11), 6818-6825.

Bremer, E. G., Schlessinger, J., & Hakomori, S.-I. (1986). Ganglioside-mediated modulation of cell growth. Specific effects of GM3 on tyrosine phosphorylation of the epidermal growth factor receptor. *Journal of Biological Chemistry, 261*(5), 2434-2440.

Brown, D. A., & London, E. (1997). Structure of detergent-resistant membrane domains: does phase separation occur in biological membranes? *Biochem Biophys Res Commun, 240*(1), 1-7. doi:10.1006/bbrc.1997.7575

Brown, D. A., & London, E. (1998). Functions of lipid rafts in biological membranes. *Annu Rev Cell Dev Biol, 14*, 111-136. doi:10.1146/annurev.cellbio.14.1.111

Brown, D. A., & London, E. (2000). Structure and Function of Sphingolipid- and Cholesterol-rich Membrane Rafts *. *Journal of Biological Chemistry, 275*(23), 17221-17224. doi:10.1074/jbc.R000005200

Brown, D. A., & Rose, J. K. (1992). Sorting of GPI-anchored proteins to glycolipid-enriched membrane subdomains during transport to the apical cell surface. *Cell, 68*(3), 533-544. doi:10.1016/0092-8674(92)90189-j

Brunngraber, E. G., Berra, B., & Zambotti, V. (1973). Altered levels of tissue glycoproteins, gangliosides, glycosaminoglycans and lipids in Niemann-Pick's disease. *Clinica Chimica Acta, 48*(2), 173-181.

Burns, A. J., & Douarin, N. M. (1998). The sacral neural crest contributes neurons and glia to the post-umbilical gut: spatiotemporal analysis of the development of the enteric nervous system. *Development, 125*(21), 4335-4347.

Collins, B. E., Ito, H., Sawada, N., Ishida, H., Kiso, M., & Schnaar, R. L. (1999). Enhanced Binding of the Neural Siglecs, Myelin-associated Glycoprotein and Schwann Cell Myelin Protein, to Chol-1 (α-Series) Gangliosides and Novel Sulfated Chol-1 Analogs*. *Journal of Biological Chemistry, 274*(53), 37637-37643. doi:https://doi.org/10.1074/jbc.274.53.37637

Constantopoulos, G., & Dekaban, A. S. (1978). Neurochemistry of the mucopolysaccharidoses: brain lipids and lysosomal enzymes in patients with four types of mucopolysaccharidosis and in normal controls. *Journal of Neurochemistry, 30*(5), 965-973.

Coskun, Ü., Grzybek, M., Drechsel, D., & Simons, K. (2011). Regulation of human EGF receptor by lipids. *Proc Natl Acad Sci U S A, 108*(22), 9044-9048. doi:10.1073/pnas.1105666108

Crane, J. F., & Trainor, P. A. (2006). Neural Crest Stem and Progenitor Cells. *Annual Review of Cell and Developmental Biology, 22*(1), 267-286. doi:10.1146/annurev.cellbio.22.010305.103814

Cumings, J. (1962). *Abnormalities in lipid metabolism in two members of a family with Niemann-Pick disease.* Paper presented at the Cerebral Sphingolipidoses. A Symposium on Tay-Sachs Disease and Allied Disorders.

D'Angelo, G., Capasso, S., Sticco, L., & Russo, D. (2013). Glycosphingolipids: synthesis and functions. *Febs j, 280*(24), 6338-6353. doi:10.1111/febs.12559

Daniotti, J. L., & Iglesias-Bartolomé, R. (2011). Metabolic pathways and intracellular trafficking of gangliosides. *IUBMB Life, 63*(7), 513-520. doi:10.1002/iub.477

Datta, A. K., & Paulson, J. C. (1995). The sialyltransferase "sialylmotif" participates in binding the donor substrate CMP-NeuAc. *J Biol Chem, 270*(4), 1497-1500. doi:10.1074/jbc.270.4.1497

Datta, A. K., Sinha, A., & Paulson, J. C. (1998). Mutation of the sialyltransferase S-sialylmotif alters the kinetics of the donor and acceptor substrates. *J Biol Chem, 273*(16), 9608-9614. doi:10.1074/jbc.273.16.9608

DeVries, G. H., & Zmachinski, C. J. (1980). The Lipid Composition of Rat CNS Axolemma-enriched Fractions. *Journal of Neurochemistry, 34*(2), 424-430. doi:https://doi.org/10.1111/j.1471-4159.1980.tb06613.x

Elleder, M. (1989). Niemann-Pick disease. *Pathology-Research and Practice, 185*(3), 293-328.

Fragaki, K., Ait-El-Mkadem, S., Chaussenot, A., Gire, C., Mengual, R., Bonesso, L., . . . Paquis-Flucklinger, V. (2013). Refractory epilepsy and mitochondrial dysfunction due to GM3 synthase deficiency. *European Journal of Human Genetics, 21*(5), 528-534. doi:10.1038/ejhg.2012.202

Futerman, A. H., Stieger, B., Hubbard, A. L., & Pagano, R. E. (1990). Sphingomyelin synthesis in rat liver occurs predominantly at the cis and medial cisternae of the Golgi apparatus. *J Biol Chem, 265*(15), 8650-8657.

Futerman, A. H., & van Meer, G. (2004). The cell biology of lysosomal storage disorders. *Nature Reviews Molecular Cell Biology, 5*(7), 554-565. doi:10.1038/nrm1423

Gault, C. R., Obeid, L. M., & Hannun, Y. A. (2010). An overview of sphingolipid metabolism: from synthesis to breakdown. *Advances in experimental medicine and biology, 688*, 1-23. doi:10.1007/978-1-4419-6741-1_1

Gordon-Lipkin, E., Cohen, J. S., Srivastava, S., Soares, B. P., Levey, E., & Fatemi, A. (2018). ST3GAL5-Related Disorders: A Deficiency in Ganglioside Metabolism and a Genetic Cause of Intellectual Disability and Choreoathetosis. *J Child Neurol, 33*(13), 825-831. doi:10.1177/0883073818791099

Hakomori, S. (1981). Glycosphingolipids in cellular interaction, differentiation, and oncogenesis. *Annu Rev Biochem, 50*, 733-764. doi:10.1146/annurev.bi.50.070181.003505

Hakomori, S.-i., Handa, K., Iwabuchi, K., Yamamura, S., & Prinetti, A. (1998). New insights in glycosphingolipid function: “glycosignaling domain,” a cell surface assembly of glycosphingolipids with signal transducer molecules, involved in cell adhesion coupled with signaling. *Glycobiology, 8*(10), xi-xviii. doi:10.1093/oxfordjournals.glycob.a018822

HAKOMORI, S.-I., YAMAMURA, S., & HANDA, K. (1998). Signal Transduction Through Glyco(sphingo)lipids: Introduction and Recent Studies on Glyco(sphingo)lipid-enriched

Microdomainsa. *Annals of the New York Academy of Sciences, 845*(1), 1-10. doi:https://doi.org/10.1111/j.1749-6632.1998.tb09657.x

Hakomori Si, S. I. (2002). The glycosynapse. *Proc Natl Acad Sci U S A, 99*(1), 225-232. doi:10.1073/pnas.012540899

Harlalka, G. V., Lehman, A., Chioza, B., Baple, E. L., Maroofian, R., Cross, H., . . . Crosby, A. H. (2013). Mutations in B4GALNT1 (GM2 synthase) underlie a new disorder of ganglioside biosynthesis. *Brain, 136*(12), 3618-3624. doi:10.1093/brain/awt270

Hiraoka, M., Ohkawa, E., Abe, A., Murata, M., Go, S., Inokuchi, J. I., & Ohguro, H. (2019). Visual Function in Mice Lacking GM3 Synthase. *Curr Eye Res, 44*(6), 664-670. doi:10.1080/02713683.2019.1576206

Hulkower, K. I., & Herber, R. L. (2011). Cell migration and invasion assays as tools for drug discovery. *Pharmaceutics, 3*(1), 107-124. doi:10.3390/pharmaceutics3010107

Indellicato, R., Parini, R., Domenighini, R., Malagolini, N., Iascone, M., Gasperini, S., . . . Trinchera, M. (2019). Total loss of GM3 synthase activity by a normally processed enzyme in a novel variant and in all ST3GAL5 variants reported to cause a distinct congenital disorder of glycosylation. *Glycobiology, 29*(3), 229-241. doi:10.1093/glycob/cwy112

Inoue, M., Fujii, Y., Furukawa, K., Okada, M., Okumura, K., Hayakawa, T., . . . Sugiura, Y. (2002). Refractory Skin Injury in Complex Knock-out Mice Expressing Only the GM3 Ganglioside*. *Journal of Biological Chemistry, 277*(33), 29881-29888. doi:https://doi.org/10.1074/jbc.M201631200

Kakio, A., Nishimoto, S., Yanagisawa, K., Kozutsumi, Y., & Matsuzaki, K. (2002). Interactions of amyloid beta-protein with various gangliosides in raft-like membranes: importance of GM1 ganglioside-bound form as an endogenous seed for Alzheimer amyloid. *Biochemistry, 41*(23), 7385-7390. doi:10.1021/bi0255874

Kawai, H., Allende, M. L., Wada, R., Kono, M., Sango, K., Deng, C., . . . Proia, R. L. (2001). Mice Expressing Only Monosialoganglioside GM3 Exhibit Lethal Audiogenic Seizures*. *Journal of Biological Chemistry, 276*(10), 6885-6888. doi:https://doi.org/10.1074/jbc.C000847200

Kawashima, N., Yoon, S. J., Itoh, K., & Nakayama, K. (2009). Tyrosine kinase activity of epidermal growth factor receptor is regulated by GM3 binding through carbohydrate to

carbohydrate interactions. *J Biol Chem, 284*(10), 6147-6155. doi:10.1074/jbc.M808171200

Keenan, T. W., Schmid, E., Franke, W. W., & Wiegandt, H. (1975). Exogenous glycosphingolipids suppress growth rate of transformed and untransformed 3T3 mouse cells. *Experimental Cell Research, 92*(2), 259-270. doi:https://doi.org/10.1016/0014-4827(75)90379-1

Kirby, M. L., Gale, T. F., & Stewart, D. E. (1983). Neural crest cells contribute to normal aorticopulmonary septation. *Science, 220*(4601), 1059-1061. doi:10.1126/science.6844926

Kracun, I., Rosner, H., Drnovsek, V., Vukelic, Z., Cosovic, C., Trbojevic-Cepe, M., & Kubat, M. (1992). Gangliosides in the human brain development and aging. *Neurochemistry International, 20*(3), 421-431. doi:https://doi.org/10.1016/0197-0186(92)90057-X

Kulesa, P. M., Bailey, C. M., Kasemeier-Kulesa, J. C., & McLennan, R. (2010). Cranial neural crest migration: new rules for an old road. *Dev Biol, 344*(2), 543-554. doi:10.1016/j.ydbio.2010.04.010

Laine, R. A., & Hakomori, S.-i. (1973). Incorporation of exogenous glycosphingolipids in plasma membranes of cultured hamster cells and concurrent change of growth behavior. *Biochemical and Biophysical Research Communications, 54*(3), 1039-1045. doi:https://doi.org/10.1016/0006-291X(73)90798-5

Lannert, H., Gorgas, K., Meissner, I., Wieland, F. T., & Jeckel, D. (1998). Functional organization of the Golgi apparatus in glycosphingolipid biosynthesis. Lactosylceramide and subsequent glycosphingolipids are formed in the lumen of the late Golgi. *J Biol Chem, 273*(5), 2939-2946. doi:10.1074/jbc.273.5.2939

Lee, J. S., Yoo, Y., Lim, B. C., Kim, K. J., Song, J., Choi, M., & Chae, J.-H. (2016). GM3 synthase deficiency due to ST3GAL5 variants in two Korean female siblings: Masquerading as Rett syndrome-like phenotype. *American Journal of Medical Genetics Part A, 170*(8), 2200-2205. doi:https://doi.org/10.1002/ajmg.a.37773

Levental, I., Levental, K. R., & Heberle, F. A. (2020). Lipid Rafts: Controversies Resolved, Mysteries Remain. *Trends in Cell Biology, 30*(5), 341-353. doi:https://doi.org/10.1016/j.tcb.2020.01.009

Li, R., Liu, Y., & Ladisch, S. (2001). Enhancement of epidermal growth factor signaling and activation of SRC kinase by gangliosides. *J Biol Chem, 276*(46), 42782-42792. doi:10.1074/jbc.M101481200

Li, T. A., & Schnaar, R. L. (2018). Chapter Two - Congenital Disorders of Ganglioside Biosynthesis. In R. L. Schnaar & P. H. H. Lopez (Eds.), *Progress in Molecular Biology and Translational Science* (Vol. 156, pp. 63-82): Academic Press.

Liu, Y., Li, R., & Ladisch, S. (2004). Exogenous ganglioside GD1a enhances epidermal growth factor receptor binding and dimerization. *J Biol Chem, 279*(35), 36481-36489. doi:10.1074/jbc.M402880200

Mandon, E. C., Ehses, I., Rother, J., van Echten, G., & Sandhoff, K. (1992). Subcellular localization and membrane topology of serine palmitoyltransferase, 3-dehydrosphinganine reductase, and sphinganine N-acyltransferase in mouse liver. *Journal of Biological Chemistry, 267*(16), 11144-11148. doi:https://doi.org/10.1016/S0021-9258(19)49887-6

Martinez, Z., Zhu, M., Han, S., & Fink, A. L. (2007). GM1 specifically interacts with alpha-synuclein and inhibits fibrillation. *Biochemistry, 46*(7), 1868-1877. doi:10.1021/bi061749a

Marton, R. M., & Pașca, S. P. (2020). Organoid and Assembloid Technologies for Investigating Cellular Crosstalk in Human Brain Development and Disease. *Trends Cell Biol, 30*(2), 133-143. doi:10.1016/j.tcb.2019.11.004

Matsuzaki, K., Kato, K., & Yanagisawa, K. (2010). Abeta polymerization through interaction with membrane gangliosides. *Biochim Biophys Acta, 1801*(8), 868-877. doi:10.1016/j.bbalip.2010.01.008

Michel, C., van Echten-Deckert, G., Rother, J., Sandhoff, K., Wang, E., & Merrill, A. H., Jr. (1997). Characterization of ceramide synthesis. A dihydroceramide desaturase introduces the 4,5-trans-double bond of sphingosine at the level of dihydroceramide. *J Biol Chem, 272*(36), 22432-22437. doi:10.1074/jbc.272.36.22432

Miljan, E. A., Meuillet, E. J., Mania-Farnell, B., George, D., Yamamoto, H., Simon, H.-G., & Bremer, E. G. (2002). Interaction of the Extracellular Domain of the Epidermal Growth Factor Receptor with Gangliosides *. *Journal of Biological Chemistry, 277*(12), 10108-10113. doi:10.1074/jbc.M111669200

Mineo, C., James, G. L., Smart, E. J., & Anderson, R. G. (1996). Localization of epidermal growth factor-stimulated Ras/Raf-1 interaction to caveolae membrane. *J Biol Chem, 271*(20), 11930-11935. doi:10.1074/jbc.271.20.11930

Moury, J. D., & Jacobson, A. G. (1990). The origins of neural crest cells in the axolotl. *Dev Biol, 141*(2), 243-253. doi:10.1016/0012-1606(90)90380-2

Palmano, K., Rowan, A., Guillermo, R., Guan, J., & McJarrow, P. (2015). The role of gangliosides in neurodevelopment. *Nutrients, 7*(5), 3891-3913. doi:10.3390/nu7053891

Pike, L. J. (2009). The challenge of lipid rafts. *J Lipid Res, 50 Suppl*(Suppl), S323-328. doi:10.1194/jlr.R800040-JLR200

Prendergast, J., Umanah, G. K. E., Yoo, S.-W., Lagerlöf, O., Motari, M. G., Cole, R. N., . . . Schnaar, R. L. (2014). Ganglioside regulation of AMPA receptor trafficking. *The Journal of neuroscience : the official journal of the Society for Neuroscience, 34*(39), 13246-13258. doi:10.1523/jneurosci.1149-14.2014

Rao, F. V., Rich, J. R., Rakić, B., Buddai, S., Schwartz, M. F., Johnson, K., . . . Strynadka, N. C. J. (2009). Structural insight into mammalian sialyltransferases. *Nature structural & molecular biology, 16*(11), 1186-1188. doi:10.1038/nsmb.1685

Regina Todeschini, A., & Hakomori, S. I. (2008). Functional role of glycosphingolipids and gangliosides in control of cell adhesion, motility, and growth, through glycosynaptic microdomains. *Biochim Biophys Acta, 1780*(3), 421-433. doi:10.1016/j.bbagen.2007.10.008

Rollhäuser-ter Horst, J. (1977). Artificial neural induction in amphibia. *Anatomy and Embryology, 151*(3), 309-316. doi:10.1007/BF00318932

Russo, D., Della Ragione, F., Rizzo, R., Sugiyama, E., Scalabrì, F., Hori, K., . . . D'Angelo, G. (2018). Glycosphingolipid metabolic reprogramming drives neural differentiation. *The EMBO Journal, 37*(7), e97674. doi:https://doi.org/10.15252/embj.201797674

Sandhoff, K., & Kolter, T. (2003). Biosynthesis and degradation of mammalian glycosphingolipids. *Philosophical transactions of the Royal Society of London. Series B, Biological sciences, 358*(1433), 847-861. doi:10.1098/rstb.2003.1265

Sargiacomo, M., Sudol, M., Tang, Z., & Lisanti, M. P. (1993). Signal transducing molecules and glycosyl-phosphatidylinositol-linked proteins form a caveolin-rich insoluble complex in MDCK cells. *Journal of Cell Biology, 122*(4), 789-807.

Sato, T. S., Handa, A., Priya, S., Watal, P., Becker, R. M., & Sato, Y. (2019). Neurocristopathies: Enigmatic Appearances of Neural Crest Cell–derived Abnormalities. *RadioGraphics, 39*(7), 2085-2102. doi:10.1148/rg.2019190086

Saul, R., Wilkes, G., & Stevenson, R. (1983). *Salt-And-Pepper'pigmentary changes with severe mental retardation: a new neurocutaneous syndrome.* Paper presented at the Proc. Greenwood Genet., Ctr.

Schnaar, R. L. (2016). Gangliosides of the Vertebrate Nervous System. *J Mol Biol, 428*(16), 3325-3336. doi:10.1016/j.jmb.2016.05.020

Schnaar, R. L., Gerardy-Schahn, R., & Hildebrandt, H. (2014). Sialic acids in the brain: gangliosides and polysialic acid in nervous system development, stability, disease, and regeneration. *Physiol Rev, 94*(2), 461-518. doi:10.1152/physrev.00033.2013

Schnitzer, J. E., McIntosh, D. P., Dvorak, A. M., Liu, J., & Oh, P. (1995). Separation of caveolae from associated microdomains of GPI-anchored proteins. *Science, 269*(5229), 1435-1439. doi:10.1126/science.7660128

Sezgin, E., Kaiser, H.-J., Baumgart, T., Schwille, P., Simons, K., & Levental, I. (2012). Elucidating membrane structure and protein behavior using giant plasma membrane vesicles. *Nature protocols, 7*(6), 1042-1051.

Simons, K., & Ikonen, E. (1997). Functional rafts in cell membranes. *Nature, 387*(6633), 569-572.

Simpson, M. A., Cross, H., Proukakis, C., Priestman, D. A., Neville, D. C. A., Reinkensmeier, G., . . . Crosby, A. H. (2004). Infantile-onset symptomatic epilepsy syndrome caused by a homozygous loss-of-function mutation of GM3 synthase. *Nature Genetics, 36*(11), 1225-1229. doi:10.1038/ng1460

Stone, M. B., Shelby, S. A., Núñez, M. F., Wisser, K., & Veatch, S. L. (2017). Protein sorting by lipid phase-like domains supports emergent signaling function in B lymphocyte plasma membranes. *Elife, 6*, e19891.

Stone, M. B., & Veatch, S. L. (2015). Steady-state cross-correlations for live two-colour super-resolution localization data sets. *Nature communications, 6*(1), 1-10.

Tajima, O., Egashira, N., Ohmi, Y., Fukue, Y., Mishima, K., Iwasaki, K., . . . Furukawa, K. (2009). Reduced motor and sensory functions and emotional response in GM3-only mice: Emergence from early stage of life and exacerbation with aging. *Behavioural Brain Research, 198*(1), 74-82. doi:https://doi.org/10.1016/j.bbr.2008.10.024

Takahashi, K., & Yamanaka, S. (2006). Induction of pluripotent stem cells from mouse embryonic and adult fibroblast cultures by defined factors. *Cell, 126*(4), 663-676. doi:10.1016/j.cell.2006.07.024

Takamiya, K., Yamamoto, A., Furukawa, K., Yamashiro, S., Shin, M., Okada, M., . . . Aizawa, S. (1996). Mice with disrupted GM2/GD2 synthase gene lack complex gangliosides but exhibit only subtle defects in their nervous system. *Proceedings of the National Academy of Sciences, 93*(20), 10662-10667. doi:10.1073/pnas.93.20.10662

Tang, F.-L., Wang, J., Itokazu, Y., & Yu, R. K. (2020). Enhanced Susceptibility to Chemoconvulsant-Induced Seizures in Ganglioside GM3 Synthase Knockout Mice. *ASN neuro, 12*, 1759091420938175.

Tettamanti, G., Bonali, F., Marchesini, S., & Zambotti, V. (1973). A new procedure for the extraction, purification and fractionation of brain gangliosides. *Biochim Biophys Acta, 296*(1), 160-170. doi:10.1016/0005-2760(73)90055-6

Van Meer, G., Voelker, D. R., & Feigenson, G. W. (2008). Membrane lipids: where they are and how they behave. *Nature Reviews Molecular Cell Biology, 9*(2), 112-124.

Vanier, M. T. (1999). Lipid changes in Niemann-Pick disease type C brain: personal experience and review of the literature. *Neurochemical research, 24*(4), 481-489.

Varki, A. (2016). Biological roles of glycans. *Glycobiology, 27*(1), 3-49. doi:10.1093/glycob/cww086

Varki, A., Cummings, R. D., Esko, J. D., Stanley, P., Hart, G. W., Aebi, M., . . . Seeberger, P. H. (2015). Essentials of Glycobiology. In A. Varki, R. D. Cummings, J. D. Esko, P. Stanley, G. W. Hart, M. Aebi, A. G. Darvill, T. Kinoshita, N. H. Packer, J. H. Prestegard, R. L. Schnaar, & P. H. Seeberger (Eds.), *Essentials of Glycobiology*. Cold Spring Harbor (NY): Cold Spring Harbor Laboratory Press

Vega-Lopez, G. A., Cerrizuela, S., Tribulo, C., & Aybar, M. J. (2018). Neurocristopathies: New insights 150 years after the neural crest discovery. *Developmental Biology, 444*, S110-S143. doi:https://doi.org/10.1016/j.ydbio.2018.05.013

Walkley, S. U., & Vanier, M. T. (2009). Secondary lipid accumulation in lysosomal disease. *Biochim Biophys Acta, 1793*(4), 726-736. doi:10.1016/j.bbamcr.2008.11.014

Wang, H., Bright, A., Xin, B., Bockoven, J. R., & Paller, A. S. (2013). Cutaneous dyspigmentation in patients with ganglioside GM3 synthase deficiency. *American Journal of Medical Genetics Part A, 161*(4), 875-879. doi:https://doi.org/10.1002/ajmg.a.35826

Wang, X.-Q., Sun, P., O'Gorman, M., Tai, T., & Paller, A. S. (2001). Epidermal growth factor receptor glycosylation is required for ganglioside GM3 binding and GM3-mediated suppresion of activation. *Glycobiology, 11*(7), 515-522. doi:10.1093/glycob/11.7.515

Wu, G., Lu, Z. H., Kulkarni, N., & Ledeen, R. W. (2012). Deficiency of ganglioside GM1 correlates with Parkinson's disease in mice and humans. *J Neurosci Res, 90*(10), 1997-2008. doi:10.1002/jnr.23090

Yamashita, T., Hashiramoto, A., Haluzik, M., Mizukami, H., Beck, S., Norton, A., . . . Proia, R. L. (2003). Enhanced insulin sensitivity in mice lacking ganglioside GM3. *Proceedings of the National Academy of Sciences, 100*(6), 3445-3449. doi:10.1073/pnas.0635898100

Yamashita, T., Wu, Y.-P., Sandhoff, R., Werth, N., Mizukami, H., Ellis, J. M., . . . Proia, R. L. (2005). Interruption of ganglioside synthesis produces central nervous system degeneration and altered axon–glial interactions. *Proceedings of the National Academy of Sciences of the United States of America, 102*(8), 2725-2730. doi:10.1073/pnas.0407785102

Yanagisawa, K., Odaka, A., Suzuki, N., & Ihara, Y. (1995). GM1 ganglioside-bound amyloid beta-protein (A beta): a possible form of preamyloid in Alzheimer's disease. *Nat Med, 1*(10), 1062-1066. doi:10.1038/nm1095-1062

Yntema, C. L., & Hammond, W. S. (1954). The origin of intrinsic ganglia of trunk viscera from vagal neural crest in the chick embryo. *J Comp Neurol, 101*(2), 515-541. doi:10.1002/cne.901010212

Yoshikawa, M., Go, S., Suzuki, S.-i., Suzuki, A., Katori, Y., Morlet, T., . . . Strauss, K. A. (2015). Ganglioside GM3 is essential for the structural integrity and function of cochlear hair cells. *Human Molecular Genetics, 24*(10), 2796-2807.

Yoshikawa, M., Go, S., Takasaki, K., Kakazu, Y., Ohashi, M., Nagafuku, M., . . . Inokuchi, J.-i. (2009). Mice lacking ganglioside GM3 synthase exhibit complete hearing loss due to selective degeneration of the organ of Corti. *Proceedings of the National Academy of Sciences, 106*(23), 9483-9488. doi:10.1073/pnas.0903279106

Yu, R. K., Tsai, Y. T., Ariga, T., & Yanagisawa, M. (2011). Structures, biosynthesis, and functions of gangliosides--an overview. *J Oleo Sci, 60*(10), 537-544. doi:10.5650/jos.60.537

CHAPTER 2

ALLELE SPECIFIC ALTERATIONS IN GLYCOLIPID BIOSYNTHESIS AND CELL SIGNALING IN GM3 SYNTHASE DEFICIENCY

INTRODUCTION

GM3 Synthase Deficiency (GM3SD) is an autosomal recessive disorder characterized by severe early-onset seizures, intellectual disability, microcephaly, cochlear degeneration, hyper- and hypo-pigmented epidermis, among other more variable clinical presentations (Bowser et al., 2019). GM3SD is caused by pathogenic variants in the *ST3GAL5* gene that encodes the sialyltransferase known as GM3 synthase. ST3Gal5 catalyzes the production of the ganglioside GM3, which is the precursor for all complex a- b-, and c-type ganglioside glycosphingolipids (GSLs) in the human brain (**Figure 2.1**). Gangliosides account for >80% of brain glycans and have been implicated in neural-glial cell interactions, neuronal proliferation and survival, membrane microdomain formation, and cell signaling (Schnaar, Gerardy-Schahn, & Hildebrandt, 2014; Sipione, Monyror, Galleguillos, Steinberg, & Kadam, 2020). Based on targeted biosynthetic knockouts in mice and on accumulated data highlighting in vitro functions of gangliosides, the significant clinical consequences of GM3SD are not unexpected (Lloyd & Furukawa, 1998; Schnaar, 2016; Yamashita et al., 2003). Nonetheless, the functional impact of ganglioside-deficiency on cell differentiation, signaling, and survival have not been studied at the cellular level.

GM3SD has been associated with three allelic combinations identified in several cohorts of patients worldwide. Salt & Pepper Syndrome was described as one of the first

cohorts of GM3SD, affecting a single family in South Carolina, USA (Boccuto et al., 2013; Saul, Wilkes, & Stevenson, 1983). The allele associated with Salt & Pepper Syndrome, c.1063G>A (p.E355K), generates a mutant form of the enzyme lacking any enzymatic activity (Indellicato et al., 2019). A more prevalent allele was identified in the Amish population, c.862C>T (p.R288X), that generates a truncated and inactive enzyme (Indellicato et al., 2019; Simpson et al., 2004). The Amish allele is estimated to have a carrier frequency of 5-6% within this population, which translates to approximately 1 in 1200 births (Bowser et al., 2019). The R288X mutation has also been reported in French and Pakistani cohorts (Fragaki et al., 2013; Gordon-Lipkin et al., 2018). Additional mutations, compound heterozygous ST3GAL5 variants (p.G201R and p.C195S), were identified in two Korean siblings (J. S. Lee et al., 2016). All of the currently identified and characterized pathogenic ST3Gal5 alleles are null for enzymatic activity and share significant overlap in their clinical presentations (Li & Schnaar, 2018).

To investigate the molecular and neural-specific changes resulting from loss of GM3, we generated induced pluripotent stem cells (iPSCs) from Salt & Pepper (SP-ST3) and Amish cohort (A-ST3) fibroblasts and differentiated them to neural crest cells (NCCs). Here, we describe the impact of loss of GM3 on neural-specific glycosylation and cellular signaling responses during differentiation and highlight differential effects of the two GM3SD alleles. Human GM3SD cells provide a novel platform to investigate structure/function relationships that connect GSL diversity to cell signaling.

MATERIAL AND METHODS

Generation of induced pluripotent stem cells

Wild-type iPSCs (WT iPSC lines K3 and hIC3) were acquired from the Duncan Lab at Medical College of Wisconsin and were reprogrammed according to Si-Tayeb et al. (2010). Generation of SP-ST3 iPSCs (from ST3Gal5 c.1063G>A (p.E355K) patient fibroblasts) and A-ST3 iPSCs (from ST3GAL5 c.862C>T (p.R288X) patient fibroblasts) was performed using the CytoTune-iPS Sendai Reprogramming Kit (Invitrogen, # A13780) and the CytoTune-iPS 2.0 Sendai Reprogramming Kit (ThermoFisher, # A16517), respectively, using the manufacturer's conditions and as described by Menendez et al. (2013). For each resulting iPSC populations, between 5 and 20 subclones were picked, expanded, and cryopreserved. Each subclone was passaged at least 10 times to ensure removal of residual reprogramming virus before further characterization. Loss of virus was monitored by staining with anti-Sendai virus antibody (Invitrogen, cat #14649482).

iPSC clones were initially tested for pluripotency by assessing expression of pluripotency markers Oct4 (Cell Signaling, # C30A3), SSEA3/4 (Santa Cruz, # sc-21704), and Sox2 (R&D, # MAB2018), and by inducing differentiation into neuroectodermal cells (Cederquist et al. (2020)). For neuroectoderm differentiation, iPSCs were seeded at 260,000 cells/cm^2 in 6 wells in Essential 8 media on matrigel. The next day, the media was changed to Essential 6 containing 100 nM LDN, 10 μM SB and 2 μM XAV until day 2 when the media was changed to Essential 6 containing 100 nM LDN, 10 μM SB. Cells were fixed and stained for PAX6 (Biolegend, # 901301/B201255) and DAPI at day 4 and

exhibited efficient differentiation into the neuroectodermal lineage (**Supplement Figure 2.1 and 2.2**). All iPSCs were tested for mycoplasma every 2 weeks.

Neural Crest differentiation of iPSCs

Patient and WT iPSCs were differentiated to neural crest cells (NCCs) according to Menendez et al. (2013). Briefly, a 60 mm dish of ~90% confluent iPSCs was dissociated with Accutase (Innovative Cell Technologies, # AT104) and resuspended to a density of ~$9.2x10^4$ cells per cm^2 on Geltrex-coated plates in neural crest media composed of DMEM/F12 without glutamine (Cellgro), 2% Probumin, Life Science Grade (Millipore), 1x Non-essential amino acids (Cellgro), 2 mM GlutaGro (Cellgro), 1x Antibiotic/Antimycotic (Cellgro), 10 µg/ml Human Transferrin, (Athens Research & Tech),1x Trace elements A, B, & C (Cellgro), 50 µg/ml L-Ascorbic acid 2-phosphate sesqimagnesium salt hydrate (Sigma), 10 ng/ml Heregulin β (Peprotech), 200 ng/ml Long R3-IGF1 (SAFC/Sigma), 8 ng/ml bFGF (RnD Systems), 2 µM GSK3 inhibitor IX (BIO) (Tocris), and 20 µM SB431542 (Tocris). Media was changed daily, and at confluence, cells were split 1:4-1:6 (vol/vol) onto Geltrex-coated plates. Cells exhibited NCC morphology between day 7-10 of differentiation. By Day 15, cells tested positive by immunohistochemistry for NC markers HNK1 (Sigma Aldrich, # C6680) and p75 (Advanced Targeting Systems, # AB-N07), and negative for iPSC markers Oct4, SSEA3/4, and Sox2 (**Supplement Figure 2.2**). When assessing cell characteristics at specific time points of differentiation, cells were collected on specified days by scraping, spun down at 200 x g for 5 minutes, and frozen after aspiration of the supernatant.

Immunofluorescence staining

Antibodies and dilutions were as follows: Anti-HNK-1 antibody (Sigma Aldrich, Monoclonal Anti-HNK-1/N-CAM (CD57), # C6680), 1:200 dilution in 5% donkey serum in PBS-T; Anti-Sox2 antibody (R&D, # MAB2018), 1:200 dilution in 5% donkey serum in PBS-T; Anti-Oct4 antibody (Santa Cruz, # sc-8628), 1:200 dilution in 5% donkey serum in PBS-T; Anti-Pax6 antibody (Santa Cruz, # sc-81649), 1:200 dilution in 5% donkey serum in PBS-T; Anti-SSEA3/4 antibody (Santa Cruz, # sc-21704), 1:200 dilution in 5% donkey serum in PBS-T; Anti-p75 antibody (Advanced Targeting Systems, # AB-N07), 1:100 dilution in 5% donkey serum prepared in 0.05% Tween-20 in PBS. All antibodies were incubated overnight at 4ºC.

Extraction and preparation of GSLs

iPSCs or iPSC-derived NCCs were homogenized and extracted with organic solvents to precipitate proteins and recover GSLs as described previously (Aoki et al., 2007). Briefly, cell pellets were Dounce homogenized in 50% methanol on ice. Ice-cold water (W), methanol (M) and chloroform (C) were added to give final ratio of C:M:W::4:8:3. The suspension was then transferred into a Teflon-lined screw cap glass tube, agitated for 2 hours at room temperature, and clarified by centrifugation. The supernatant was saved and the resulting pellet was re-extracted three times with fresh 4:8:3 solvent. All supernatants were combined as the lipid extract. Lipid extracts were dried under a nitrogen stream and subjected to saponification to remove glycerophospholipids (Nimrichter et al., 2008). Saponification was completed using 0.5M KOH in methanol-water (95:5, M/W, v/v) at 37 ºC for 6 hours. Following neutralization with 10% acetic acid on ice, the solution was adjusted to 50% M/W, and then directly loaded onto a Sep-Pak

tC18 cartridge column (Waters, Sep-Pak Vac 1cc, 100 mg resin) equipped with a glass syringe (10 ml) that was previously washed with methanol and pre-equilibrated with distilled water. The initial flow-through from the loading was collected and re-applied to the column to enhance recovery. The loaded column was washed with a total of 30 ml of water. GSLs were then eluted with 3 ml of methanol and dried under a nitrogen stream. Free fatty acids resulting from saponification of glycerophospholipids were removed from the dried GSLs by wash with hexane and redrying under nitrogen. Initial analyses of WT and GM3SD GSLs were performed by thin-layer chromatography (TLC) using the following solvent systems: C/M/W (60:35:8) for neutral GSLs; C/M/0.2% $CaCl_2$ (55:45:10) for gangliosides; C/M/W (60:40:10) for GSL mixtures. Orcinol–H_2SO_4, resorcinol, Dittmer-Lester, and Ninhydrin reagents were used for the detection of sugar, sialic acid, phosphate, and primary amine groups, respectively.

Analysis of GSLs by mass spectrometry

Nanospray ionization mass spectrometry (NSI-MS) was performed on permethylated glycolipids. For MS of permethylated glycolipids in positive ion mode,~0.4 nmol of permethylated total glycolipids were dissolved in 50 µl of 1 mM sodium acetate in methanol/water (1:1) for infusion into a linear ion trap mass spectrometer (Orbi-LTQ; ThermoFisher Scientific) using a nanospray source at a syringe flow rate of 0.40 µl/min and capillary temperature set to 210 ^oC (Anumula & Taylor, 1992; Aoki et al., 2007; Nimrichter et al., 2008; Vukelić et al., 2005). The instrument was tuned with a mixture of permethylated standard neutral or ganglioside GSLs. For fragmentation by collision-induced dissociation (CID) in MS/MS and MS^n, a normalized collision energy of 30 – 35% was used.

Detection and relative quantification of the prevalence of individual glycolipids were accomplished using the total ion mapping (TIM) and neutral loss scan (NL scan) functionality of the Xcalibur software package version 2.0 (ThermoFisher Scientific) as previously described (Aoki et al., 2007). For TIM, the m/z range from 600 to 2000 was automatically scanned in successive 2.8 mass unit windows with a window-to-window overlap of 0.8 mass units, which allowed the naturally occurring isotopes of each glycolipid species to be summed into a single response, thereby increasing detection sensitivity. Most glycolipid components were identified as singly, doubly, and triply charged, sodiated species (M + Na) in positive mode. Peaks for all charge states were summed for quantification. Preliminary analysis demonstrated that the major fragment ions in CID MS/MS scans of glycolipid preparations correspond to the neutral loss of the ceramide moiety, leaving intact glycolipid oligosaccharide ions. Therefore, an MS workflow was defined for NL scans in which the highest intensity peak detected by full MS was subjected to CID fragmentation. If an MS/MS profile contained an ion with m/z equivalent to loss of the most prevalent ceramide moiety, MS^n fragmentation was initiated. Following this data-dependent acquisition, the workflow returned to full MS, excluded the parent ion just fragmented, and chose the peak of next highest intensity for the same MS/MS and MS^n analysis. Glycomics data and metadata were obtained and are presented in accordance with MIRAGE standards and the Athens Guidelines (Neelamegham et al., 2019; Varki et al., 2015; York et al., 2014).

Selective Exo-Enzymatic labeling of cell surface glycoproteins

Selective Exo-Enzymatic labelling (SEEL) and proteomics were conducted on WT and SP-ST3 iPSCs and NCCs according to Sun et al. (2016). Recombinant rat α-(2,6)-

sialyltransferase (ST6Gal1) was prepared as previously described in Meng et al. (2013). Biotinylated CMP-sialic acid was synthesized as described previously according to Sun et al. (2016). For labeling of cell-surface glycoproteins, approximately $9x10^7$ NCCs from WT and SP-ST3 lines were dissociated from the cell culture dish by manual trituration in Dulbecco's phosphate-buffered saline (DPBS) and the cells were transferred to Eppendorf tubes. The cells were pelleted and resuspended in serum-free DMEM with 42 µg/ml ST6Gal1, 34 µM CMP-Sia-C5-biotin, 13.3 µg/ml BSA, 13.3 µg/ml alkaline phosphatase and 2 µl *Arthrobacter ureafaciens* (AU) neuraminidase. Each reaction was in a final volume of 350 µl per tube and was incubated for 2 hours at 37 °C. After the SEEL labeling incubation, labeled cells were lysed in RIPA buffer and biotinylated proteins were captured by immunoprecipitation (IP) from 1 mg lysate using anti-biotin antibody. Precipitated proteins were resolved by SDS-PAGE, visualized by silver stain, and subjected to in-gel trypsinization as previously described Sun et al. (2016). The resulting peptides and glycopeptides were analyzed by LC-MS/MS using a Lumos Tribrid mass spectrometer (ThermoFisher). Proteins identified by peptides detected at <10 spectral matches (PSMs) were excluded from analysis, as were peptides identified as nuclear or cytosolic by GO annotation. Spectral counts for cell surface and secreted proteins that met threshold criteria were normalized to the spectral counts detected for human transferrin receptor in WT and SP-ST3 IPs. Data was processed for the enrichment of membrane raft and endosome associated proteins using R-Studio using the UniProtR analysis package (Soudy et al., 2020).

Identification of Receptor Tyrosine Kinases in WT and GM3SD cells

Protein (300 µg) was harvested from WT and SP-ST3 iPSC and NCC (d19 of differentiation) lysates using the manufacturer's protocol in Lysis buffer 17 (R&D Systems, # ARY001B). The cell lysates were mixed with HRP-conjugated pan-phosphotyrosine antibody and allowed to incubate for 1 hour on ice, rocking on the RTK array after blocking the array in Array Buffer 1 for 1 hour. Relative RTK phosphorylation/phosphorylation was subsequently detected by chemiluminescence.

Western blot analysis

Antibodies for detection of cell surface proteins and by western blot of cell lysates were used at 1:1000 dilution as provided and were from the following sources: anti-ErbB3 (Cell Signaling, HER3/ErbB3, D22C5 XP Rabbit mAb, # 12708); anti-EGFR (Santa Cruz, EGFR A-10, # sc-373746); anti-caspase 3 (Santa Cruz, caspase-3 Antibody 31A1067, # sc-56053); anti-sortilin (BD Biosciences, Neurotensin Receptor 3 antibody, # 612100); anti-Notch2 (DSHB, Notch2 C651.6DbHN); anti-ß-actin (Santa Cruz, Actin Antibody 2Q1055, # Sc-58673).

Protein concentrations in lysates were measured by BCA assay and aliquots containing 25 µg were reduced, alkylated, resolved by SDS-PAGE, and transferred to PVDF membranes for probing with primary antibodies. Primary antibody binding was detected by HRP-conjugated secondary antibodies and chemiluminescence. Densitometric quantification was performed with ImageJ Software. For developmental time courses that assessed the change in abundance of receptors across differentiation from iPSC to NCC, signal intensities for receptor proteins were normalized to ß-actin

(loading control) and then expressed as log_2-fold changes relative to the normalized signal intensity detected in iPSC (d0 of differentiation).

Pharmacologic inhibition of EGFR activation by erlotinib

WT and SP-ST3 iPSCs were differentiated to NCCs for 10 days. Beginning at d10, vehicle (DMSO) or erlotinib in vehicle (100 μM final concentration in media) was added to a media change and the cells were incubated for 24 or 48 additional hours prior to imaging or harvest for analysis. At harvest timepoints, the media was removed from the wells and centrifuged to collect floating cells. Adherent cells were also scraped and pelleted for collection. Adherent and floating cells were lysed prior to analysis by BCA assay and analyzed separately by western blot for the relative abundance of cleaved and uncleaved caspase 3.

RESULTS

GM3 synthase deficiency impacts neural-specific GSL biosynthesis

Significant changes in GSL synthesis are apparent when comparing the GSL profiles of iPSCs and NCCs by thin-layer chromatography, whether the cells are WT or GM3SD deficient (**Figure 2.2**). WT and GM3SD iPSC GSL profiles are dominated by hexosyl-, lactosyl-, globotriaosyl- and globotetraosylceramide (Gb3 and Gb4, respectively). The induced pluripotent stem cell marker SSEA-3, itself a GSL, was detected in WT and GM3SD iPSC GSL profiles, whether the iPSCs were of SP-ST3 or A-ST3 origin. Upon differentiation of WT iPSCs to NCCs, LacCer is efficiently shunted toward the production of GM3 and subsequently toward the more complex gangliosides GD3, GM1, and GD1. Differentiation of GM3SD iPSCs does not result in significant reduction of LacCer or in the appearance of GM3 in the GSL profile. Higher resolution analysis of GSL profiles by NSI-MS^n of their permethylated derivatives validates the lack of GM3 in GM3SD iPSCs and NCCs and the resulting lack of a-, b-, or c-series gangliosides **(Figures 2.3 and 2.4)**. The complex sialylated GSLs detected in GM3SD NCCs were detected only as o-series gangliosides, sialylated on the external Gal residue (GM1b, GD1c, see **Figure 2.1**). In the absence of GM3 and GM3-derived GSLs, the GM3SD NCCs retained high levels of LacCer and elevated levels of Gb3- and Gb4Cer compared to wildtype NCCs.

GSL ceramide moieties impart physicochemical characteristics that facilitate their incorporation into specialized membrane microdomains referred to as lipid rafts and as detergent resistant membranes (DRMs) (Brown & London, 1997). Heterogeneity in GSL ceramides derives from the chemical nature of the sphingosine base and its amide-linked

fatty acid. These components can differ based on degree of saturation, hydrocarbon chain length, and presence or absence of a sphingosine hydroxyl group. The heterogeneity of GSL ceramides is well resolved by NSI-MS^n, in which each GSL glycan head group is detected in association with a family of m/z values that reflect lipid differences (**Figures 2.3 and 2.4**). The ratio of longer chain fatty acid-containing ceramides to shorter chain-containing ceramides was higher for several of the GSLs in the GM3SD patients compared to wild-type, whether profiled in iPSCs or NCCs; LacCer and globoside Gb4 exhibit this difference particularly well. In addition, the ratio of long-chain to short-chain ceramides was even greater when comparing LacCer of SP-ST3 and A-ST3. For both iPSCs and NCCs, A-ST3 has a higher abundance of longer chain fatty acid-containing ceramide in LacCer than SP-ST3 and the C:24 form of fucosylated lactotetraosylceramide (Fuc-Lc4) is predominant in A-ST3 NCCs while the C:16 form is predominant in SP-ST3 NCCs.

While the GSL profiles of SP-ST3 and A-ST3 iPSCs and NCCs presented similar deficiencies in GM3 and GM3-derived GSLs, more subtle differences were detected between the cells derived from the two GM3SD patient alleles. The non-sialylated GSLs Gb4 and Lc4 were more abundant in SP-ST3 compared to A-ST3 iPSCs. However, upon differentiation to neural crest, Gb4 and Lc4 were increased in A-ST3 but decreased in SP-ST3 NCCs relative to the abundances of these GSLs in their respective iPSCs. Alternatively, sialylated gangliosides GM1b and GD1c, which are both products of ST3Gal2, were increased in SP-ST3 NCCs more than in A-ST3 NCCs. Additionally, extended LacNAc structures uncapped by sialic acid at their non-reducing termini were more abundant in A-ST3 NCCs, whereas extended LacNAc structures were more likely

to be sialylated in SP-ST3 NCCs (**Figure 2.5**). In general, SP-ST3 NCCs synthesized more alternatively sialylated gangliosides (GSLs sialylated by sialyltransferases other than ST3Gal5) compared to A-ST3 cells.

GM3 synthase deficiency alters the cell surface proteome

Glycosphingolipids partition into plasma membrane microdomains enriched in proteins, frequently GPI-anchored, that participate in adhesion, signaling, and adaptor functions. Since GM3 and several of its downstream GSL products have been demonstrated to be enriched in lipid rafts, we employed a robust cell-surface capture technology to assess whether altered ganglioside biosynthesis impacted the presentation of cell surface proteins (Brown & Rose, 1992; K. Sandhoff & Kolter, 2003; Simons & Ikonen, 1997). This technology, called Selective Exo-Enzymatic Labeling (SEEL), installs a biotin moiety onto the N-linked glycans of cell-surface glycoproteins, allowing their subsequent high-affinity capture for proteomic analysis (Mbua et al., 2013; Sun et al., 2016). Our SEEL-based proteomics first removed sialic acids from cell surface glycoproteins by sialidase digestion to unmask Gal residues for subsequent labeling with a recombinant sialyltransferase (ST6Gal1) that placed a biotin-modified sialic acid residue onto all N-linked glycans of membrane glycoproteins (other than high-Man glycans or glycans lacking Gal extension). Since the ST6Gal1 enzyme is highly membrane impermeant, enrichment for membrane proteins by SEEL far exceeds similar approaches that utilize various charged, low molecular weight, chemical cross-linkers to tag cell surface proteins. We applied SEEL to NCCs derived from WT and SP-ST3 iPSCs at day 35 of differentiation, captured the resulting biotinylated proteins by immunoprecipitation

with anti-biotin antibody, and resolved the precipitated proteins by SDS-PAGE (**Figure 2.7A**).

Subsequent in-gel tryptic digestion and LC-MS/MS analysis identified 120 proteins in WT and 160 proteins in SP-ST3 detected at > 10 spectral counts. GO analysis indicated that 96% of the identified proteins were cell surface or cell-surface associated and 4% were nuclear or cytoplasmic. Thus, our SEEL enrichment achieved a stringent enrichment of cell-surface glycoproteins and provided a pool of protein identities for further analysis. After filtering the total protein identifications to exclude the low-level of contamination with cytoplasmic and nuclear proteins, quantification by spectral counts demonstrated that 73% of the identified cell surface proteins were increased and 27% were decreased in abundance in SP-ST3 NCCs compared to WT NCCs (**Table 2.2**).

To assess the impact of GM3SD on the membrane raft and the endocytic pathway proteome, we filtered the identified membrane proteins for GO assignments to “membrane raft” (GO:0045121) and “endosome” (GO:0005768). Of the total protein identifications, 28% of WT (33 proteins) and 20% of SP-ST3 (32 proteins) were annotated with these GO classifications. Among the lipid raft protein identifications, 11 were increased and 3 were decreased in SP-ST3 compared to WT (**Figure 2.7B**). Among the raft-associated proteins, several adhesion receptors (CAD13, CAD15, ICAM1) were detected in WT NCCs that were absent or significantly reduced in SP-ST3 NCCs, while other adhesion receptors (DAG1, ITA1, CAD2) were enriched in SP-ST3 NCCs compared to WT. Several endocytic receptors, signaling, and adaptor proteins were increased in abundance at the plasma membrane in SP-ST3 NCCs in comparison to WT, while a

single signaling receptor, a receptor tyrosine kinase (ErbB2) and two peptide hormone processing enzymes (ECE1, LNPEP) were reduced.

A major component of raft/endosomal membrane trafficking, SORT1 (Number 153 in **Table 2.2**), was not detected on SP-ST3 NCCs by SEEL labeling. However, western blot analysis of whole cell lysates demonstrated that SP-ST3 cells express SORT1 at levels similar to WT NCCs (**Figure 2.6A**). Likewise, Notch2 (Number 154 in **Table 2.2**), a cell surface receptor important for NCC differentiation into peripheral neurons and other NC-derived cell types, was also not detected by cell surface labeling of SP-ST3 NCC cells, despite being expressed and detected in whole cell lysates (**Figure 2.6B**). The emergent landscape of the changes in the cell-surface proteome of ganglioside deficient NCCs is one in which the abundances of more lipid raft and endocytic proteins are increased compared to WT than decreased, while some proteins expected to be at the cell surface appear to be sequestered within an intracellular pool.

Receptor tyrosine kinases are impacted by GM3 synthase deficiency

To assess whether GM3SD impacts subsets of signaling pathways more than others, we queried receptor tyrosine kinases (RTK)s for changes in abundance or phosphorylation state. Whole-cell lysates prepared from WT and SP-ST3 iPSCs and NCCs (day 19 of differentiation) were incubated on RTK blots and the captured RTKs were subsequently visualized by probing with anti-phosphotyrosine antibody. The major RTKs detected in WT and GM3SD iPSC lysates were EGFR, ErbB3, InsR, and IGF-2, each of which were detected at approximately equal intensity comparing WT to GM3SD (**Figure 2.8A**). Upon differentiation to NCCs, ErbB3 intensity was increased, while EGFR, InsR, and IGF-1 intensities were not substantially modified (**Figure 2.8B**). However,

ErbB3 intensity was not detected in GM3SD NCC lysates. EGFR was similar to WT in GM3SD NCC lysates, while InsR and IGF-1 intensities were slightly decreased. Other changes in less abundant or less phosphorylated RTKs (ErbB4 and Axl) were also detected (**Figures 2.8A-B**). This sandwich capture/detection method reports changes in expression level and/or phosphorylation of the arrayed RTKs but cannot resolve changes in the relative phosphorylation state or relative protein expression of an individual RTK. Therefore, we separately assessed the expression levels of EGFR and ErbB3 receptors.

GM3 synthase deficiency uncouples EGFR and ErbB3 from neural crest differentiation

EGFR (ErbB1) possesses a glycan binding domain in its extracellular region that interacts with gangliosides, in particular GM3 (Miljan et al., 2002). EGFR also forms a heterodimer with ErbB3, thought to be a poor kinase by itself, to facilitate signaling in response to heregulin/neuregulin binding (Black, Longo, & Carroll, 2019; Shih, Telesco, & Radhakrishnan, 2011; Steinkamp et al., 2014). While the role of ganglioside binding to EGFR is incompletely understood, our GM3SD cells provide an opportunity to understand how gangliosides impact these important growth factor receptors across differentiation. To understand whether the differences in ErbB3 detected by RTK blot resulted from altered phosphorylation or from differential protein expression/stability, we probed cell lysates with phosphorylation-independent antibodies for EGFR and ErbB3 across the time course of differentiation from iPSCs to NCCs (**Figure 2.9**). As WT iPSCs differentiate toward NCCs, they exhibit a reproducible and complementary expression profile in which EGFR increases early in differentiation, almost 8-fold compared to iPSCs, and then decreases upon completion of the differentiation process (**Figure 2.9A and 2.9B**). ErbB3

mirrors the EGFR profile, exhibiting an early decrease in abundance that transforms into a greater than 8-fold increased abundance in NCCs compared to iPSCs. The evolving time course of EGFR and ErbB3 expression during differentiation from iPSCs to NCCs was highly reproducible across biological replicates, with the maximum variability occurring during times of greatest change in receptor expression (d0-d15 of differentiation).

We assessed EGFR and ErbB3 expression in SP-ST3 and A-ST3 cells across the same differentiation course from iPSCs to NCCs and compared the GM3SD cells to WT (**Figure 2.9C-F**). Both the SP-ST3 and A-ST3 cell populations exhibit significant variation from WT across all timepoints of differentiation. For EGFR, 67, 44, and 22% of SP-ST3 expression values lie 1, 2, or 3 standard deviations, respectively, above or below from the mean of the WT values at a similar time point. For EGFR in A-ST3, 75, 66, and 56% of the values lie 1, 2, or 3 standard deviations, respectively, above or below the WT mean. Thus, EGFR is more variable in A-ST3 than in SP-ST3. For ErbB3, 73, 51, and 35% of SP-ST3 expression values lie 1, 2, or 3 standard deviations, respectively, above or below the mean of the WT values at a similar time point. For ErbB3 in A-ST3, 69, 25, and 16% of the values lie 1, 2, or 3 standard deviations, respectively, above or below the WT mean. Thus, in contrast to EGFR expression, ErbB3 is more variable in SP-ST3 than in A-ST3. The deviation detected for EGFR and ErbB3 in the SP-ST3 cells is consistent with the RTK blot, namely ErbB3 affected more than EGFR at d19 of differentiation (see **Figure 2.8**). The broad scatter of EGFR and ErbB3 receptor expression across the differentiation course from iPSCs to NCCs in GM3SD, unlike in WT, demonstrates that RTK signaling

is highly variable across the deficient cell preparations and does not follow the regulated course of expression associated with differentiation to a neural fate.

EGFR/ErbB3-dependent cell survival is compromised in GM3 synthase deficiency cells

EGFR and ErbB3 signaling support cell survival (Holbro et al., 2003; Wee & Wang, 2017). Therefore, we investigated the impact of altered expression of these essential RTKs on cell survival by assessing the appearance of cleaved caspase 3, an apoptotic effector, in differentiating SP-ST3 cells (**Figure 2.10A**). While cleaved caspase 3 was detected in both WT and SP-ST3 iPSCs, it decreased to undetectable levels by the mid-point of differentiation of WT iPSCs to NCCs but remained present through d13 as SP-ST3 iPSCs differentiated to NCCs. This result suggested that GM3SD cells are intrinsically predisposed toward cell death. In order to test the hypothesis that ganglioside deficiency engenders enhanced sensitivity to cell death, we stressed the EGFR/ErbB3 signaling pathway by exposing cells to erlotinib, a pharmacologic inhibitor of EGFR signaling, at the midpoint (d11 – d13) of iPSC differentiation to NCCs (Rukazenkov et al., 2009). Exposure of WT cells to 100 μM erlotinib for 24 hours resulted in a 4-fold increase in the ratio of cleaved to full-length caspase 3, from 0.05 to 0.2. After 48 hours of exposure to erlotinib, this ratio increased to 0.3 in WT cells (**Figure 2.10B,C**). Consistent with the broad variance in the expression levels of EGFR and ErbB3 detected at the equivalent time points along the differentiation course (see **Figure 2.9C-F**), the magnitude of the cleaved caspase 3 response of SP-ST3 cells to erlotinib was also variable but was reproducibly higher when the cells were challenged with vehicle alone or when treated with 100 μM erlotinib for 24 hours. At 48 hours, cleaved caspase 3 levels in treated SP-

ST3 cells were closer to WT levels, but still significantly variable around the WT mean (**Figure 2.10C**). We observed that treatment with erlotinib resulted in significant detachment of presumably apoptotic cells from the surface of the tissue culture well (**Figure 2.10D**). GM3SD cells dissociated from the surface of the culture well to a much greater extent than WT cells and significant levels of cleaved caspase 3 was detected in association with the floating cell population (**Figure 2.10B**).

DISCUSSION

Complex gangliosides are essential components of the extracellular leaflet of the plasma membrane of neural cells. Subsets of these GSLs, including GM3, preferentially partition into lipid microdomains that are also enriched in cell-signaling receptors and adhesion molecules (Brown & Rose, 1992; K. Sandhoff & Kolter, 2003). Therefore, mutations in the biosynthetic enzymes responsible for generating GSLs would be expected to impart significant pathology. Surprisingly, however, the first reports of a mouse knockout of ST3Gal5 described a relatively normal animal capable of surviving and reproducing (Yamashita et al., 2003). Subsequent analysis demonstrated more subtle defects such as cochlear neuronal cell death, reduced male fertility, altered insulin receptor signaling, and skewed inflammatory responses (R. Sandhoff et al., 2005; Yamashita et al., 2003; Yamashita et al., 2005; Yoshikawa et al., 2015; Yoshikawa et al., 2009) . The relatively mild nature of the mouse ST3Gal5 knockout phenotype has been proposed to result from the ability of that organism to efficiently extend LacCer to longer ganglioseries cores which can be sialylated on their external Gal residues to generate o-series GSLs (**Figure 2.1**) capable of at least partially compensating for loss of the a-, b-, and c-series gangliosides (Collins et al., 1999) . Our previously published work on SP-ST3 patient fibroblasts and the results presented here for patient iPSCs and NCCs demonstrate that humans do not possess a similarly robust capacity to produce significant amounts of o-series gangliosides (Boccuto et al., 2013). In the absence of this alternative GSL biosynthetic capacity, patients with GM3SD manifest significant neurologic complications that are not currently well modeled in the mouse. Therefore, we took advantage of iPSC technology to investigate the cellular consequences of altered

ganglioside biosynthesis in regard to human neural cell differentiation in two different alleles of GM3SD.

Consistent with our previous report on SP-ST3 fibroblasts, GSL profiles of iPSCs and NCCs from both GM3SD alleles were devoid of GM3 and GM3-derived glycolipids (Boccuto et al., 2013; Simpson et al., 2004). This absence of a-, b-, and c-series gangliosides was mirrored by a significant increase in LacCer, the precursor to GM3, and smaller increases in globo- and lacto-series GSLs and GM1b. Thus, a hallmark of the human ST3Gal5 deficiency is a partial rerouting of LacCer into other biosynthetic pathways in association with significant precursor accumulation. The extent to which the clinical phenotypes of GM3SD arise from elevated LacCer, reduced complex ganglioside biosynthesis, or a combination of both remains unknown, but the iPSCs and NCCs we describe here provide a useful platform to investigate the contribution of GSL imbalance at the cellular level.

While the shifts in abundance of major GSLs were similar in the two GM3SD alleles, subtle variations distinguished the SP-ST3 and A-ST3 profiles. In particular, minor GSLs with extended LacNAc structures were differentially sialylated in NCCs. Non-sialylated extended LacNAc structures were more abundant in A-ST3 NCCs, whereas extended LacNAc structures were more likely to be sialylated in SP-ST3 NCCs. We also detected increases in the sialylated-GSLs GM1b and GD1c in SP-ST3 relative to A-ST3, and increased abundance of the asialo-GSLs Gb4/Lc4 in A-ST3 relative to SP-ST3. In general, SP-ST3 NCCs appear to synthesize more alternatively sialylated (non-ST3GAL5 derived) GSLs when compared to A-ST3. The relative abundance of these minor GSLs in NCCs derived from the two alleles indicate that they may utilize the donor substrate

CMP-NeuAc differently, suggesting a broader look at the total sialylated glycome and glycoproteome is warranted.

The molecular nature of the two ST3Gal5 mutations fails to suggest an obvious mechanism by which the two alleles might differentially impact alternative sialylation. The SP-ST3 allele preserves the L- and S-motifs characteristic of all sialyltransferases (STs), which both contribute to CMP-NeuAc and acceptor (LacCer for ST3Gal5) binding (Datta & Paulson, 1995; Rao et al., 2009). The A-ST3 is truncated between the L- and S-motifs and may, therefore, be less capable of binding CMP-NeuAc. Thus, it could be proposed that the A-ST3 allele might be able to sequester CMP-Sialic acid and therefore negatively impact donor availability for other sialyltransferases. However, the GSLs of SP-ST3-derived NCCs are more highly sialylated than the A-ST3-derived NCCs. Thus, the mechanism for the differential appearance of minor, alternatively sialylated GSLs most likely requires a more nuanced shift in the function and organization of the secretory pathway, perhaps in response to altered cell-surface signaling, or in the association of non-functional ST3Gal5 protein with other glycosyltransferases, which has been proposed to be a feature of GSL biosynthesis (Maccioni, Quiroga, & Ferrari, 2011; Maccioni, Quiroga, & Spessott, 2011).

Because membrane dynamics are important components of protein stability and signaling at the cell surface, we investigated whether differences in GSL composition impact cell surface proteins. Our SEEL-based capture of cell surface glycoproteins in WT and SP-ST3 NCCs identified substantial enrichment and loss of several membrane raft associated proteins whose GO functions indicate roles in cell adhesion, cell signaling, axon pathfinding, neurogenesis, nervous system development, and cell migration. While

gross changes in CNS architecture have not been associated with GM3SD, delayed neurologic development and reduced cranial growth are characteristic of the deficiency (Bowser et al., 2019). Thus, altered GSL composition appears to be accompanied by the cell surface presentation of an aberrant set of growth factor and cell adhesion proteins in GM3SD neural cells, which may generate cacophonous signaling and disrupted migration that contribute to defective developmental progression.

Although the molecular mechanisms by which specific GSLs contribute to the self-associative generation or stabilization of signaling microdomains remain elusive, direct interactions between GM3 and RTKs such as EGFR (ErbB1) have been functionally and structurally demonstrated (E. G. Bremer, Hakomori, Bowen-Pope, Raines, & Ross, 1984; Eric G Bremer, Schlessinger, & Hakomori, 1986; Laine & Hakomori, 1973; Miljan et al., 2002; Wang, Sun, & Paller, 2003). Weak, potentially disruptive binding between EGFR or other RTKs and the alternatively sialylated GSLs produced by GM3SD cells may significantly impact the efficiency of receptor partition into signaling domains, the efficacy of their signaling activity, or the extent of their existence at the cell surface (**Figure 2.11**). In support of the hypothesis that GM3SD cells are subject to dysregulated signaling, the expression of EGFR and ErbB3 in GM3SD cells departs significantly from WT across their differentiation from iPSCs to NCCs. The reproducible and phasic shift from early EGFR to later ErbB3 signaling seen in WT cells is degraded to an almost random pattern of receptor expression across differentiation in both GM3SD alleles. Importantly, dysregulation of ErbB3 in mice has been shown to be embryonic lethal and is associated with cardiac and peripheral nervous system defects, including loss of Schwann cell precursors (Black et al., 2019). EGFR-null mice are also embryonic lethal; however,

numerous conditional knockout studies have shown its role in a variety of developmental processes including innervation of the skin, abnormal valvular differentiation in the heart, and differentiation of the hair follicle and normal hair development (Barrick et al., 2009; T.-C. Lee & Threadgill, 2009; Maklad et al., 2009). In addition, a loss-of-function EGFR missense mutation identified in a young male patient presented with severe inflammatory skin, bowel, and lung disease and the patient died at 2.5 years of age from complications (Campbell et al., 2014).

Despite altered EGFR and ErbB3 expression, GM3SD cells as a population acquire expression of neural crest differentiation markers and concomitantly lose pluripotency markers as expected. However, the progression of differentiation of GM3SD cells is also associated with higher apoptosis than is observed in WT cells, which is significantly exacerbated by antagonism of EGFR signaling by erlotinib. Thus, at least within the neural crest lineage, significant dys-coordination of RTK protein expression as a result of altered GSL biosynthesis does not block the ability of a population of iPSCs to generate NCCs, but the progression comes at the cost of decreased cell viability. Whether other neural crest cell behaviors, such as motility, targeted migration, or capacity to differentiate into specific peripheral neuronal or endocrine fates, are similarly impacted by altered GSL biosynthesis is currently unknown but is a target of future studies using these cell populations.

While, in general, iPSCs derived from both GM3SD patient populations exhibited highly dys-coordinated EGFR and ErbB3 signaling during differentiation to NCCs, more subtle differences were detected between the two alleles. EGFR expression was more disrupted, and usually elevated, in A-ST3 cells, while ErbB3 expression was more

disrupted, and usually suppressed, in SP-ST3 cells. Additionally, ErbB3 expression in SP-ST3 cells was more frequently increased above WT than decreased, consistent with increased EGFR expression in this cell type and the propensity for EGFR to form heterodimers with ErbB3. It remains to be determined whether the subtle differences in the abundance of alternatively sialylated GSLs detected in the two cell populations might contribute to this differential skew in signaling receptor expression or stability. Perhaps the alternatively sialylated GSLs detected in the SP-ST3 cells are capable of facilitating dynamics of EGFR recycling/signaling/stability that are more similar to WT than are the non-sialylated GSLs detected in the A-ST3 cells. Additional lipid perturbation and targeted biosynthetic disruptions may provide more insight into the GSL and signaling receptor structure/function interactions that drive RTK expression/recycling/signaling. The ganglioside deficient cells we have generated provide a basis for adding-back or further restricting GSL biosynthesis to test specific structure/function hypotheses relevant for neural cell development and function.

Our results demonstrate the importance of investigating glycosylation changes associated with mutations in glycan biosynthetic enzymes in appropriate cell types. We previously described collateral changes in N-linked and O-linked glycosylation of glycoproteins expressed by SP-ST3 fibroblasts (Boccuto et al., 2013). Such collateral changes are of interest because ST3Gal5 does not act on glycans linked to proteins; it is absolutely GSL-specific. Thus, the matrix of regulatory processes that control cellular glycosylation are responsive to changes that span glycan classes. This phenomenon has recently been demonstrated very clearly in glyco-engineered human cell lines (Huang et al., 2021). The results presented here provide the first characterization of GSL

biosynthetic, cell signaling, and cellular survival changes associated with GM3SD. We have identified global changes in GSL biosynthesis and signaling receptor expression between GM3SD and WT cells, but also more subtle changes that differentiate GM3SD alleles. As additional cohorts of GM3SD patients are identified and become available for analysis at the cellular level, the results reported here will provide a framework for assessing functional differences that may provide insight into clinical phenotypes. The iPSC platform we have characterized also presents opportunities to assess the potency of molecular and small-molecule therapeutic interventions that might resolve these cellular phenotypes and impact broader glycomic consequences associated with GM3SD.

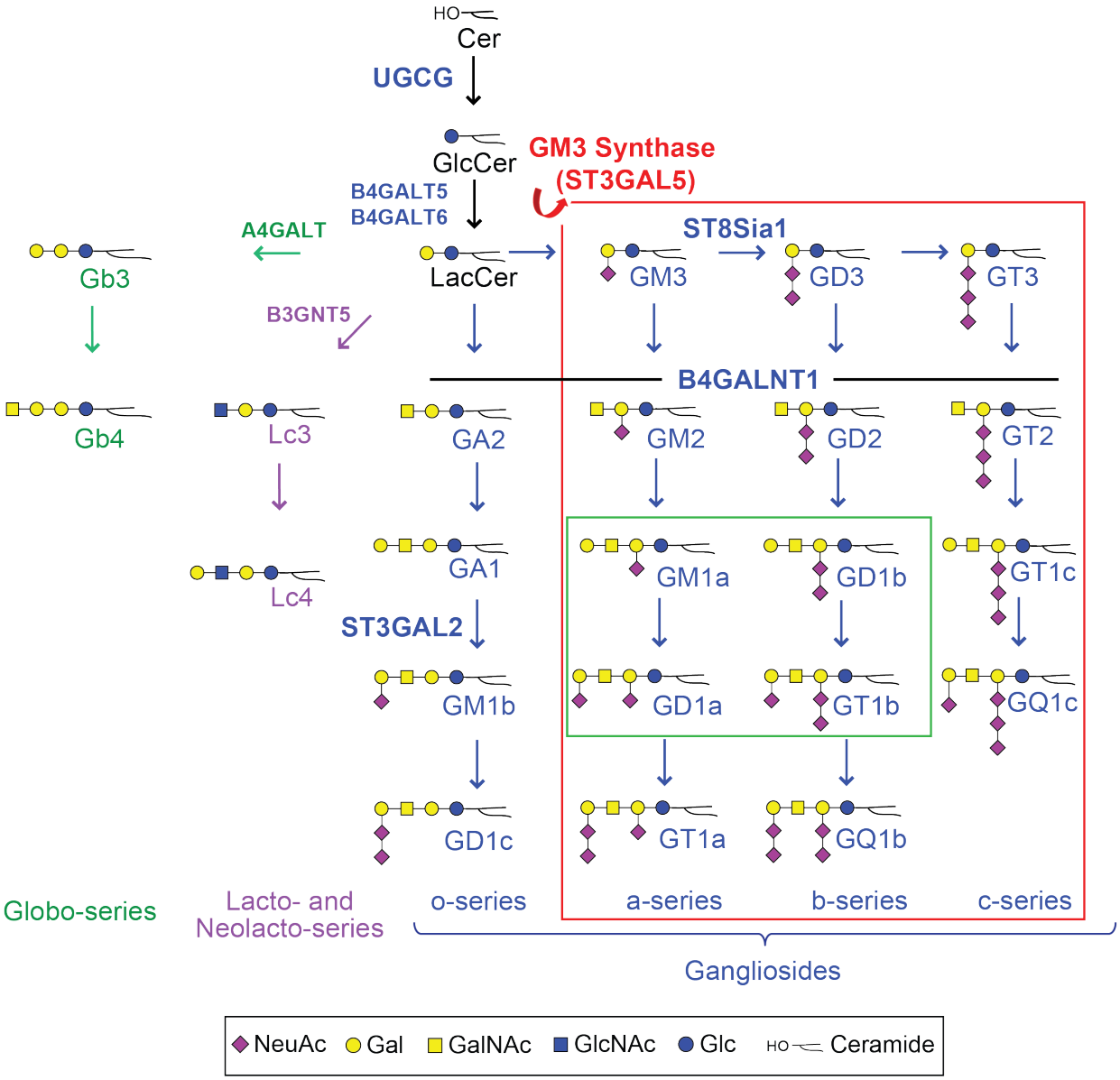

Figure 2.1. Glycosphingolipid biosynthetic pathways.
Ceramide (Cer) is glucosylated to form glucosylceramide (GlcCer), which can then be elongated with a galactose to form lactosylceramide (LacCer). LacCer can be further glycosylated to form a multitude of glycosphingolipids (GSLs) and gangliosides, or sialylated GSLs. Sialylation of LacCer by ST3Gal5, or GM3 Synthase, forms the ganglioside GM3. GM3 is the necessary precursor molecule to form all a-, b-, and c-series gangliosides (RED BOX). The four major gangliosides found in the brain are GM1a, GD1a, GD1b and GT1b (GREEN BOX).
Adapted from Boccuto et al. (2013).

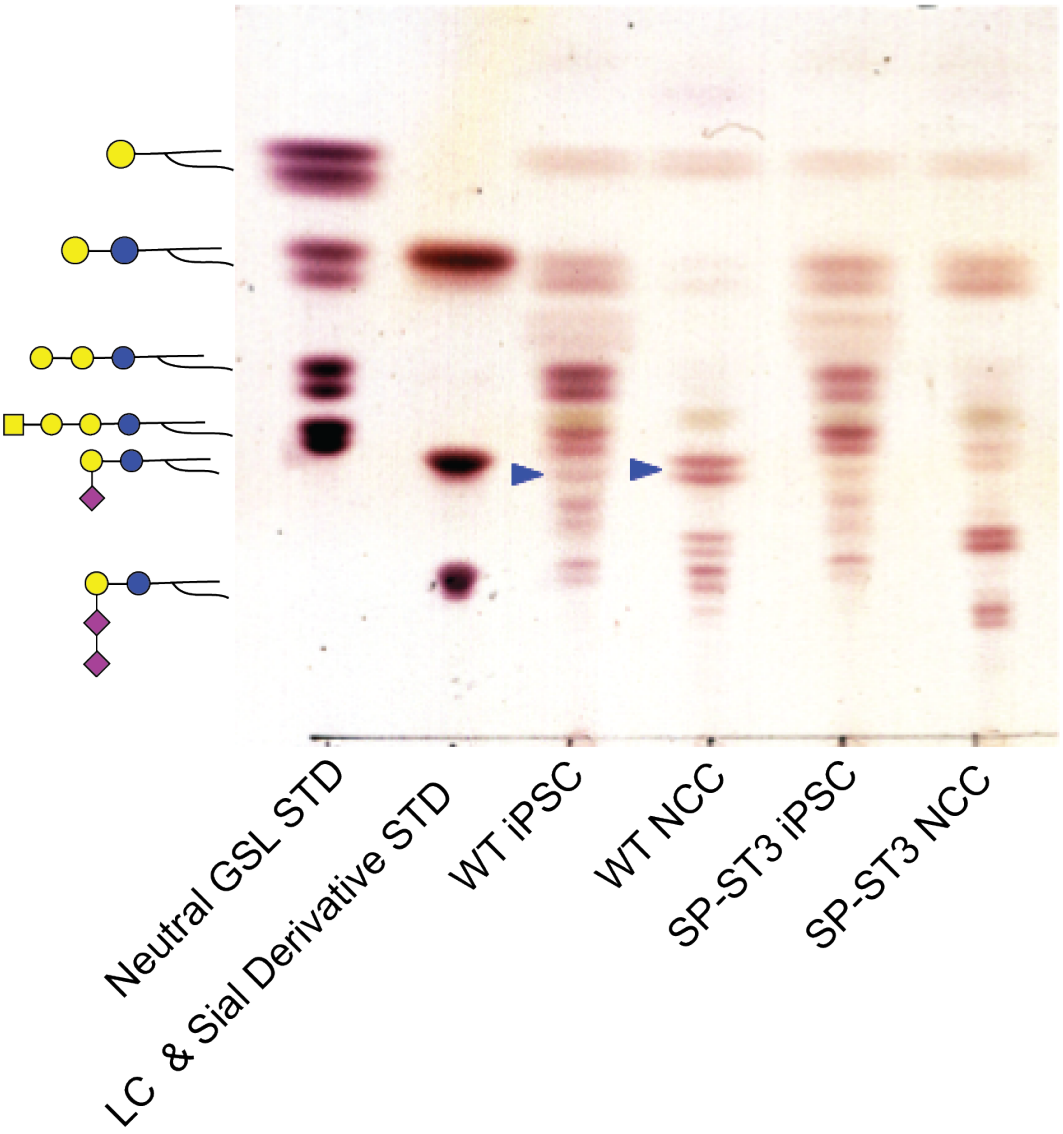

Figure 2.2 Differentiation of iPSCs to NCCs corresponds with Robust Changes in GSL Profiles

(A) Thin-layer chromatography analysis of glycolipid extracts from wildtype and SP-ST3 iPSCs and NCCs shows a loss of GM3 and GM3-derived gangliosides in SP-ST3 iPSCs and NCCs. Cartoon depictions of the GSL and ganglioside standards are shown on the left of the TLC plate. The blue arrows indicate GM3 in wildtype iPSC and NCC glycolipid extract.

Figure 2.3 iPSCs derived from GM3SD patients fail to produce GM3
Spectra from NSI-MS/MS^n analysis shows glycolipid profiles of wild-type (A), SP-ST3 (B), and A-ST3 (C) iPSCs. GM3 in wild type iPSCs is indicated by the red arrow. Lack of GM3 is indicated in SP-ST3 and A-ST3 spectra. These spectra primarily show neutral GSLs. The green arrow shows the differences in ceramide fatty acid composition in lactosylceramide (LacCer) in wild type, SP-ST3 and A-ST3 iPSCs.

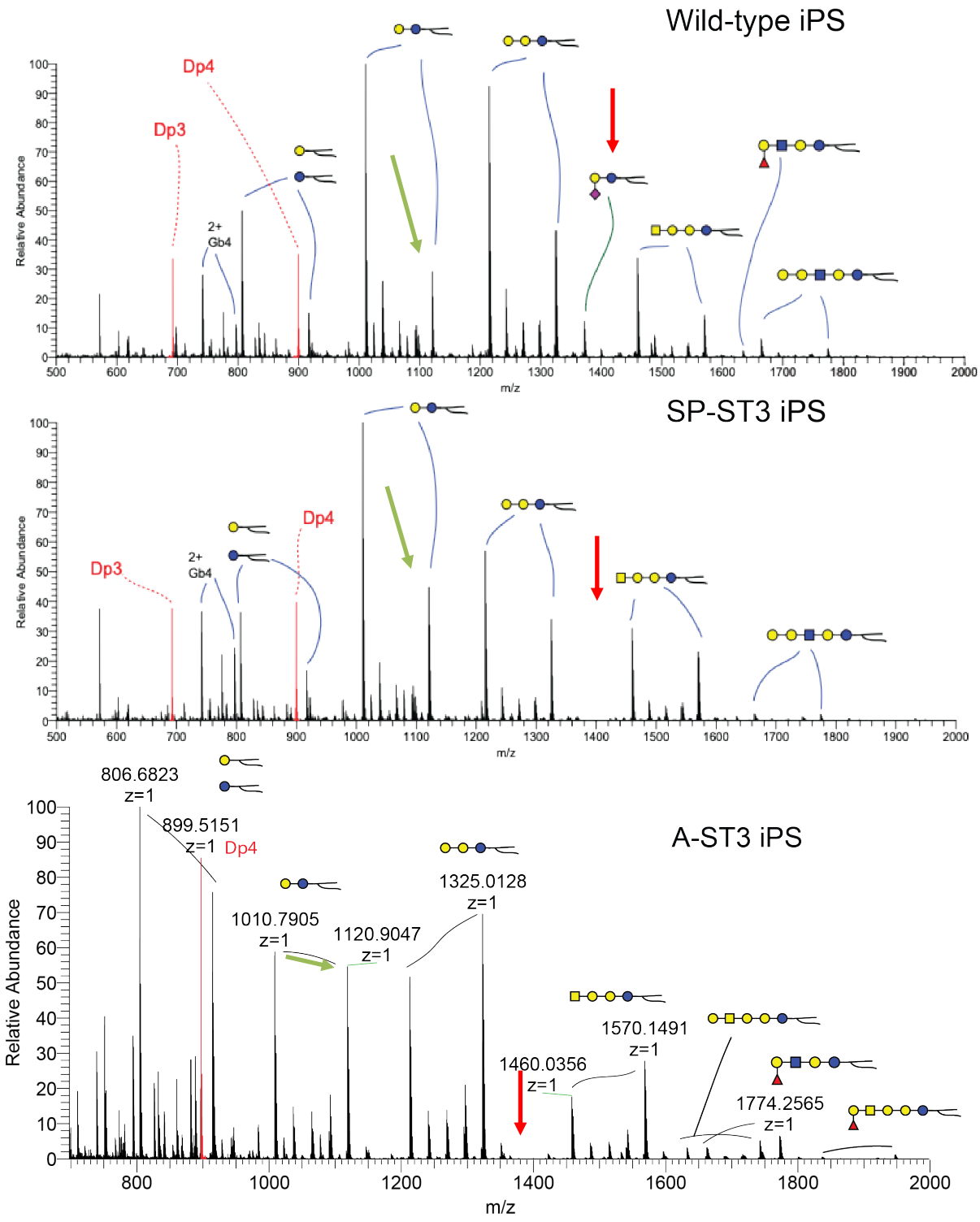
Wild-type iPS
Dp4
Dp3
2+
Gb4
Relative Abundance
m/z
SP-ST3 iPS
Dp4
Dp3
2+
Gb4
Relative Abundance
m/z
A-ST3 iPS
806.6823
z=1
899.5151
z=1
Dp4
1010.7905
z=1
1120.9047
z=1
1325.0128
z=1
1460.0356
z=1
1570.1491
z=1
1774.2565
z=1
Relative Abundance
m/z

Figure 2.4 GM3-deficient NCCs produce neutral GSLs and o-series gangliosides. Spectra from NSI-MS/MS^n analysis shows glycolipid profiles of wild-type (A), SP-ST3 (B), and A-ST3 (C) NCCs GM3 and GM3-derivatives in wild type NCCs are indicated by the red arrows. Lack of GM3 is indicated in SP-ST3 and A-ST3 spectra. SP-ST3 and A-ST3 spectra primarily show neutral GSLs and o-series gangliosides which are indicated by the blue arrows. The green arrow shows the differences in ceramide fatty acid composition in lactosylceramide (LacCer) in wild type, SP-ST3 and A-ST3 NCCs.

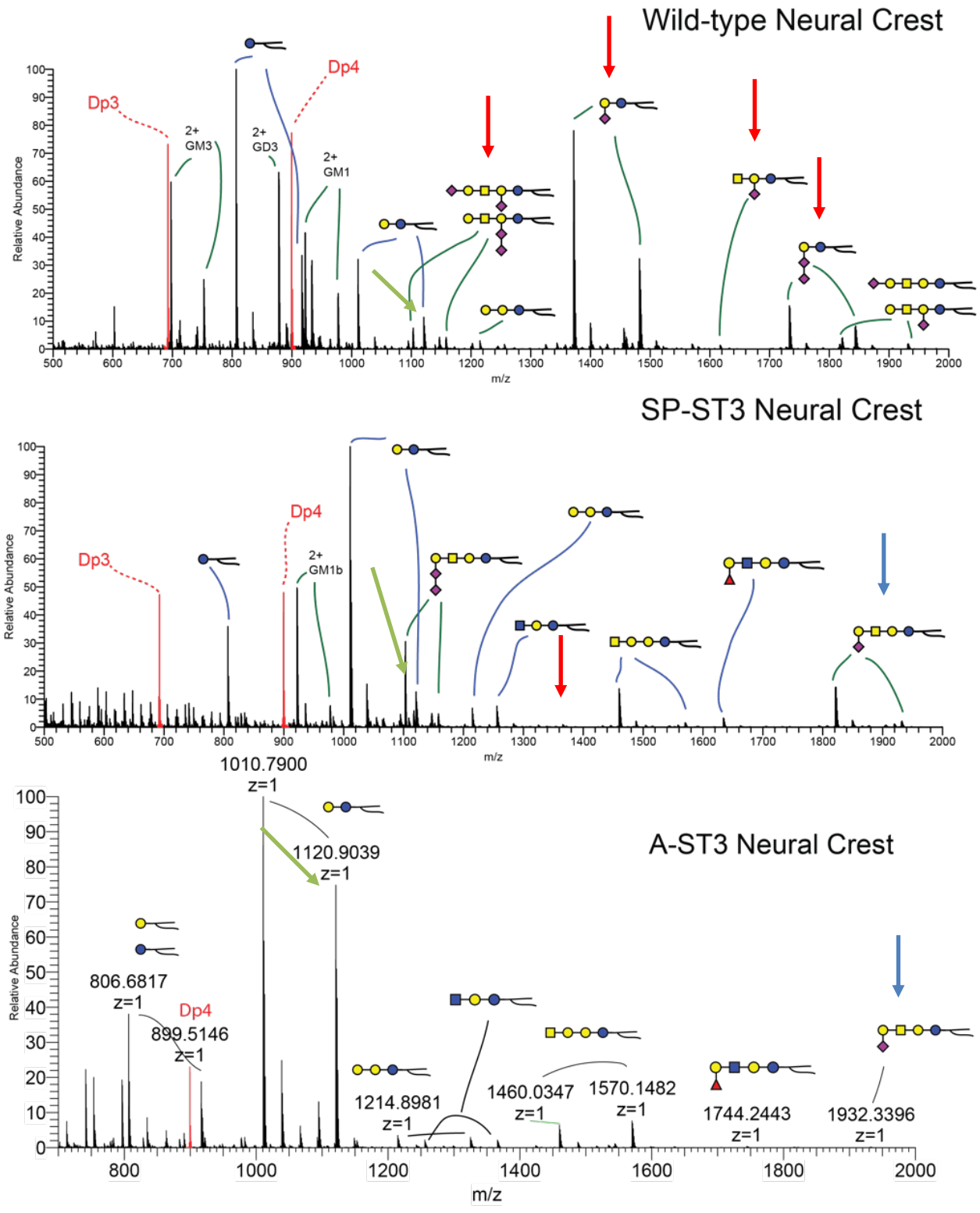
Wild-type Neural Crest
Dp3
Dp4
2+ GM3
2+ GD3
2+ GM1
Relative Abundance
m/z
SP-ST3 Neural Crest
Dp3
Dp4
2+ GM1b
Relative Abundance
m/z
1010.7900
z=1
A-ST3 Neural Crest
1120.9039
z=1
806.6817
z=1
Dp4
899.5146
z=1
1214.8981
z=1
1460.0347
z=1
1570.1482
z=1
1744.2443
z=1
1932.3396
z=1
Relative Abundance
m/z

Table 2.1 Quantification of glycosphingolipids from MS analysis of WT, SP-ST3, and A-ST3 iPSCs and NCCs

			LacCer	Gb3	Lc3	Gb4,Lc4	Fuc-Lc4	GM3	GM2	GM1a	GM1b	GD1a	GD1b	GD1c
iPS cells	Conc. pmol/1x10^6 cells	WT	277.8	326.1	0	173.8	14.1	33.6	0	2.6	6	0	0	0
		SP-ST3	230.4	158.9	0	188.4	0	0	0	0	20.6	0	0	0
		A-ST3	36.1	43.3	0.2	26.4	18.3	0	0	0	0.2	0	0	0
Neural Crest cells	Conc. pmol/1x10^6 cells	WT	35.1	3.1	1.2	8.3	0.0	145.6	1.0	4.6	41.8	63.7	0.8	5.5
		SP-ST3	138.4	7.9	9.0	25.6	8.5	0	0	0	92.1	0	0	44.5
		A-ST3	175.7	7.4	4.8	37.1	3.2	0	0	0	3.7	0	0	0.3

Figure 2.5 Differences in extended LacNAc structures and ganglioside sialic acid distribution in SP-ST3 and A-ST3 NCCs by MS.
(A) MS analysis shows peaks corresponding to a lower abundance extended N-Acetyllactosamine (LacNAc) structure, indicated by the red arrow, that is uncapped by sialic acid and is not found in SP-ST3. (B) MS analysis shows peaks corresponding to the sialylated form of the extended LacNAc structure seen in Figure 2.4A that is also indicated by the red arrow. Another red arrow also shows peaks that corresponds to GD1c, an o-series gangliosides not sialylated by GM3 synthase, in SP-ST3 that is bared detected in A-ST3.

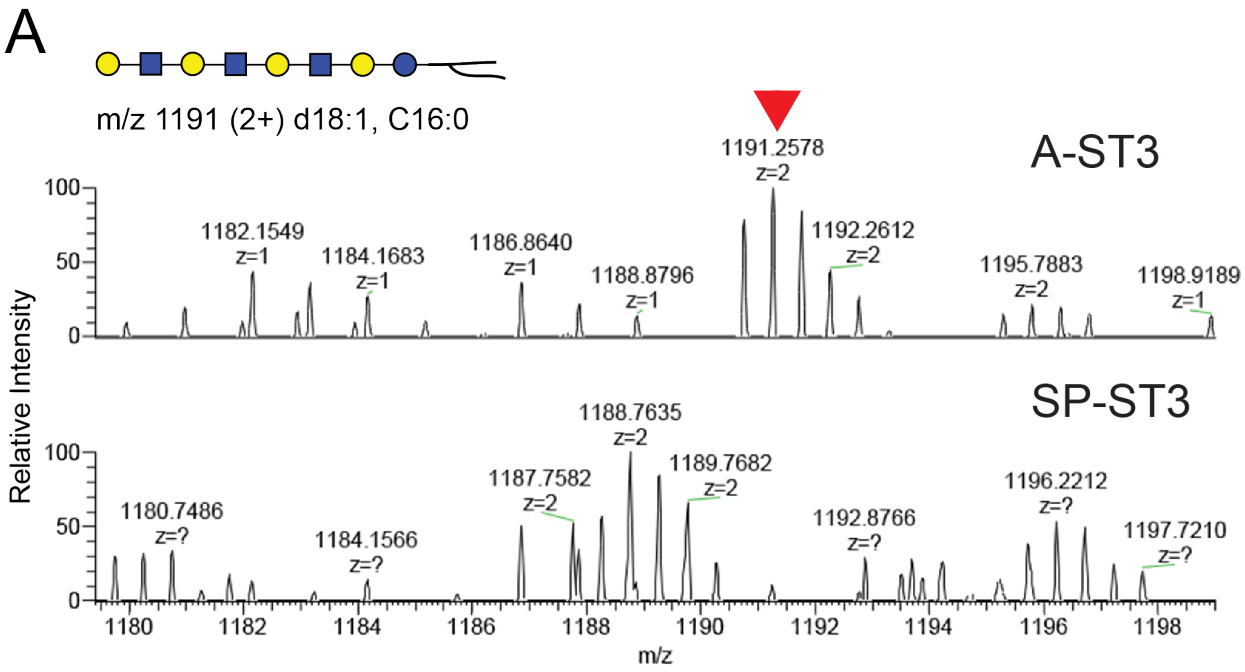
A
m/z 1191 (2+) d18:1, C16:0
A-ST3
1191.2578
z=2
1182.1549
z=1
1184.1683
z=1
1186.8640
z=1
1188.8796
z=1
1192.2612
z=2
1195.7883
z=2
1198.9189
z=1
SP-ST3
1188.7635
z=2
1187.7582
z=2
1189.7682
z=2
1180.7486
z=?
1184.1566
z=?
1192.8766
z=?
1196.2212
z=?
1197.7210
z=?
Relative Intensity
m/z

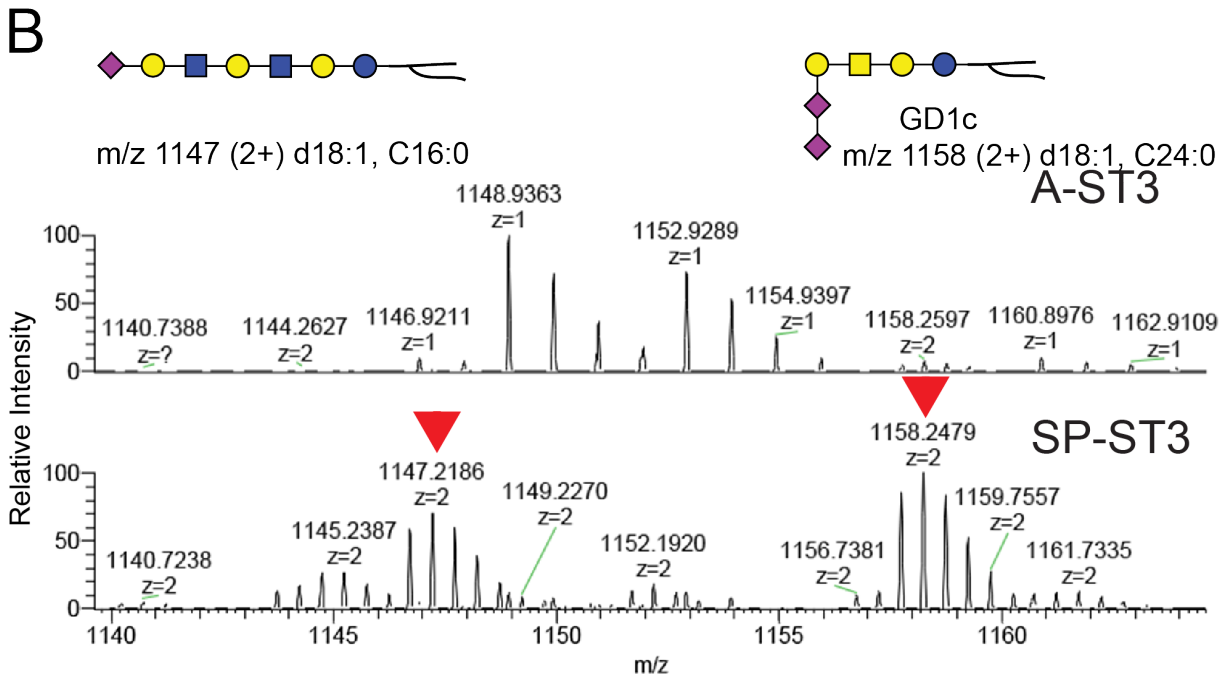
B
m/z 1147 (2+) d18:1, C16:0
GD1c
m/z 1158 (2+) d18:1, C24:0
A-ST3
1148.9363
z=1
1152.9289
z=1
1154.9397
z=1
1140.7388
z=?
1144.2627
z=2
1146.9211
z=1
1158.2597
z=2
1160.8976
z=1
1162.9109
z=1
SP-ST3
1158.2479
z=2
1147.2186
z=2
1149.2270
z=2
1159.7557
z=2
1145.2387
z=2
1152.1920
z=2
1156.7381
z=2
1161.7335
z=2
1140.7238
z=2
Relative Intensity
m/z

Table 2.2 Up- or downregulated SP-ST3 proteins from SEEL experiment

#	Accession	Description	WT	SP-ST3	Noramlized SP-ST3 (normalized to Transferrin Receptor)	Upregulated/ Downregulated in SP-ST3 (WT/SP-ST3)
1	P43146	Netrin receptor DCC OS=Homo	0	12	19.908	0
2	Q15303	Receptor tyrosine-protein kinas	0	17	28.203	0
3	P98164	Low-density lipoprotein recepto	0	19	31.521	0
4	Q96JQ0	Protocadherin-16 OS=Homo sa	0	17	28.203	0
5	P23471	Receptor-type tyrosine-protein p	0	45	74.655	0
6	P24821	Tenascin OS=Homo sapiens GN	0	66	109.494	0
7	Q9HAR2	Adhesion G protein-coupled rec	0	18	29.862	0
8	O00192	Armadillo repeat protein deleted	0	12	19.908	0
9	Q9Y6N8	Cadherin-10 OS=Homo sapiens	0	10	16.59	0
10	P55283	Cadherin-4 OS=Homo sapiens	0	18	29.862	0
11	P55285	Cadherin-6 OS=Homo sapiens	0	35	58.065	0
12	Q13740	CD166 antigen OS=Homo sapie	0	58	96.222	0
13	Q02246	Contactin-2 OS=Homo sapiens	0	15	24.885	0
14	P26232	Catenin alpha-2 OS=Homo sap	0	74	122.766	0
15	O60716	Catenin delta-1 OS=Homo sapi	0	35	58.065	0
16	P17813	Endoglin OS=Homo sapiens GN	0	20	33.18	0
17	P54762	Ephrin type-B receptor 1 OS=Ho	0	16	26.544	0
18	Q92945	Far upstream element-binding p	0	10	16.59	0
19	P07900	Heat shock protein HSP 90-alph	0	42	69.678	0
20	P26012	Integrin beta-8 OS=Homo sapie	0	10	16.59	0
21	Q8N2Q7	Neuroligin-1 OS=Homo sapiens	0	16	26.544	0
22	Q9NZ94	Neuroligin-3 OS=Homo sapiens	0	11	18.249	0
23	Q8N0W4	Neuroligin-4, X-linked OS=Hom	0	18	29.862	0
24	O95206	Protocadherin-8 OS=Homo sap	0	14	23.226	0
25	Q9NT68	Teneurin-2 OS=Homo sapiens (	0	22	36.498	0

26	O14786	Neuropilin-1 OS=Homo sapiens	1	25	41.475	0.02411091
27	Q5VU97	VWFA and cache domain-conta	1	24	39.816	0.025115531
28	Q6UXK5	Leucine-rich repeat neuronal pr	1	24	39.816	0.025115531
29	Q08174	Protocadherin-1 OS=Homo sap	1	24	39.816	0.025115531
30	P12111	Collagen alpha-3(VI) chain OS=	1	16	26.544	0.037673297
31	Q92859	Neogenin OS=Homo sapiens G	5	61	101.199	0.049407603
32	P48029	Sodium- and chloride-depende	2	14	23.226	0.086110394
33	O43157	Plexin-B1 OS=Homo sapiens G	6	36	59.724	0.100462126
34	Q6UXS9	Inactive caspase-12 OS=Homo	2	11	18.249	0.109595046
35	P35221	Catenin alpha-1 OS=Homo sap	4	21	34.839	0.114813858
36	Q96JA1	Leucine-rich repeats and immu	8	33	54.747	0.146126728
37	Q9BQE3	Tubulin alpha-1C chain OS=Ho	4	16	26.544	0.150693189
38	P01130	Low-density lipoprotein recepto	23	89	147.651	0.155772734
39	Q14114	Low-density lipoprotein recepto	4	14	23.226	0.172220787
40	Q86VP6	Cullin-associated NEDD8-disso	3	10	16.59	0.180831826
41	O75487	Glypican-4 OS=Homo sapiens G	4	13	21.567	0.18546854
42	Q24JP5	Transmembrane protein 132A O	12	37	61.383	0.195493866
43	O95490	Adhesion G protein-coupled rec	20	58	96.222	0.207852674
44	P10721	Mast/stem cell growth factor rec	7	20	33.18	0.210970464
45	P05186	Alkaline phosphatase, tissue-no	4	11	18.249	0.219190093
46	O00592	Podocalyxin OS=Homo sapiens	9	24	39.816	0.226039783
47	P18084	Integrin beta-5 OS=Homo sapie	7	18	29.862	0.234411627
48	P23468	Receptor-type tyrosine-protein p	19	39	64.701	0.293658522
49	O94813	Slit homolog 2 protein OS=Hom	10	20	33.18	0.301386377
50	P78504	Protein jagged-1 OS=Homo sap	10	19	31.521	0.317248818
51	O60462	Neuropilin-2 OS=Homo sapiens	25	46	76.314	0.327593888
52	P06756	Integrin alpha-V OS=Homo sap	44	80	132.72	0.331525015
53	Q9NT99	Leucine-rich repeat-containing	22	40	66.36	0.331525015
54	Q2VWP7	Protogenin OS=Homo sapiens G	13	23	38.157	0.340697644
55	P15586	N-acetylglucosamine-6-sulfatas	6	10	16.59	0.361663653

56	Q8NFZ4	Neuroligin-2 OS=Homo sapiens	15	25	41.475	0.361663653
57	Q9UHN6	Transmembrane protein 2 OS=H	54	90	149.31	0.361663653
58	Q14118	Dystroglycan OS=Homo sapien	27	44	72.996	0.369883281
59	A1A5C7	Solute carrier family 22 member	16	26	43.134	0.37093708
60	O43490	Prominin-1 OS=Homo sapiens (	33	52	86.268	0.382528864
61	P23229	Integrin alpha-6 OS=Homo sapi	45	68	112.812	0.398893735
62	P56199	Integrin alpha-1 OS=Homo sapi	8	12	19.908	0.401848503
63	P09619	Platelet-derived growth factor re	16	24	39.816	0.401848503
64	Q8NE01	Metal transporter CNNM3 OS=H	16	23	38.157	0.419320177
65	Q9H6X2	Anthrax toxin receptor 1 OS=Ho	10	14	23.226	0.430551968
66	Q9P273	Teneurin-3 OS=Homo sapiens (	44	60	99.54	0.442033353
67	Q96J84	Kin of IRRE-like protein 1 OS=H	77	105	174.195	0.442033353
68	P13591	Neural cell adhesion molecule 1	114	155	257.145	0.443329639
69	Q15375	Ephrin type-A receptor 7 OS=Ho	41	55	91.245	0.44933969
70	P55011	Solute carrier family 12 member	45	60	99.54	0.452079566
71	P11362	Fibroblast growth factor recepto	28	37	61.383	0.456152355
72	P19022	Cadherin-2 OS=Homo sapiens	25	30	49.77	0.502310629
73	P11279	Lysosome-associated membran	31	37	61.383	0.505025821
74	Q5IJ48	Protein crumbs homolog 2 OS=	42	49	81.291	0.516662361
75	P29317	Ephrin type-A receptor 2 OS=Ho	59	67	111.153	0.530799888
76	Q13683	Integrin alpha-7 OS=Homo sapi	24	27	44.793	0.535798004
77	P50993	Sodium/potassium-transporting	355	396	656.964	0.540364464
78	Q9H0X4	Protein FAM234A OS=Homo sa	19	21	34.839	0.545365826
79	Q8IWT6	Volume-regulated anion channe	31	34	56.406	0.549586923
80	P54760	Ephrin type-B receptor 4 OS=Ho	48	52	86.268	0.55640562
81	Q8IVU1	Immunoglobulin superfamily DC	42	45	74.655	0.562587904
82	Q92673	Sortilin-related receptor OS=Ho	51	53	87.927	0.580026613
83	O75051	Plexin-A2 OS=Homo sapiens G	32	33	54.747	0.584506914
84	Q13332	Receptor-type tyrosine-protein p	40	41	68.019	0.58807098
85	P29320	Ephrin type-A receptor 3 OS=Ho	21	21	34.839	0.602772755

86	P29323	Ephrin type-B receptor 2 OS=Hc	112	111	184.149	0.60820314
87	Q15758	Neutral amino acid transporter E	39	38	63.042	0.618635196
88	Q5ZPR3	CD276 antigen OS=Homo sapie	87	84	139.356	0.624300353
89	Q9Y666	Solute carrier family 12 member	21	20	33.18	0.632911392
90	Q7Z5N4	Protein sidekick-1 OS=Homo sa	21	20	33.18	0.632911392
91	P11047	Laminin subunit gamma-1 OS=I	17	16	26.544	0.640446052
92	A8MVW0	Protein FAM171A2 OS=Homo s	26	24	39.816	0.653003818
93	O94856	Neurofascin OS=Homo sapiens	12	11	18.249	0.657570278
94	O15031	Plexin-B2 OS=Homo sapiens G	176	158	262.122	0.671443068
95	P00533	Epidermal growth factor recepto	53	45	74.655	0.709932356
96	Q9HCM3	UPF0606 protein KIAA1549 OS	13	11	18.249	0.712367801
97	P08648	Integrin alpha-5 OS=Homo sapi	71	59	97.881	0.725370603
98	P13637	Sodium/potassium-transporting	460	381	632.079	0.727757132
99	P05556	Integrin beta-1 OS=Homo sapie	199	160	265.44	0.749698614
100	Q07954	Prolow-density lipoprotein recep	188	150	248.85	0.755475186
101	Q9UIW2	Plexin-A1 OS=Homo sapiens G	83	64	106.176	0.781720916
102	Q92692	Nectin-2 OS=Homo sapiens GN	13	10	16.59	0.783604581
103	P54764	Ephrin type-A receptor 4 OS=Hc	42	32	53.088	0.791139241
104	P43121	Cell surface glycoprotein MUC1	140	105	174.195	0.803697006
105	P18433	Receptor-type tyrosine-protein p	30	22	36.498	0.821962847
106	Q12913	Receptor-type tyrosine-protein p	11	8	13.272	0.828812538
107	P11717	Cation-independent mannose-6	131	95	157.605	0.831191904
108	Q06418	Tyrosine-protein kinase recepto	18	13	21.567	0.83460843
109	O75976	Carboxypeptidase D OS=Homo	17	12	19.908	0.853928069
110	Q9UBG0	C-type mannose receptor 2 OS=	61	43	71.337	0.855096233
111	Q92542	Nicastrin OS=Homo sapiens GN	43	30	49.77	0.863974282
112	P08195	4F2 cell-surface antigen heavy	165	113	187.467	0.880154907
113	P51805	Plexin-A3 OS=Homo sapiens G	34	23	38.157	0.891055376
114	P54753	Ephrin type-B receptor 3 OS=Hc	24	16	26.544	0.904159132
115	Q92823	Neuronal cell adhesion molecu	131	87	144.333	0.907623343

116	Q9C0C4	Semaphorin-4C OS=Homo sap	37	24	39.816	0.929274663
117	Q8NB49	Phospholipid-transporting ATPa	19	12	19.908	0.954390195
118	P10586	Receptor-type tyrosine-protein p	75	47	77.973	0.961871417
119	Q15043	Zinc transporter ZIP14 OS=Hom	16	10	16.59	0.964436407
120	O75054	Immunoglobulin superfamily me	67	41	68.019	0.985018892
121	P02786	Transferrin receptor protein 1 O	307	185	306.915	1.00027695
122	Q9Y289	Sodium-dependent multivitamin	10	6	9.954	1.004621258
123	Q96GP6	Scavenger receptor class F mer	36	20	33.18	1.084990958
124	Q5KU26	Collectin-12 OS=Homo sapiens	120	64	106.176	1.130198915
125	Q9BY67	Cell adhesion molecule 1 OS=H	44	23	38.157	1.153130487
126	Q58EX2	Protein sidekick-2 OS=Homo sa	152	78	129.402	1.174634086
127	Q9P2B2	Prostaglandin F2 receptor nega	43	22	36.498	1.178146748
128	O75882	Attractin OS=Homo sapiens GN	16	8	13.272	1.205545509
129	P02787	Serotransferrin OS=Homo sapie	173	86	142.674	1.212554495
130	O15439	Multidrug resistance-associated	15	7	11.613	1.291655903
131	P08069	Insulin-like growth factor 1 recep	43	20	33.18	1.295961423
132	Q96F46	Interleukin-17 receptor A OS=H	11	5	8.295	1.32610006
133	P32004	Neural cell adhesion molecule L	66	29	48.111	1.371827649
134	Q93050	V-type proton ATPase 116 kDa	32	14	23.226	1.377766296
135	P42892	Endothelin-converting enzyme	28	12	19.908	1.406469761
136	Q9UIQ6	Leucyl-cystinyl aminopeptidase	119	46	76.314	1.559346909
137	Q6N022	Teneurin-4 OS=Homo sapiens (	95	35	58.065	1.636097477
138	Q8TDY8	Immunoglobulin superfamily DC	22	8	13.272	1.657625075
139	Q13444	Disintegrin and metalloproteina	16	5	8.295	1.928872815
140	P23470	Receptor-type tyrosine-protein p	13	4	6.636	1.959011453
141	P33527	Multidrug resistance-associated	43	13	21.567	1.993786804
142	P50895	Basal cell adhesion molecule O	131	39	64.701	2.024698227
143	Q6UVK1	Chondroitin sulfate proteoglyca	140	38	63.042	2.220741728
144	Q9Y6N7	Roundabout homolog 1 OS=Ho	106	28	46.452	2.281925428
145	Q14126	Desmoglein-2 OS=Homo sapie	25	6	9.954	2.511553144

146	Q9H3T3	Semaphorin-6B OS=Homo sapi	17	4	6.636	2.561784207
147	P04626	Receptor tyrosine-protein kinas	32	7	11.613	2.755532593
148	P26006	Integrin alpha-3 OS=Homo sapi	40	8	13.272	3.013863773
149	P25391	Laminin subunit alpha-1 OS=Hc	12	2	3.318	3.616636528
150	Q14542	Equilibrative nucleoside transpc	13	2	3.318	3.918022905
151	P05362	Intercellular adhesion molecule	63	8	13.272	4.746835443
152	P53708	Integrin alpha-8 OS=Homo sapi	28	0	0	Inf
153	Q04721	Neurogenic locus notch homolc	40	0	0	Inf
154	Q99523	Sortilin OS=Homo sapiens GN=	55	0	0	Inf
155	P20594	Atrial natriuretic peptide recepto	20	0	0	Inf
156	Q9NY47	Voltage-dependent calcium cha	11	0	0	Inf
157	P55290	Cadherin-13 OS=Homo sapiens	12	0	0	Inf
158	P55291	Cadherin-15 OS=Homo sapiens	17	0	0	Inf
159	P54756	Ephrin type-A receptor 5 OS=Hc	48	0	0	Inf
160	Q13797	Integrin alpha-9 OS=Homo sapi	22	0	0	Inf
161	P08581	Hepatocyte growth factor recept	11	0	0	Inf
162	O95980	Reversion-inducing cysteine-ric	10	0	0	Inf
163	Q01973	Inactive tyrosine-protein kinase	25	0	0	Inf
164	Q6AZY7	Scavenger receptor class A mer	12	0	0	Inf
165	O60503	Adenylate cyclase type 9 OS=H	10	0	0	Inf

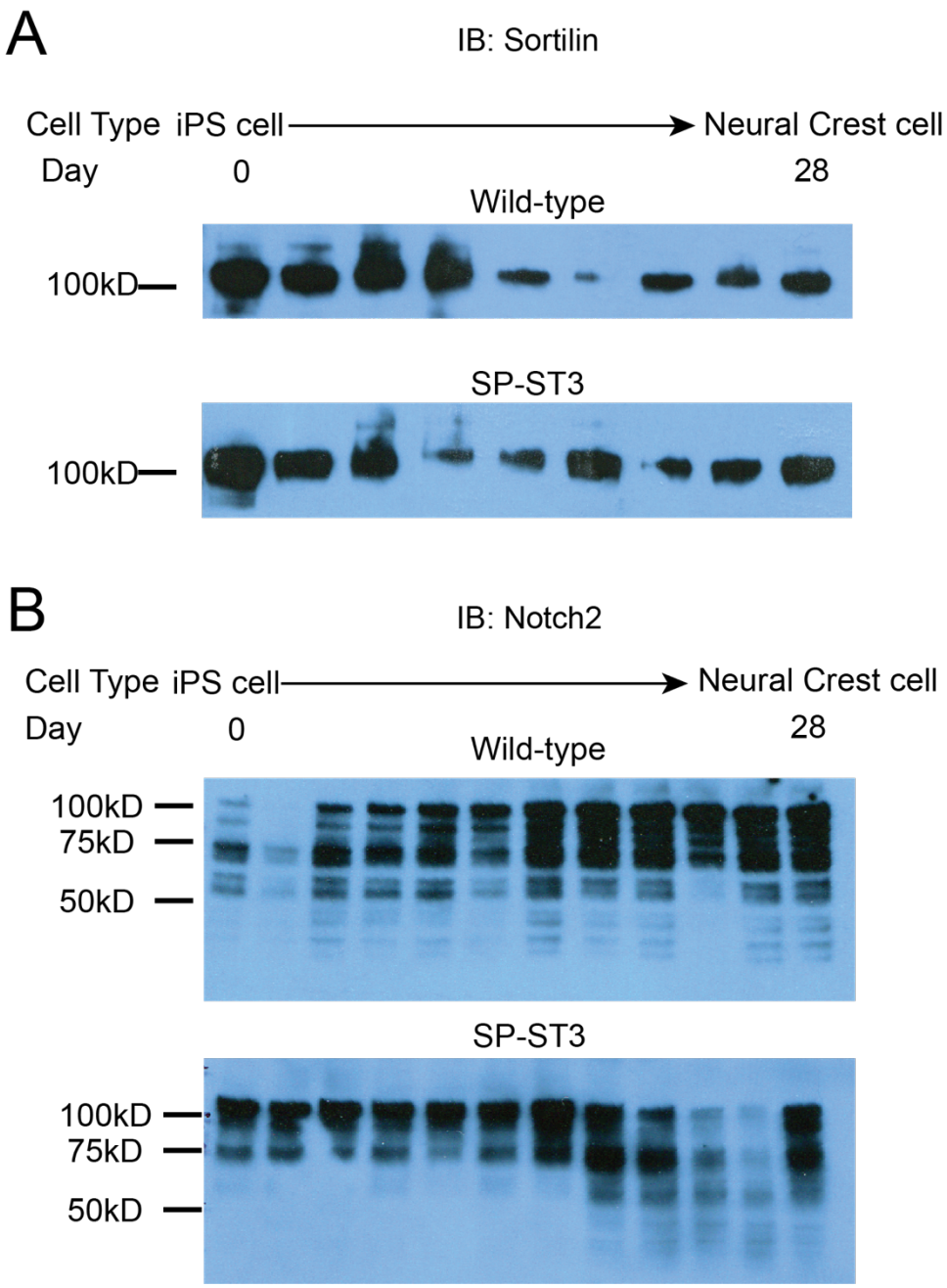

Figure 2.6 Notch2 and Sortilin expression in WT and SP-ST3 cells during differentiation.
Western blot analysis shows that the proteins Sortilin (A) and Notch2 (2) are expressed throughout NCC differentiation in both WT and SP-ST3 cells, although Notch2 appears to show a different pattern of expression. 25ug of protein used for each lane. However, peptides from these proteins were only identified in WT cell during our SEEL experiment (see Table 2.2)

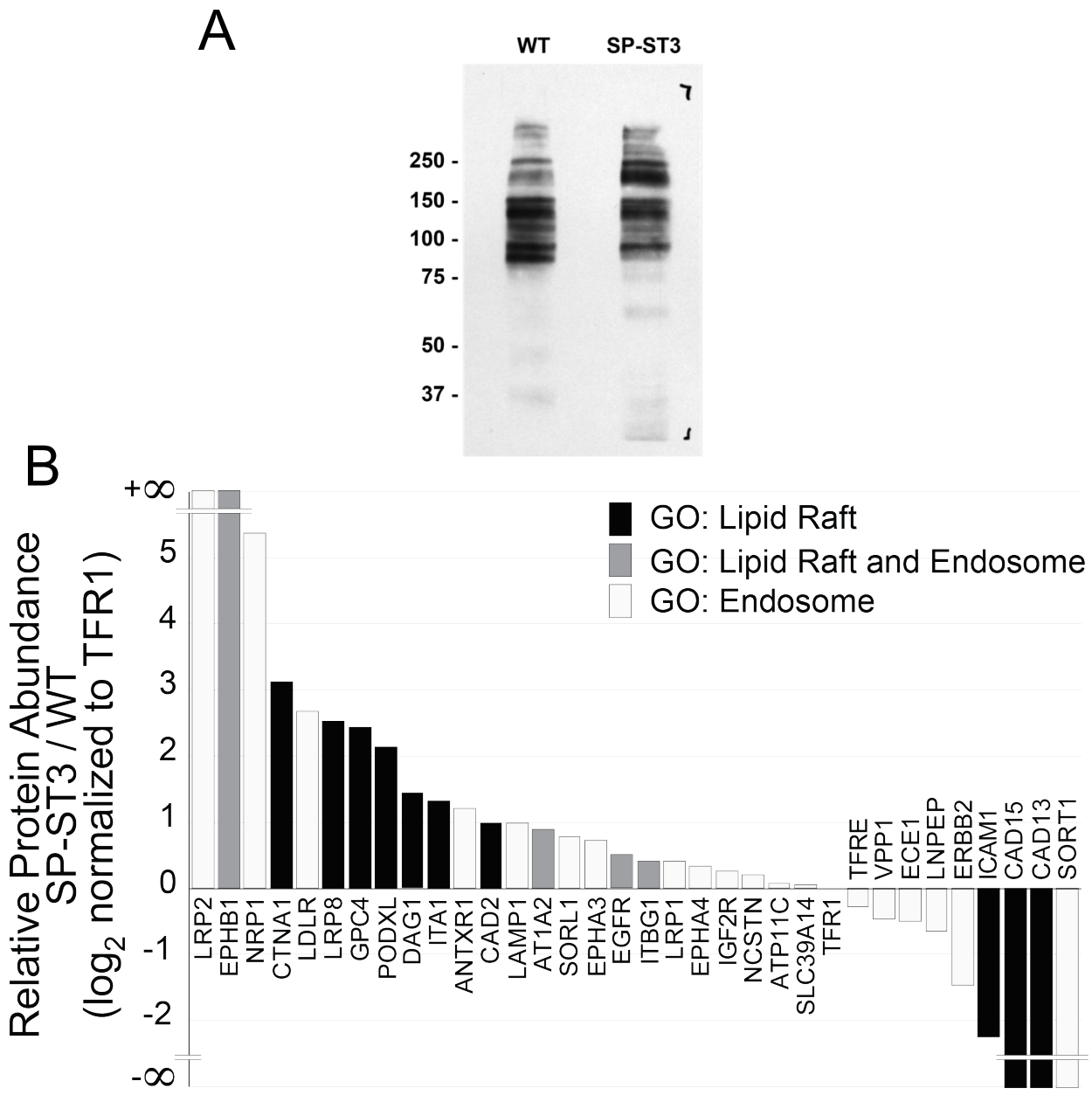

Figure 2.7 Cell surface protein abundance is altered in GM3SD cells. NC cells differentiated from WT or SP-ST3 iPSCs were subjected to selective-exoenzymatic labeling (SEEL) to install a biotin moiety specifically on cell surface glycoproteins. (**A**) Labeled proteins were resolved by SDS-PAGE and probed by western blot with anti-biotin antibody, revealing the presence of changes in the abundance of membrane proteins. (**B**) Gel-resolved proteins were harvested by in-gel digestion with trypsin and identified by LC-MS/MS. Identified proteins assigned to the indicated GO categories were compared to assess the integrity of lipid rafts and the endosomal pathway. Of the 35 proteins in these GO categories that were detected above threshold of confidence in either cell type, more were increased than decreased, with 11 raft proteins increased and 3 decreased in GM3SD cells.

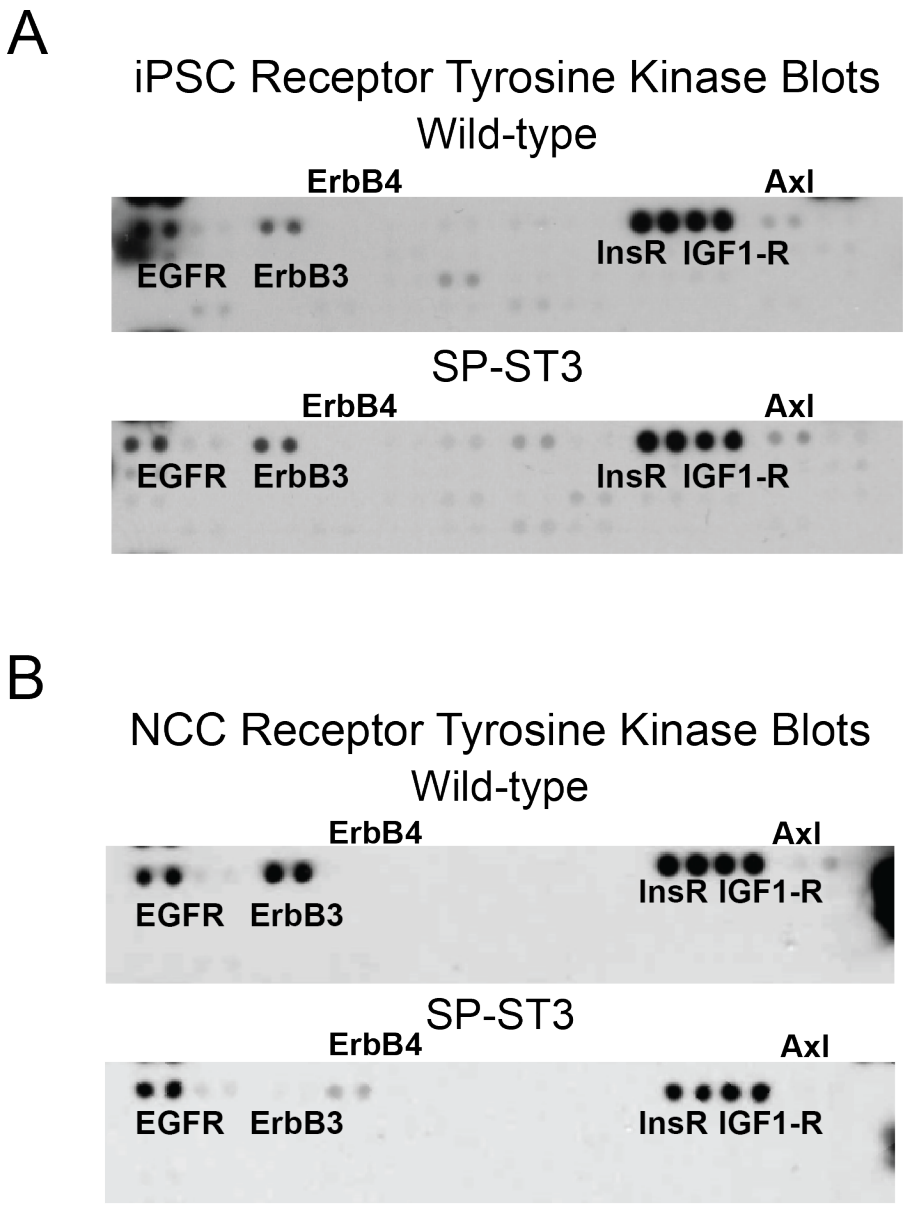

Figure 2.8 Expression/phosphorylation of receptor tyrosine kinases in WT and GM3SD cells. Blots prepared with anti-RTK antibodies were overlayed with whole cell lysates from (**A**) iPSCs or (**B**) NCCs harvested at d19 of differentiation. Bound RTKs were then detected by sandwich with anti-phosphotyrosine antibody. Signal associated with ErbB3 increases in WT cells upon differentiation to NCCs, but ErbB3 is reduced in SP-ST3 NCCs. Other more subtle changes in RTK detection were also evident in SP-ST3 NCCs compared to WT.

Figure 2.9 Dynamics of EGFR and ErbB3 expression during neural crest differentiation. Protein-specific, not phospho-specific, antibodies against EGFR and ErbB3 were used to quantify receptor expression in WT and GM3SD cells across full time courses of differentiation from iPSCs to NCCs (n=3 independent differentiations for each cell type). Receptor abundance was normalized to actin (loading control) and then expressed as the $\log_2$ ratio of the abundance detected at the indicated day of differentiation relative to the abundance detected at d0 (iPSC) for the same differentiation course. (**A**) As WT cells differentiate to NCCs, EGFR and ErbB3 expression mirror each other, with EGFR expression high at early to mid-time points and ErbB3 expression high as cells assume the full NCC fate. For simplicity of presentation and to provide a baseline reference for comparison with GM3SD cells, WT values were combined into bins that span 4 days of differentiation (mean±SEM, n=4-6 determinations for each bin, total of 30 data points for each receptor). (**B**) Representative EGFR and ErbB3 western blots from one differentiation course of WT cells. (**C**) Individual time points for EGFR abundance are plotted for three independent differentiations of GM3SD cells (n=27 data points for SP-ST3, n=32 data points for A-ST3); WT EGFR profile is reproduced from panel A for reference. (**D**) Representative EGFR western blots from one differentiation course of SP-ST3 and A-ST3 cells. (**E**) Individual time points for ErbB3 abundance are plotted for three independent differentiations of GM3SD cells (n=37 data points for SP-ST3, n=32 data points for A-ST3); WT ErbB3 profile is reproduced from panel A for reference. (**F**) Representative ErbB3 western blots from one differentiation course of SP-ST3 and A-ST3 cells.

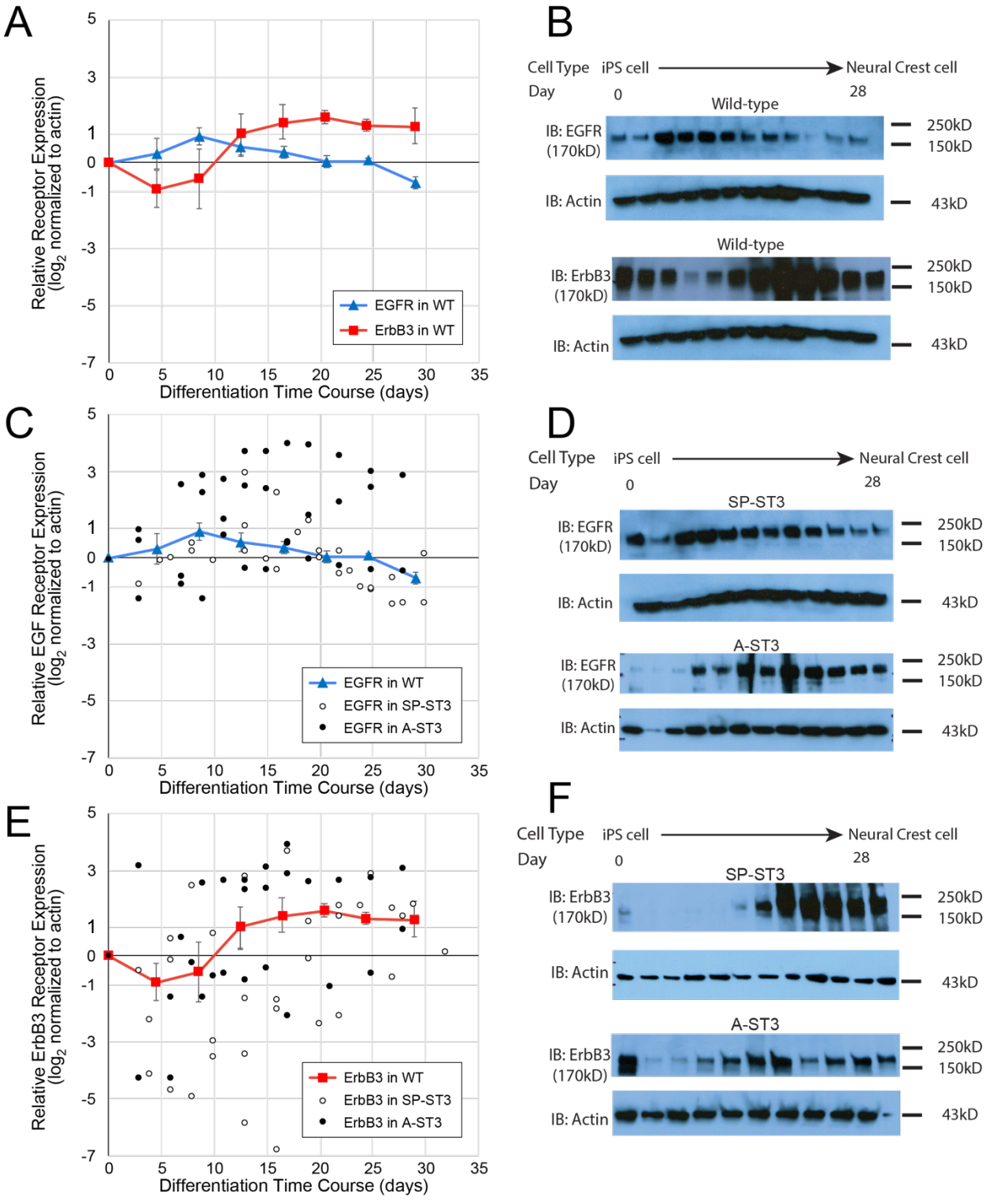
A
Relative Receptor Expression (log2 normalized to actin)
Differentiation Time Course (days)
EGFR in WT
ErbB3 in WT
B
Cell Type iPS cell Neural Crest cell
Day 0 28
Wild-type
IB: EGFR (170kD)
IB: Actin
250kD
150kD
43kD
Wild-type
IB: ErbB3 (170kD)
IB: Actin
C
Relative EGF Receptor Expression (log2 normalized to actin)
Differentiation Time Course (days)
EGFR in WT
EGFR in SP-ST3
EGFR in A-ST3
D
Cell Type iPS cell Neural Crest cell
Day 0 28
SP-ST3
IB: EGFR (170kD)
IB: Actin
A-ST3
E
Relative ErbB3 Receptor Expression (log2 normalized to actin)
Differentiation Time Course (days)
ErbB3 in WT
ErbB3 in SP-ST3
ErbB3 in A-ST3
F
Cell Type iPS cell Neural Crest cell
Day 0 28
SP-ST3
IB: ErbB3 (170kD)
IB: Actin
A-ST3

Figure 2.10 Apoptosis is enhanced in GM3SD cells during differentiation to NCCs. (**A**) Apoptosis, reported by the abundance of cleaved Caspase3, is detected in WT and GM3SD iPSC cultures (***d0***). As WT cells differentiate to NCCs, cleaved Caspase3 is barely detectable at the midpoint of the differentiation course (***d13***), whereas it remains at or above iPSC levels in SP-ST3 cells at the same time point. (**B**) Treatment of WT or SP-ST3 cells with Erlotinib, an EGFR antagonist, induces increased Caspase3 cleavage. (**C**) SP-ST3 cells are more sensitive to Erlotinib (SP-ST3 data points represent treatment during 3 independent differentiations and are plotted on top of WT bars that represent mean±SEM for n=3 independent differentiations) and (**D**) exhibit greater dissociation from the surface of the culture dish.

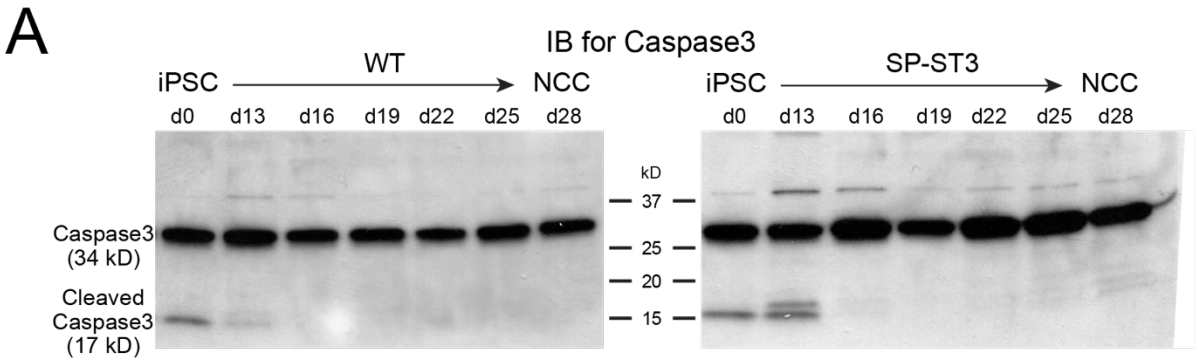
A
IB for Caspase3
WT
iPSC
NCC
SP-ST3
iPSC
NCC
d0 d13 d16 d19 d22 d25 d28
d0 d13 d16 d19 d22 d25 d28
kD
37
25
20
15
Caspase3
(34 kD)
Cleaved
Caspase3
(17 kD)

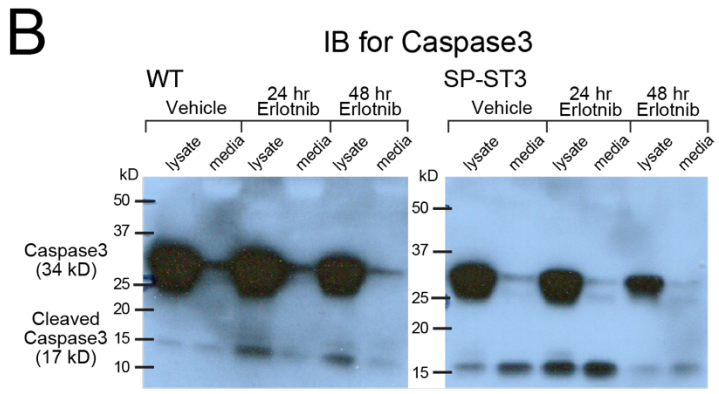
B
IB for Caspase3
WT
SP-ST3
Vehicle
24 hr
Erlotnib
48 hr
Erlotnib
lysate
media
kD
50
37
25
20
15
10
Caspase3
(34 kD)
Cleaved
Caspase3
(17 kD)

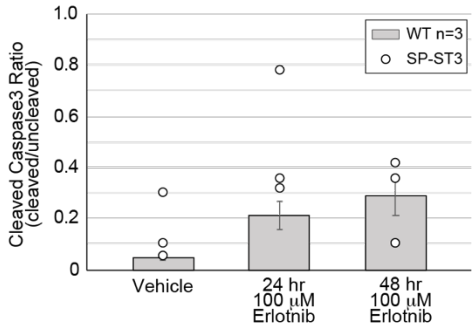
C
Cleaved Caspase3 Ratio
(cleaved/uncleaved)
1.0
0.8
0.6
0.4
0.2
0
WT n=3
SP-ST3
Vehicle
24 hr
100 μM
Erlotnib
48 hr
100 μM
Erlotnib

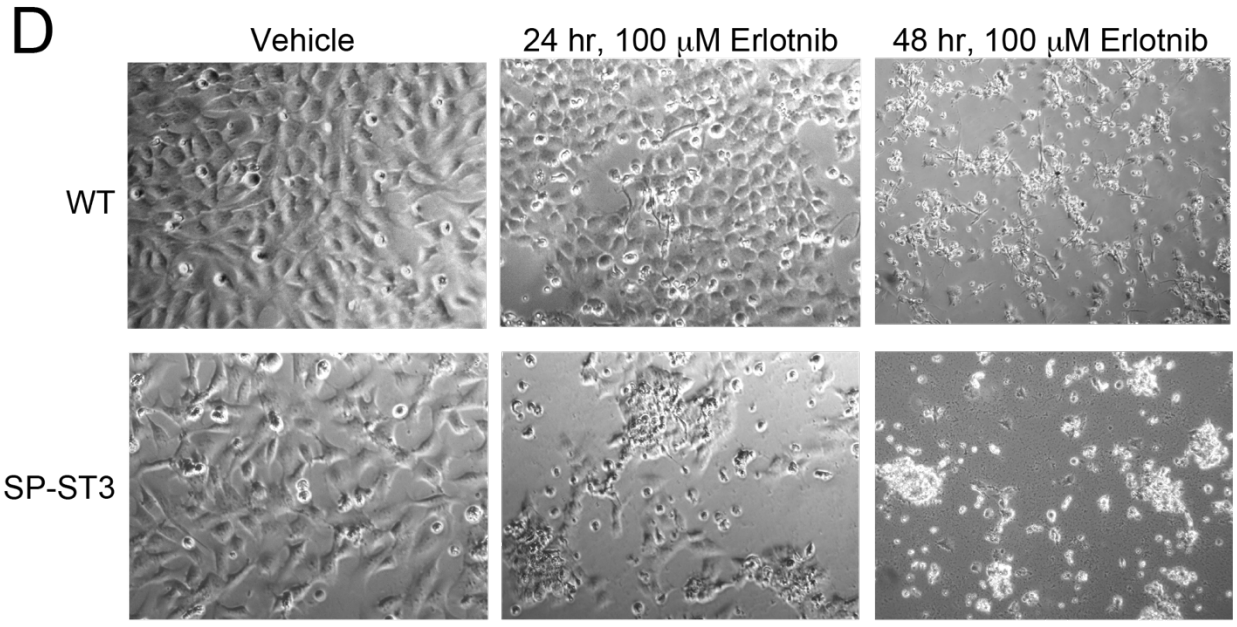
D
Vehicle
24 hr, 100 μM Erlotnib
48 hr, 100 μM Erlotnib
WT
SP-ST3

Figure 2.11. GSL composition impacts lipid rafts and cell signaling in GM3SD. Cell surface signaling receptor functions are regulated by their migration in-and-out of membrane signaling domains and by the balance of their internalization/reinsertion kinetics. In WT and GM3SD cells, lipid raft characteristics reflect the physicochemical properties of the GSLs, phospholipids, and sterols that constitute the plasma membrane. (**A**) When cells are able to synthesize GM3 and its subsequent end-products, lipid rafts (***shaded green***) facilitate the association of signaling receptors and adaptor/scaffold proteins to appropriately stimulate downstream effectors (***lightning bolts***). Membrane recycling also buffers signaling responses by internalizing surface receptors and shuttling additional signaling capacity from intracellular storage. (**B**) In the absence of GM3 and any of the biosynthetic products derived from GM3, GSL compositions are shifted toward greater abundance of neutral lipids and toward the appearance of alternatively sialylated species. The characteristics of the resulting lipid rafts (***shaded red***) will reflect the ability of these GSLs to interact with receptors and with each other. In general, we propose that GM3SD generates new populations of lipid rafts that are more heterogeneous in their size and/or functionality than in WT. Some rafts may be too small or unstable to accommodate the signaling machinery of specific receptors while others may be larger than in WT, resulting in enhanced signaling and greater residency time for surface receptors. Additionally, altered accessibility of some receptors to surface derivatization (SEEL) indicates that the normal buffering function provided by membrane recycling is also impacted by GSL imbalance.

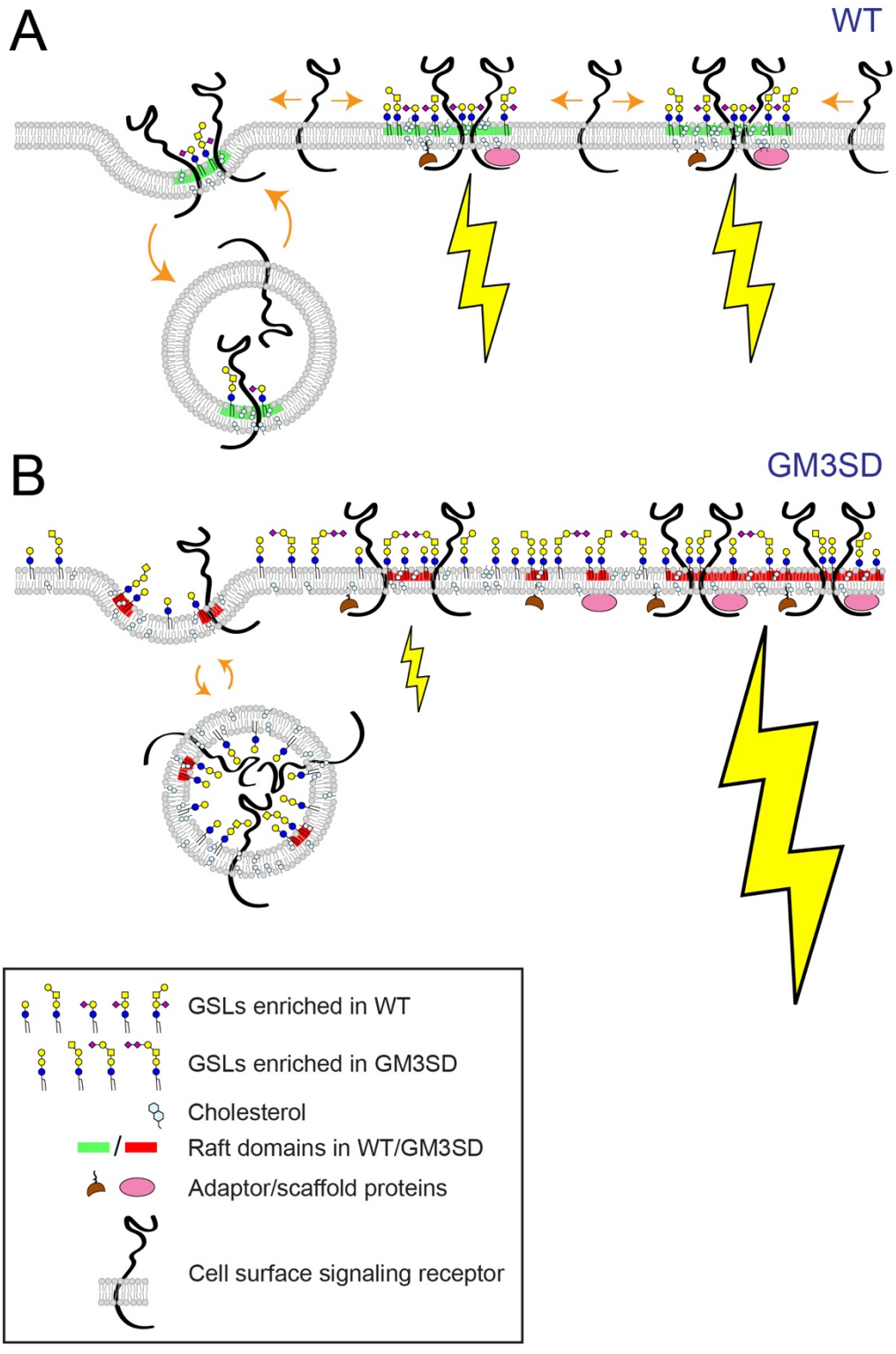
A
WT
B
GM3SD
GSLs enriched in WT
GSLs enriched in GM3SD
Cholesterol
Raft domains in WT/GM3SD
Adaptor/scaffold proteins
Cell surface signaling receptor

REFERENCES

Anumula, K. R., & Taylor, P. B. (1992). A comprehensive procedure for preparation of partially methylated alditol acetates from glycoprotein carbohydrates. *Anal Biochem, 203*(1), 101-108. doi:10.1016/0003-2697(92)90048-c

Aoki, K., Perlman, M., Lim, J. M., Cantu, R., Wells, L., & Tiemeyer, M. (2007). Dynamic developmental elaboration of N-linked glycan complexity in the Drosophila melanogaster embryo. *J Biol Chem, 282*(12), 9127-9142. doi:10.1074/jbc.M606711200

Barrick, C. J., Roberts, R. B., Rojas, M., Rajamannan, N. M., Suitt, C. B., O'Brien, K. D., . . . Threadgill, D. W. (2009). Reduced EGFR causes abnormal valvular differentiation leading to calcific aortic stenosis and left ventricular hypertrophy in C57BL/6J but not 129S1/SvImJ mice. *American Journal of Physiology-Heart and Circulatory Physiology, 297*(1), H65-H75. doi:10.1152/ajpheart.00866.2008

Black, L. E., Longo, J. F., & Carroll, S. L. (2019). Mechanisms of Receptor Tyrosine-Protein Kinase ErbB-3 (ERBB3) Action in Human Neoplasia. *The American Journal of Pathology, 189*(10), 1898-1912. doi:10.1016/j.ajpath.2019.06.008

Boccuto, L., Aoki, K., Flanagan-Steet, H., Chen, C.-F., Fan, X., Bartel, F., . . . Schwartz, C. E. (2013). A mutation in a ganglioside biosynthetic enzyme, ST3GAL5, results in salt & pepper syndrome, a neurocutaneous disorder with altered glycolipid and glycoprotein glycosylation. *Human Molecular Genetics, 23*(2), 418-433. doi:10.1093/hmg/ddt434

Bowser, L. E., Young, M., Wenger, O. K., Ammous, Z., Brigatti, K. W., Carson, V. J., . . . Strauss, K. A. (2019). Recessive GM3 synthase deficiency: Natural history, biochemistry, and therapeutic frontier. *Mol Genet Metab, 126*(4), 475-488. doi:10.1016/j.ymgme.2019.01.013

Bremer, E. G., Hakomori, S., Bowen-Pope, D. F., Raines, E., & Ross, R. (1984). Ganglioside-mediated modulation of cell growth, growth factor binding, and receptor phosphorylation. *J Biol Chem, 259*(11), 6818-6825.

Bremer, E. G., Schlessinger, J., & Hakomori, S.-I. (1986). Ganglioside-mediated modulation of cell growth. Specific effects of GM3 on tyrosine phosphorylation of the epidermal growth factor receptor. *Journal of Biological Chemistry, 261*(5), 2434-2440.

Brown, D. A., & London, E. (1997). Structure of detergent-resistant membrane domains: does phase separation occur in biological membranes? *Biochem Biophys Res Commun, 240*(1), 1-7. doi:10.1006/bbrc.1997.7575

Brown, D. A., & Rose, J. K. (1992). Sorting of GPI-anchored proteins to glycolipid-enriched membrane subdomains during transport to the apical cell surface. *Cell, 68*(3), 533-544. doi:10.1016/0092-8674(92)90189-j

Campbell, P., Morton, P. E., Takeichi, T., Salam, A., Roberts, N., Proudfoot, L. E., . . . McGrath, J. A. (2014). Epithelial inflammation resulting from an inherited loss-of-function mutation in EGFR. *J Invest Dermatol, 134*(10), 2570-2578. doi:10.1038/jid.2014.164

Cederquist, G. Y., Tchieu, J., Callahan, S. J., Ramnarine, K., Ryan, S., Zhang, C., . . . Studer, L. (2020). A Multiplex Human Pluripotent Stem Cell Platform Defines Molecular and Functional Subclasses of Autism-Related Genes. *Cell Stem Cell, 27*(1), 35-49.e36. doi:10.1016/j.stem.2020.06.004

Collins, B. E., Ito, H., Sawada, N., Ishida, H., Kiso, M., & Schnaar, R. L. (1999). Enhanced Binding of the Neural Siglecs, Myelin-associated Glycoprotein and Schwann Cell Myelin Protein, to Chol-1 (α-Series) Gangliosides and Novel Sulfated Chol-1 Analogs*. *Journal of Biological Chemistry, 274*(53), 37637-37643. doi:https://doi.org/10.1074/jbc.274.53.37637

Datta, A. K., & Paulson, J. C. (1995). The sialyltransferase "sialylmotif" participates in binding the donor substrate CMP-NeuAc. *J Biol Chem, 270*(4), 1497-1500. doi:10.1074/jbc.270.4.1497

Fragaki, K., Ait-El-Mkadem, S., Chaussenot, A., Gire, C., Mengual, R., Bonesso, L., . . . Paquis-Flucklinger, V. (2013). Refractory epilepsy and mitochondrial dysfunction due to GM3 synthase deficiency. *European Journal of Human Genetics, 21*(5), 528-534. doi:10.1038/ejhg.2012.202

Gordon-Lipkin, E., Cohen, J. S., Srivastava, S., Soares, B. P., Levey, E., & Fatemi, A. (2018). ST3GAL5-Related Disorders: A Deficiency in Ganglioside Metabolism and a Genetic Cause of Intellectual Disability and Choreoathetosis. *J Child Neurol, 33*(13), 825-831. doi:10.1177/0883073818791099

Holbro, T., Beerli, R. R., Maurer, F., Koziczak, M., Barbas, C. F., & Hynes, N. E. (2003). The ErbB2/ErbB3 heterodimer functions as an oncogenic unit: ErbB2 requires ErbB3 to

drive breast tumor cell proliferation. *Proceedings of the National Academy of Sciences, 100*(15), 8933-8938. doi:10.1073/pnas.1537685100

Huang, Y. F., Aoki, K., Akase, S., Ishihara, M., Liu, Y. S., Yang, G., . . . Fujita, M. (2021). Global mapping of glycosylation pathways in human-derived cells. *Dev Cell*. doi:10.1016/j.devcel.2021.02.023

Indellicato, R., Parini, R., Domenighini, R., Malagolini, N., Iascone, M., Gasperini, S., . . . Trinchera, M. (2019). Total loss of GM3 synthase activity by a normally processed enzyme in a novel variant and in all ST3GAL5 variants reported to cause a distinct congenital disorder of glycosylation. *Glycobiology, 29*(3), 229-241. doi:10.1093/glycob/cwy112

Laine, R. A., & Hakomori, S.-i. (1973). Incorporation of exogenous glycosphingolipids in plasma membranes of cultured hamster cells and concurrent change of growth behavior. *Biochemical and Biophysical Research Communications, 54*(3), 1039-1045. doi:https://doi.org/10.1016/0006-291X(73)90798-5

Lee, J. S., Yoo, Y., Lim, B. C., Kim, K. J., Song, J., Choi, M., & Chae, J.-H. (2016). GM3 synthase deficiency due to ST3GAL5 variants in two Korean female siblings: Masquerading as Rett syndrome-like phenotype. *American Journal of Medical Genetics Part A, 170*(8), 2200-2205. doi:https://doi.org/10.1002/ajmg.a.37773

Lee, T.-C., & Threadgill, D. W. (2009). Generation and validation of mice carrying a conditional allele of the epidermal growth factor receptor. *genesis, 47*(2), 85-92. doi:https://doi.org/10.1002/dvg.20464

Li, T. A., & Schnaar, R. L. (2018). Chapter Two - Congenital Disorders of Ganglioside Biosynthesis. In R. L. Schnaar & P. H. H. Lopez (Eds.), *Progress in Molecular Biology and Translational Science* (Vol. 156, pp. 63-82): Academic Press.

Lloyd, K. O., & Furukawa, K. (1998). Biosynthesis and functions of gangliosides: recent advances. *Glycoconjugate Journal, 15*(7), 627-636. doi:10.1023/A:1006924128550

Maccioni, H. J. F., Quiroga, R., & Ferrari, M. L. (2011). Cellular and molecular biology of glycosphingolipid glycosylation. *Journal of Neurochemistry, 117*(4), 589-602. doi:https://doi.org/10.1111/j.1471-4159.2011.07232.x

Maccioni, H. J. F., Quiroga, R., & Spessott, W. (2011). Organization of the synthesis of glycolipid oligosaccharides in the Golgi complex. *FEBS Letters, 585*(11), 1691-1698. doi:https://doi.org/10.1016/j.febslet.2011.03.030

Maklad, A., Nicolai, J. R., Bichsel, K. J., Evenson, J. E., Lee, T.-C., Threadgill, D. W., & Hansen, L. A. (2009). The EGFR Is Required for Proper Innervation to the Skin. *Journal of Investigative Dermatology, 129*(3), 690-698. doi:https://doi.org/10.1038/jid.2008.281

Mbua, N. E., Li, X., Flanagan-Steet, H. R., Meng, L., Aoki, K., Moremen, K. W., . . . Boons, G.-J. (2013). Selective Exo-Enzymatic Labeling of N-Glycans on the Surface of Living Cells by Recombinant ST6Gal I. *Angewandte Chemie International Edition, 52*(49), 13012-13015. doi:https://doi.org/10.1002/anie.201307095

Menendez, L., Kulik, M. J., Page, A. T., Park, S. S., Lauderdale, J. D., Cunningham, M. L., & Dalton, S. (2013). Directed differentiation of human pluripotent cells to neural crest stem cells. *Nat Protoc, 8*(1), 203-212. doi:10.1038/nprot.2012.156

Meng, L., Forouhar, F., Thieker, D., Gao, Z., Ramiah, A., Moniz, H., . . . Moremen, K. W. (2013). Enzymatic basis for N-glycan sialylation: structure of rat α2,6-sialyltransferase (ST6GAL1) reveals conserved and unique features for glycan sialylation. *J Biol Chem, 288*(48), 34680-34698. doi:10.1074/jbc.M113.519041

Miljan, E. A., Meuillet, E. J., Mania-Farnell, B., George, D., Yamamoto, H., Simon, H.-G., & Bremer, E. G. (2002). Interaction of the Extracellular Domain of the Epidermal Growth Factor Receptor with Gangliosides *. *Journal of Biological Chemistry, 277*(12), 10108-10113. doi:10.1074/jbc.M111669200

Neelamegham, S., Aoki-Kinoshita, K., Bolton, E., Frank, M., Lisacek, F., Lütteke, T., . . . Group, T. S. D. (2019). Updates to the Symbol Nomenclature for Glycans guidelines. *Glycobiology, 29*(9), 620-624. doi:10.1093/glycob/cwz045

Nimrichter, L., Burdick, M. M., Aoki, K., Laroy, W., Fierro, M. A., Hudson, S. A., . . . Schnaar, R. L. (2008). E-selectin receptors on human leukocytes. *Blood, 112*(9), 3744-3752. doi:10.1182/blood-2008-04-149641

Rao, F. V., Rich, J. R., Rakić, B., Buddai, S., Schwartz, M. F., Johnson, K., . . . Strynadka, N. C. J. (2009). Structural insight into mammalian sialyltransferases. *Nature structural & molecular biology, 16*(11), 1186-1188. doi:10.1038/nsmb.1685

Rukazenkov, Y., Speake, G., Marshall, G., Anderton, J., Davies, B. R., Wilkinson, R. W., . . . Swaisland, A. (2009). Epidermal growth factor receptor tyrosine kinase inhibitors: similar but different? *Anticancer Drugs, 20*(10), 856-866. doi:10.1097/CAD.0b013e32833034e1

Sandhoff, K., & Kolter, T. (2003). Biosynthesis and degradation of mammalian glycosphingolipids. *Philosophical transactions of the Royal Society of London. Series B, Biological sciences, 358*(1433), 847-861. doi:10.1098/rstb.2003.1265

Sandhoff, R., Geyer, R., Jennemann, R., Paret, C., Kiss, E., Yamashita, T., . . . Gröne, H.-J. (2005). Novel Class of Glycosphingolipids Involved in Male Fertility *. *Journal of Biological Chemistry, 280*(29), 27310-27318. doi:10.1074/jbc.M502775200

Saul, R., Wilkes, G., & Stevenson, R. (1983). *Salt-And-Pepper'pigmentary changes with severe mental retardation: a new neurocutaneous syndrome.* Paper presented at the Proc. Greenwood Genet., Ctr.

Schnaar, R. L. (2016). Gangliosides of the Vertebrate Nervous System. *J Mol Biol, 428*(16), 3325-3336. doi:10.1016/j.jmb.2016.05.020

Schnaar, R. L., Gerardy-Schahn, R., & Hildebrandt, H. (2014). Sialic acids in the brain: gangliosides and polysialic acid in nervous system development, stability, disease, and regeneration. *Physiol Rev, 94*(2), 461-518. doi:10.1152/physrev.00033.2013

Shih, A., Telesco, S., & Radhakrishnan, R. (2011). Analysis of Somatic Mutations in Cancer: Molecular Mechanisms of Activation in the ErbB Family of Receptor Tyrosine Kinases. *Cancers, 3*, 1195-1231. doi:10.3390/cancers3011195

Si-Tayeb, K., Noto, F. K., Nagaoka, M., Li, J., Battle, M. A., Duris, C., . . . Duncan, S. A. (2010). Highly efficient generation of human hepatocyte-like cells from induced pluripotent stem cells. *Hepatology, 51*(1), 297-305. doi:10.1002/hep.23354

Simons, K., & Ikonen, E. (1997). Functional rafts in cell membranes. *Nature, 387*(6633), 569-572.

Simpson, M. A., Cross, H., Proukakis, C., Priestman, D. A., Neville, D. C. A., Reinkensmeier, G., . . . Crosby, A. H. (2004). Infantile-onset symptomatic epilepsy syndrome caused by a homozygous loss-of-function mutation of GM3 synthase. *Nature Genetics, 36*(11), 1225-1229. doi:10.1038/ng1460

Sipione, S., Monyror, J., Galleguillos, D., Steinberg, N., & Kadam, V. (2020). Gangliosides in the Brain: Physiology, Pathophysiology and Therapeutic Applications. *Frontiers in Neuroscience, 14*(1004). doi:10.3389/fnins.2020.572965

Soudy, M., Anwar, A. M., Ahmed, E. A., Osama, A., Ezzeldin, S., Mahgoub, S., & Magdeldin, S. (2020). UniprotR: Retrieving and visualizing protein sequence and functional information from Universal Protein Resource (UniProt knowledgebase). *Journal of Proteomics, 213*, 103613. doi:https://doi.org/10.1016/j.jprot.2019.103613

Steinkamp, M. P., Low-Nam, S. T., Yang, S., Lidke, K. A., Lidke, D. S., & Wilson, B. S. (2014). erbB3 Is an Active Tyrosine Kinase Capable of Homo- and Heterointeractions. *Molecular and Cellular Biology, 34*(6), 965-977. doi:10.1128/mcb.01605-13

Sun, T., Yu, S.-H., Zhao, P., Meng, L., Moremen, K. W., Wells, L., . . . Boons, G.-J. (2016). One-Step Selective Exoenzymatic Labeling (SEEL) Strategy for the Biotinylation and Identification of Glycoproteins of Living Cells. *Journal of the American Chemical Society, 138*(36), 11575-11582. doi:10.1021/jacs.6b04049

Varki, A., Cummings, R. D., Aebi, M., Packer, N. H., Seeberger, P. H., Esko, J. D., . . . Kornfeld, S. (2015). Symbol Nomenclature for Graphical Representations of Glycans. *Glycobiology, 25*(12), 1323-1324. doi:10.1093/glycob/cwv091

Vukelić, Ž., Zamfir, A. D., Bindila, L., Froesch, M., Peter-Katalinić, J., Usuki, S., & Yu, R. K. (2005). Screening and sequencing of complex sialylated and sulfated glycosphingolipid mixtures by negative ion electrospray Fourier transform ion cyclotron resonance mass spectrometry. *Journal of the American Society for Mass Spectrometry, 16*(4), 571-580. doi:10.1016/j.jasms.2005.01.013

Wang, X.-Q., Sun, P., & Paller, A. S. (2003). Ganglioside GM3 Blocks the Activation of Epidermal Growth Factor Receptor Induced by Integrin at Specific Tyrosine Sites *. *Journal of Biological Chemistry, 278*(49), 48770-48778. doi:10.1074/jbc.M308818200

Wee, P., & Wang, Z. (2017). Epidermal Growth Factor Receptor Cell Proliferation Signaling Pathways. *Cancers (Basel), 9*(5). doi:10.3390/cancers9050052

Yamashita, T., Hashiramoto, A., Haluzik, M., Mizukami, H., Beck, S., Norton, A., . . . Proia, R. L. (2003). Enhanced insulin sensitivity in mice lacking ganglioside GM3. *Proceedings of the National Academy of Sciences, 100*(6), 3445-3449. doi:10.1073/pnas.0635898100

Yamashita, T., Wu, Y.-P., Sandhoff, R., Werth, N., Mizukami, H., Ellis, J. M., . . . Proia, R. L. (2005). Interruption of ganglioside synthesis produces central nervous system degeneration and altered axon–glial interactions. *Proceedings of the National Academy of Sciences of the United States of America, 102*(8), 2725-2730. doi:10.1073/pnas.0407785102

York, W. S., Agravat, S., Aoki-Kinoshita, K. F., McBride, R., Campbell, M. P., Costello, C. E., . . . Kettner, C. (2014). MIRAGE: the minimum information required for a glycomics experiment. *Glycobiology, 24*(5), 402-406. doi:10.1093/glycob/cwu018

Yoshikawa, M., Go, S., Suzuki, S.-i., Suzuki, A., Katori, Y., Morlet, T., . . . Inokuchi, J.-i. (2015). Ganglioside GM3 is essential for the structural integrity and function of cochlear hair cells. *Human Molecular Genetics, 24*(10), 2796-2807. doi:10.1093/hmg/ddv041

Yoshikawa, M., Go, S., Takasaki, K., Kakazu, Y., Ohashi, M., Nagafuku, M., . . . Inokuchi, J.-i. (2009). Mice lacking ganglioside GM3 synthase exhibit complete hearing loss due to selective degeneration of the organ of Corti. *Proceedings of the National Academy of Sciences, 106*(23), 9483-9488. doi:10.1073/pnas.0903279106

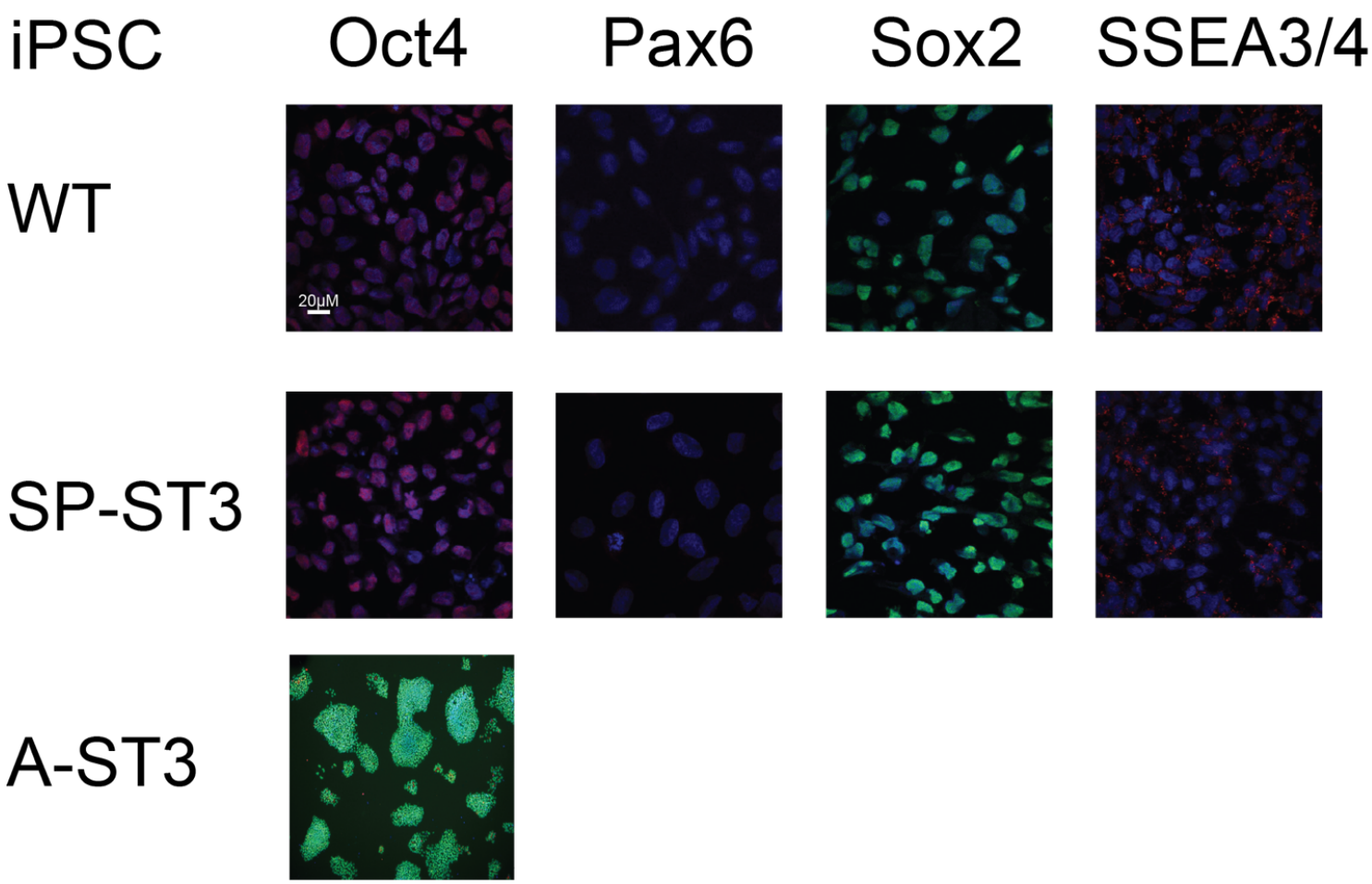

Supplemental Figure 2.1 Immunofluorescence staining for iPSC markers.
WT iPSCs stain positive for Oct 4 (red), Sox2 (green), and SSEA3/4 (red), and negative for Pax 6. DAPI in blue. Taken at 60X
SP-ST3 iPSCs iPSCs stain positive for Oct 4 (red), Sox2 (green), and SSEA3/4 (red), and negative for Pax 6. DAPI in blue. Taken at 60X
A-ST3 stain positive for Oct4 (green). DAPI in blue. Taken at 4X

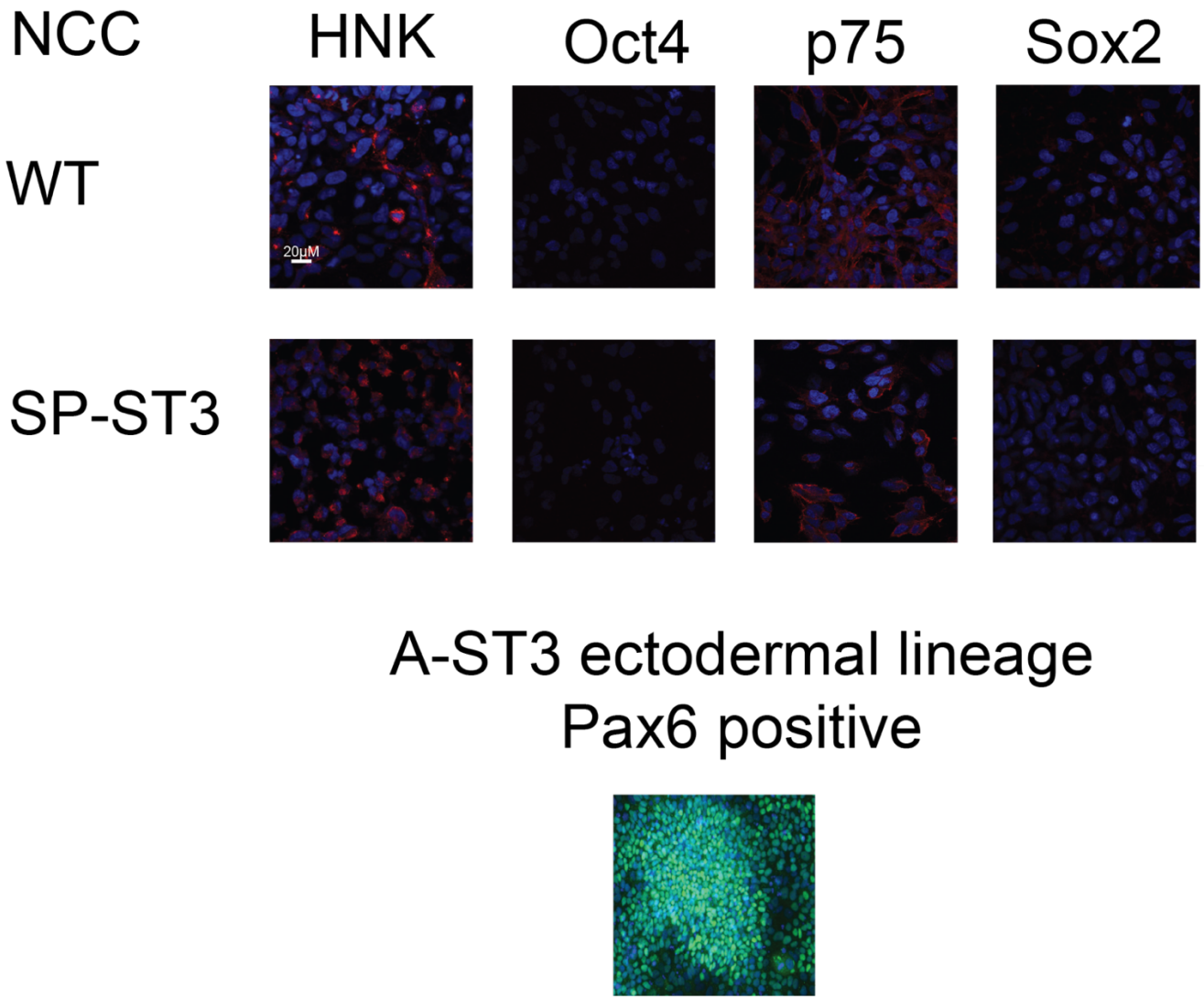

Supplemental Figure 2.2 1 Immunofluorescence staining for NCC and ectodermal markers.
WT NCCSs stain positive for HNK-1 (red) and p75(red)and negative for Oct4 and Sox2. DAPI in blue. Taken at 60X
SP-ST3 NCCSs stain positive for HNK-1 (red) and p75(red)and negative for Oct4 and Sox2. DAPI in blue. Taken at 60X
A-ST3 stain positive for Pax6 (green). DAPI in blue. Taken at 4X

CHAPTER 3

DISCUSSION

This chapter will provide conclusive remarks about the major findings from this project, discuss future directions for this research, and elaborate on how this work fits into the overall context of the field and the significance of this work to the areas of glycolipid biology, rare disease research, and modeling neurological disorders.

Conclusions from our Research

GM3SD is one of two disorders of glycolipid biosynthesis identified in humans (Saul, Wilkes, & Stevenson, 1983; Simpson et al., 2004). The disease is caused by variants in *ST3GAL5*, which encodes the sialyltransferase GM3 Synthase, and appears to result in the loss of all GM3 and GM3-derived gangliosides. There are now five known variants in the *ST3GAL5* that have been identified in patient populations with the disease, all of which result in loss-of-function of GM3 Synthase (Boccuto et al., 2013; Gordon-Lipkin et al., 2018; Indellicato et al., 2019; Lee et al., 2016; Simpson et al., 2004). The results presented in Chapter 2 of this dissertation showed some of the glycosylation and cell signaling molecular changes that occur in two patients with different variants of GM3SD-causing mutations.

Consistent with previously reported glycolipid analyses of GM3SD patient fibroblasts, neither iPSCS nor NCCs from SP-ST3 or A-ST3 had any GM3 or GM3-derived gangliosides (Boccuto et al., 2013; Bowser et al., 2019; Simpson et al., 2004). However, we did find increased LacCer levels relative to wildtype levels in the GM3

deficient cell lines. The increase in LacCer levels is in contrast to what was seen in the previously published Salt and Pepper, GM3-deficient fibroblasts, where high levels of LacCer were not detected, but rather increased levels of globo-series GSLs (Boccuto et al., 2013). Increased globosides and lower LacCer levels, relative to wildtype fibroblasts, was also observed in GM3-deficient fibroblasts from the French cohort as well, with the same p.Arg288X mutation as the Amish cohort (Fragaki et al., 2013). However, increased levels of LacCer were reported to be in the plasma of GM3-deficient Amish patients (Aoki, Heaps, Strauss, & Tiemeyer, 2019). The increase in LacCer may have a significant impact on the cells, as increased LacCer has been associated with apoptosis in some cells (Bodas, Min, & Vij, 2015; Martin, Williams, & Chatterjee, 2006). We have previously reported findings on apoptosis in the mid- to hind-brain region of zebrafish that had *ST3GAL5* knocked down by morpholino injection, and in Chapter 2 of this work we found an increase in susceptibility to apoptosis by EGFR inhibition in SP-ST3 differentiating NCCs compared to wildtype (Boccuto et al., 2013).

Apoptosis is a key and necessary feature during neural crest development in many vertebrates. As with many aspects of development though, proper timing and location are critical (Graham, Francis-West, Brickell, & Lumsden, 1994; Graham, Heyman, & Lumsden, 1993; Trainor, Sobieszczuk, Wilkinson, & Krumlauf, 2002). Identifying cleaved-caspase 3 expression, an indicator of apoptosis, during neural crest differentiation, therefore, might not initially seem like a notable phenotype. However, our work showed that SP-ST3 cells exhibited increased cleaved-caspase 3 expression during neural crest differentiation, and improper amount or timing of the apoptotic cells

could be an indication of a misstep in neural crest development that could have lasting effects on the remaining population of cells. For instance, it is important to remember that we generated a pool of neural crest cells that presumably can be further differentiated to several neural crest-derived lineages. However, we don't know the future fates of the population of neural crest cells that are experiencing enhanced apoptosis in our SP-ST3 differentiation or if the particular population of cells that die off were needed to provided necessary signaling for proper further differentiation or migration of surrounding neural crest cells. Possible experiments to address these questions will be discussed in the "Future Directions" section. Furthermore, we also demonstrated that the SP-ST3 cells appear to be more sensitive to apoptosis induced by EGFR inhibition. Enhanced sensitivity could indicate that the SP-ST3 cells are more primed for apoptotic events that could be occurring later in the developmental process than what we're seeing within the window of our cell culture differentiation.

Variations were detected on comparing the GSL profiles of the two GM3-deficient patient lines we studied as well. In particular differences in sialylated versus non-sialylated GSLs between the two patient neural crest lines were seen. We observed increased GM1b and GD1c in SP-ST3 relative to A-ST3, and increased Gb4/Lc4 in A-ST3 relative to SP-ST3, along with increased sialylated LacNAc structures in SP-ST3, while those same motifs were non-sialylated in A-ST3. The two mutations appear to result in differences in the utilization of sialic acid to modify their non-GM3 Synthase-derived gangliosides; therefore, it would be of interest to analyze the glycoprotein profiles of the two lines and compare sialic acid content and sialic acid containing molecules overall between both cell lines. It was speculated in the previous publication

on the Salt and Pepper patient fibroblasts that differences in LacCer levels and utilization in GM3-deficient fibroblasts might reflect a possible difference in the variant sub-Golgi localization for the Salt and Pepper patient and the Amish cohort since the Amish variant results in a truncated protein and is presumably unable to bind LacCer if any translation product is actually produced (Boccuto et al., 2013). The S-motif is responsible for binding LacCer, and the p.Arg288X variant in the Amish cohort results in a truncation that cuts off the S-motif, while the Salt and Pepper variant is in the S-motif, but results in loss-of-function of the enzyme (Datta & Paulson, 1995). It is unknown if the Salt and Pepper variant is actually translated or, if it is produced, still allows for binding and sequestration of LacCer. However, with regards to our data on sialylation distribution between SP-ST3 and A-ST3 neural crest cells, it's important to note that both the L-motif and the S-motif are needed to bind the donor nucleotide, CMP-Neu5Ac, and that enzyme lacking the S-motif disrupts the flux of sialic acid in the cells (Rao et al., 2009).

The changes in glycolipid profile between the two cell lines could impact other molecules at the cell surface. Because gangliosides are a major component of lipid rafts, it begs the question: what are the lipid rafts of GM3-deficient cells comprised of or do the patient cells make proper or even functional lipid rafts? While this question has yet to be answered, our data leads us to believe the lipid raft composition in SP-ST3 and A-ST3 cells could differ based on the findings that their GSL profiles are different. Several membrane raft and endosome associated proteins came out in our SEEL experiment, some being up-regulated in SP-ST3 GM3-deficient NCCs, while others were down-regulated. There was a high proportion of membrane raft associated

proteins – 11 out of 14 of the filtered proteins in our experiment **(Figure 2.7B**) – that were upregulated in SP-ST3 relative to wildtype. The high abundance of membrane raft associated proteins seen in the SP-ST3 SEEL results could indicate higher retention of membrane raft proteins within lipid rafts at the cell surface in SP-ST3 NCCs and could result in improper cell signaling in these cells. There are also some membrane raft and endosome associated proteins that are down-regulated in SP-ST3 NCCs. It is likely that some proteins that are not able to bind to the alternatively sialylated gangliosides, or in some cases, the appropriate binding partners for particular proteins may not be brought into the correct vicinity to help retain those proteins at the cell surface.

When we followed-up on the SEEL experiment by looking at whole cell expression of certain proteins, we found that even though Notch2 and Sortilin were not detected in the SP-ST3 SEEL data, they were expressed throughout differentiation. This indicates that either Notch2 and Sortilin are not properly glycosylated or that they are not being properly trafficked or retained at the cell surface in SP-ST3 NCCs. The downregulation of sortilin abundance at the cell surface could suggest dysregulation of endocytosis in SP-ST3 NCCs. The downregulation of cell surface Notch2 abundance could be significant for further differentiation of neural crest-derived lineages as Notch2 is known to be required for cardiac neural crest development (Varadkar et al., 2008). Additionally, even though we were able to detect Notch2 by western blot analysis, the expression pattern does appear to differ between SP-ST3 and WT throughout the differentiation process (**Figure 2.6**)**.** The difference in bands seen between the two cell types suggests differences in processing, as Notch2 undergoes several cleavage steps before a portion of the intracellular domain travels to the nucleus to act as a

transcription factor. ADAM10 and γ-secretase are proteases involved in Notch2 processing, and they are both themselves cell surface transmembrane proteins that could be improperly trafficked or retained at the SP-ST3 cell surface during NC differentiation.

A major function of gangliosides is to facilitate cell signaling through either indirect means via lipid raft formation or directly by binding with signaling proteins, including RTKs, with carbohydrate binding domains (Simons & Toomre, 2000). Therefore, we explored the expression of RTKs in our GM3-deficient cells. Analysis of RTKs showed differences in EGFR and ErbB3 expression in GM3-deficient cells during differentiation from iPSC to NCC when compared to wild-type, and subtle differences were seen in these particular RTKs expression between the two GM3SD mutations as well. With the two patient lines expressing different GSL profiles, the findings that there are differences in their RTK expression as well is consistent. SP-ST3 showed more alternatively sialylated gangliosides compared to A-ST3, and it's possible that EGFR is able to bind to some of these other gangliosides, though not likely with the same affinity for GM3 (Miljan et al., 2002). The upregulation of EGFR in SP-ST3 could be influencing the cells' ability to survive during neural crest differentiation, as we found that inhibition of EGFR activity had a severe impact on apoptosis in SP-ST3 cells.

ErbB3 also showed differential expression between wild-type, SP-ST3 and A-ST3 cells during neural crest differentiation. ErbB3 is a binding partner for EGFR, and its dysregulation could impact the expression of ErbB3. The improper regulation of ErbB3 could have a significant impact on the overall phenotype of the patients as loss of ErbB3 in mice is embryonic lethal and associated with several cardiac and peripheral

neuron defects, including loss of Schwann cell precursors (Black, Longo, & Carroll, 2019). Because we only took the patient-derived iPSCs to neural crest and did not differentiate them further into other neuronal cell types, it is unclear whether or not the cell signaling changes that occur earlier in neural crest development have any impact on the later differentiation potential of the GM3-deficient cells.

Future Directions

This work has provided valuable insight into the glycolipid profile and resulting cell surface molecular changes that occur with two different mutations in the GM3 synthase enzyme. The differences in glycolipid expression between the two patient cell lines, while not unreasonable, were unexpected. The difference in glycolipid expression between the two patient variants of course brings about the question: how do the glycolipid profiles for the other *ST3GAL5* variants differ from what we've observed in our studies? The Italian cohort, for instance, also has a variant within the S-motif, similar to SP-ST3, so would we expect to see a similar glycolipid profile as well (Indellicato et al., 2019)? Combine those potential findings with the fact that the Korean cohort exhibits variants in the L-motif rather than the S-motif, and we may be able to tease apart the significances of the different conserved motifs with regard to non-GM3 derived glycolipid diversity (Lee et al., 2016).

Beyond looking at the GM3SD-variant diversity and glycolipid diversity, it will also be very important to dive into comprehensive glycoprotein profiling for GM3SD patient cells. Assessing the glycoprotein profile for these patients will provide further knowledge of sialic acid utilization in GM3-deficient backgrounds. Furthermore, additional cell surface glycoproteome analyses could shed light on which cell surface molecules (N-

linked or O-linked depending on the recombinant sialyltransferase used for SEEL labeling) are being affected by loss of GM3-derived gangliosides. Lipidomics could point to global changes in the lipid profile that could be occurring as a result of the GSL profile changes seen in GM3SD. Sphingomyelin is also generated from a ceramide tail and is another key lipid molecule in neural development and also important for lipid rafts and signaling. As a final assessment of global changes, RNAseq and proteomics could be performed on GM3SD patient cells to help provide a better understanding of what cell signaling pathways are most affected.

Regarding the cell signaling molecular changes that we identified in Chapter 2, further studies will need to be conducted to determine if EGFR has a different carbohydrate binding partner in GM3-deficient cells, as it typically binds to GM3 (Bremer, Schlessinger, & Hakomori, 1986). It is possible that even between the two variant lines we tested, EGFR could be binding with different gangliosides considering their ganglioside profiles differ. Additionally, it could be that the preferred carbohydrate binding partner when GM3 is not available is being expressed differentially between SP-ST3 and A-ST3 resulting in the difference in EGFR expression that we observed in the two lines. This could result in the EGFR protein not being retained at the cell surface or perhaps it's being trafficked improperly, resulting in degradation. New EGFR binding partners in GM3-deficient cells could be identified by performing a glycolipid-protein overlay, where lipid extract from GM3-deficient cells is run on a TLC plate with known GSL standards, the plate is then coated with a thin coating of poly(isobutylmethacrylate) plastic polymer. This coating freezes the lipids in place in an orientation that still allows for binding of proteins. His-tagged EGFR is then laid over the TLC plate, followed by

anti-his tag secondary antibody after washes. The bound protein is then detected by 3,3'-Diaminobenzidine (DAB) staining. This process would allow us to see which glycolipids within the GM3-deficient cells' lipid extract can be bound by EGFR and help shed light on alternative GSL binding partners for cell surface proteins when GM3-derived gangliosides are not available.

Lastly, the differences in GSL profiles seen between patient fibroblasts, plasma, iPSCs, and NCCs highlights the cell-type specificity of glycosylation, and our results reinforce the need to look at phenotypically relevant cell types. Investigating the cell-type specific glycosylation and resulting cell signaling molecular changes that occurred in GM3-deficient NCCs was informative. However, the fact remains that the GM3SD patient iPSCs could both be differentiated to NCCs in a similar timeline to wildtype. Considering the changes in cell signaling molecules and cell surface N-linked glycans that we observed in our studies, it could be argued that the patient NCCs were not functioning in the same fashion as wildtype. It is also possible that the apoptosis cellular phenotype could be playing a role in the remaining NCC population. As mentioned, we know that some SP-ST3 cells express increased cleaved-caspase 3 relative to WT, indicating increased apoptosis. It is unclear if a specific population of NCCs are undergoing apoptosis, and if loss of this population could result in downstream consequences during further neural crest differentiation. To investigate the fate of specific cells within our NCC culture additional studies could be conducted to look at more global changes caused by GM3 deficiency that could help pinpoint pathways and possible mechanisms that lead to the phenotypic defects seen in patients. Furthermore, single-cell variability could be playing a role with regards to the importance of

maintaining the appropriate population of NCCs for the development of NC-derived cell lineages. Single-cell RNAseq of NCCs could help decipher if key subtypes of NCCs are changed or lost in SP-ST3 NCC differentiation. Another possibility is that disease-relevant cellular phenotypes arise upon further differentiation from NCC to its terminal cell type, or that there are inherent issues in cell migration that affect how patient neural crest cells get to their required locations in the body. This latter scenario is given support by the results of our SEEL experiment that showed many differential changes in cell adhesion molecules and cell motility molecules in SP-ST3 NCCs compared to wildtype. Cellular mechanisms behind the disease phenotypes may become more apparent in some of the neural crest-derived cell types such as peripheral neurons, Schwann cells, and even melanocytes. Inner hair cells would be another interesting cell type to attempt to differentiate to as we know that *St3gal5*-null mice lack inner hair cells, resulting in a deaf phenotype (Yoshikawa et al., 2015). Studies investigating the migratory capabilities of iPSC-derived neural crest cells could also lend some insight into whether or not GM3-deficient neural crest cells are able to properly migrate and further differentiate in GM3SD patients.

Significance

In a 2018 book series titled Progress in Molecular Biology and Translational Science, the volume on Gangliosides in Health and Disease has a chapter on Congenital Disorders of Ganglioside Biosynthesis, in which the authors state, “To date, nervous system gangliosides have not been analyzed in the affected subjects, although glycosphingolipids in plasma and cultured fibroblasts have been reported,” and concludes that, “these data imply profound alterations of brain gangliosides, plasma and

fibroblast ganglioside patterns are simple compared to those in the nervous system and a more thorough biochemical analysis awaits the availability of post-mortem brain tissue“ (Li & Schnaar, 2018). However, access to tissue will be very difficult considering the scarcity of patients. Add to that our newfound understanding that different patient mutations not only result in different phenotypic profiles, but also glycolipid profiles, it would be most beneficial to be able to compare neural tissues from multiple patients – making post-mortem brain tissue even less feasible. Furthermore, through the results of our recent study - the first to look at GM3SD mutations in iPSCs and, more importantly, a neural lineage-derived from iPSCs - we have learned that investigating the differentiation time courses are also an important factor to consider. Therefore, the iPSC to neural cell-type disease model we've demonstrated holds great value to enriching our knowledge of congenital disorders of glycolipid biosynthesis and understanding the relationship between GSLs and cell signaling molecules.

This model could be used to study the only other currently identified congenital disorder of ganglioside biosynthesis, GM2/GD2 Synthase Deficiency, which is a form of Hereditary Spastic Paraplegia (HSP). This disorder is caused by a mutation in the GM2/GD2 Synthase enzyme or B4GALNT1(Harlalka et al., 2013). This enzyme transfers an N-Acetylgalactosamine, or GalNAc, onto GM3/GD3 in a β-1,4 linkage to generate GM2/GD2. Over 40 patients have been identified, belonging to 12 different pedigrees with 12 different gene mutations (Li & Schnaar, 2018). The disorder is characterized by weakness and spasticity of the lower limb, which often onsets in childhood or adulthood but progresses with severity and is also accompanied by Intellectual Disability (ID) (Boukhris et al., 2013). While the mouse model for GM2/GD2

Synthase Deficiency (*B4galnt1*-null mouse) does phenocopy the hallmark phenotypes of the disease – progressive motor neuropathy and ID – the same limitations to accessing patient tissues, especially in phenotypically relevant tissue types remains for this rare disorder (Bhuiyan et al., 2019; Takamiya et al., 1996). Therefore, utilizing an iPSC to neural time course model to identify molecular changes that could provide insights to disease mechanisms would be applicable.

An ever-growing body of work demonstrates the important role of gangliosides in neurodegenerative disorders, such as Alzheimer's (Dukhinova et al., 2019; Sipione, Monyror, Galleguillos, Steinberg, & Kadam, 2020). The information gleaned about neurological function in the absence of the majority of complex gangliosides could prove invaluable to the Alzheimer's field. Recent work investigating the impact of GM3 on amyloid deposits and other Alzheimer's phenotypes reported that $ST3^{-/-}$5XFAD mice, an Alzheimer's mouse model in a GM3-deficient background, lack central nervous system (CNS) amyloid deposits and don't exhibit AD-related neuroinflammation (Dukhinova ref here?). Additionally, the mice don't show neuronal loss or synaptic dysfunctions and performed normally in a cognitive test. Furthermore, the researchers showed that treatment of wildtype 5XFAD mice with a sialic-acid specific lectin improved AD pathology (Dukhinova et al., 2019). GM3-deficient cell lines could aid in the study of this relationship between gangliosides and neurodegenerative disorders in the future.

Lastly, it's important to also consider beyond just the disease-focused applications of this work and circle back to the fact that GM3SD is a very rare disorder of glycosylation, which highlights the essential nature of properly functioning ganglioside biosynthesis. The results presented in this dissertation clearly demonstrates that

expression of cell signaling molecules changes when ganglioside biosynthesis is disrupted. Gangliosides are a key component to lipid rafts, and the field is still trying to fully understand lipid raft composition and function (Brown & London, 1998; Levental, Levental, & Heberle, 2020). A GM3-deficient cell line provides a valuable tool to understand how lipid rafts are formed and function in the absence of certain gangliosides.

Furthermore, the shift in GSL expression from neutral globo- and lacto-series GSLs to complex gangliosides has been shown to be a key driver in neural differentiation (Russo et al., 2018). The GM3SD patient cells can only produce a limited variety of complex gangliosides, and our work shows that the different patient variants result in different GSL profiles. Attempting to differentiat these cells to neural cell types allows for the further study of how the GSL repertoire affects neural cell types and could help identify other key drivers and players in the differentiation process.

We showed that EGFR had altered expression in the GM3-deficient patient cells, but we also demonstrated that the expression differed between the two patient lines with different mutation in GM3 Synthase. EGFR is known to bind with the ganglioside GM3 in wildtype cells (Bremer et al., 1986; Coskun, Grzybek, Drechsel, & Simons, 2011; Wang, Sun, & Paller, 2003). While it is unknown specifically what GSL EGFR is interacting with in the absence of GM3 in our patient cells, it’s possible that EGFR is binding with different GSLs or gangliosides in the two different patient cell lines. This could result in changes in EGFR signaling as it has been demonstrated that EGFR signaling can be augmented or diminished depending on the GSL the protein is interacting with (Coskun et al., 2011; Liu, Li, & Ladisch, 2004; Park, Kwak, Shayman, &

Kim, 2012). Furthermore, our SEEL labeling experiment showed numerous cell surface, and notably cell signaling molecules, that were differentially expressed between wildtype and the SP-ST3 GM3-deficient neural crest cells. These surface molecules are likely interacting with a different repertoire of GSLs compared to their normal binding partners in wildtype. The GM3SD patient cells lines could be used to uncover a whole new set of possible protein-GSL interactions that could help us better understand the interplay between cell surface proteins and glycolipids.

This work builds off of numerous publications that present the glycosphingolipid profiles of GM3-deficient animals and patient tissues. However, it is the first work to present this information in human neural tissues differentiated from patient-derived iPSCs. Moreover, by utilizing these patient-derived cells from individuals with a rare neurological disorder, we have been able to show that different genetic variants in a key glycosphingolipid biosynthetic enzyme actually results in variations in the GSL profile expressed by the patient cells. Furthermore, this work also demonstrates that the changes in the GSL repertoire then result in differences in receptor tyrosine kinase expression – reinforcing the intricate and intimate connection between glycolipids and cell signaling molecules. This experiment of nature, and the experiments that we've already conducted, and will conduct in the future, utilizing these patient-derived cells, take us many steps closer to understanding the basic biology of glycolipids and their role in cell signaling and proper neural development.

References

Aoki, K., Heaps, A. D., Strauss, K. A., & Tiemeyer, M. (2019). Mass spectrometric quantification of plasma glycosphingolipids in human GM3 ganglioside deficiency. *Clinical Mass Spectrometry, 14*, 106-114. doi:https://doi.org/10.1016/j.clinms.2019.03.001

Bhuiyan, R. H., Ohmi, Y., Ohkawa, Y., Zhang, P., Takano, M., Hashimoto, N., . . . Furukawa, K. (2019). Loss of Enzyme Activity in Mutated B4GALNT1 Gene Products in Patients with Hereditary Spastic Paraplegia Results in Relatively Mild Neurological Disorders: Similarity with Phenotypes of B4galnt1 Knockout Mice. *Neuroscience, 397*, 94-106. doi:https://doi.org/10.1016/j.neuroscience.2018.11.034

Black, L. E., Longo, J. F., & Carroll, S. L. (2019). Mechanisms of Receptor Tyrosine-Protein Kinase ErbB-3 (ERBB3) Action in Human Neoplasia. *The American Journal of Pathology, 189*(10), 1898-1912. doi:10.1016/j.ajpath.2019.06.008

Boccuto, L., Aoki, K., Flanagan-Steet, H., Chen, C.-F., Fan, X., Bartel, F., . . . Schwartz, C. E. (2013). A mutation in a ganglioside biosynthetic enzyme, ST3GAL5, results in salt & pepper syndrome, a neurocutaneous disorder with altered glycolipid and glycoprotein glycosylation. *Human Molecular Genetics, 23*(2), 418-433. doi:10.1093/hmg/ddt434

Bodas, M., Min, T., & Vij, N. (2015). Lactosylceramide-accumulation in lipid-rafts mediate aberrant-autophagy, inflammation and apoptosis in cigarette smoke induced emphysema. *Apoptosis, 20*(5), 725-739. doi:10.1007/s10495-015-1098-0

Boukhris, A., Schule, R., Loureiro, J. L., Lourenço, C. M., Mundwiller, E., Gonzalez, M. A., . . . Stevanin, G. (2013). Alteration of ganglioside biosynthesis responsible for complex hereditary spastic paraplegia. *Am J Hum Genet, 93*(1), 118-123. doi:10.1016/j.ajhg.2013.05.006

Bowser, L. E., Young, M., Wenger, O. K., Ammous, Z., Brigatti, K. W., Carson, V. J., . . . Strauss, K. A. (2019). Recessive GM3 synthase deficiency: Natural history, biochemistry, and therapeutic frontier. *Mol Genet Metab, 126*(4), 475-488. doi:10.1016/j.ymgme.2019.01.013

Bremer, E. G., Schlessinger, J., & Hakomori, S.-I. (1986). Ganglioside-mediated modulation of cell growth. Specific effects of GM3 on tyrosine phosphorylation of the epidermal growth factor receptor. *Journal of Biological Chemistry, 261*(5), 2434-2440.

Brown, D. A., & London, E. (1998). Functions of lipid rafts in biological membranes. *Annu Rev Cell Dev Biol, 14*, 111-136. doi:10.1146/annurev.cellbio.14.1.111

Coskun, Ü., Grzybek, M., Drechsel, D., & Simons, K. (2011). Regulation of human EGF receptor by lipids. *Proc Natl Acad Sci U S A, 108*(22), 9044-9048. doi:10.1073/pnas.1105666108

Datta, A. K., & Paulson, J. C. (1995). The sialyltransferase "sialylmotif" participates in binding the donor substrate CMP-NeuAc. *J Biol Chem, 270*(4), 1497-1500. doi:10.1074/jbc.270.4.1497

Dukhinova, M., Veremeyko, T., Yung, A. W. Y., Kuznetsova, I. S., Lau, T. Y. B., Kopeikina, E., . . . Ponomarev, E. D. (2019). Fresh evidence for major brain gangliosides as a target for the treatment of Alzheimer's disease. *Neurobiology of Aging, 77*, 128-143. doi:https://doi.org/10.1016/j.neurobiolaging.2019.01.020

Fragaki, K., Ait-El-Mkadem, S., Chaussenot, A., Gire, C., Mengual, R., Bonesso, L., . . . Paquis-Flucklinger, V. (2013). Refractory epilepsy and mitochondrial dysfunction due to GM3 synthase deficiency. *European Journal of Human Genetics, 21*(5), 528-534. doi:10.1038/ejhg.2012.202

Gordon-Lipkin, E., Cohen, J. S., Srivastava, S., Soares, B. P., Levey, E., & Fatemi, A. (2018). ST3GAL5-Related Disorders: A Deficiency in Ganglioside Metabolism and a Genetic Cause of Intellectual Disability and Choreoathetosis. *J Child Neurol, 33*(13), 825-831. doi:10.1177/0883073818791099

Graham, A., Francis-West, P., Brickell, P., & Lumsden, A. (1994). The signalling molecule BMP4 mediates apoptosis in the rhombencephalic neural crest. *Nature, 372*(6507), 684-686. doi:10.1038/372684a0

Graham, A., Heyman, I., & Lumsden, A. (1993). Even-numbered rhombomeres control the apoptotic elimination of neural crest cells from odd-numbered rhombomeres in the chick hindbrain. *Development, 119*(1), 233-245.

Harlalka, G. V., Lehman, A., Chioza, B., Baple, E. L., Maroofian, R., Cross, H., . . . Crosby, A. H. (2013). Mutations in B4GALNT1 (GM2 synthase) underlie a new disorder of ganglioside biosynthesis. *Brain, 136*(12), 3618-3624. doi:10.1093/brain/awt270

Indellicato, R., Parini, R., Domenighini, R., Malagolini, N., Iascone, M., Gasperini, S., . . . Trinchera, M. (2019). Total loss of GM3 synthase activity by a normally processed enzyme in a novel variant and in all ST3GAL5 variants reported to cause a distinct congenital disorder of glycosylation. *Glycobiology, 29*(3), 229-241. doi:10.1093/glycob/cwy112

Lee, J. S., Yoo, Y., Lim, B. C., Kim, K. J., Song, J., Choi, M., & Chae, J.-H. (2016). GM3 synthase deficiency due to ST3GAL5 variants in two Korean female siblings: Masquerading as Rett syndrome-like phenotype. *American Journal of Medical Genetics Part A, 170*(8), 2200-2205. doi:https://doi.org/10.1002/ajmg.a.37773

Levental, I., Levental, K. R., & Heberle, F. A. (2020). Lipid Rafts: Controversies Resolved, Mysteries Remain. *Trends in Cell Biology, 30*(5), 341-353. doi:https://doi.org/10.1016/j.tcb.2020.01.009

Li, T. A., & Schnaar, R. L. (2018). Chapter Two - Congenital Disorders of Ganglioside Biosynthesis. In R. L. Schnaar & P. H. H. Lopez (Eds.), *Progress in Molecular Biology and Translational Science* (Vol. 156, pp. 63-82): Academic Press.

Liu, Y., Li, R., & Ladisch, S. (2004). Exogenous ganglioside GD1a enhances epidermal growth factor receptor binding and dimerization. *J Biol Chem, 279*(35), 36481-36489. doi:10.1074/jbc.M402880200

Martin, S. F., Williams, N., & Chatterjee, S. (2006). Lactosylceramide is required in apoptosis induced by N-Smase. *Glycoconjugate Journal, 23*(3), 147-157. doi:10.1007/s10719-006-7920-8

Miljan, E. A., Meuillet, E. J., Mania-Farnell, B., George, D., Yamamoto, H., Simon, H.-G., & Bremer, E. G. (2002). Interaction of the Extracellular Domain of the Epidermal Growth Factor Receptor with Gangliosides *. *Journal of Biological Chemistry, 277*(12), 10108-10113. doi:10.1074/jbc.M111669200

Park, S. Y., Kwak, C. Y., Shayman, J. A., & Kim, J. H. (2012). Globoside promotes activation of ERK by interaction with the epidermal growth factor receptor. *Biochim Biophys Acta, 1820*(7), 1141-1148. doi:10.1016/j.bbagen.2012.04.008

Rao, F. V., Rich, J. R., Rakić, B., Buddai, S., Schwartz, M. F., Johnson, K., . . . Strynadka, N. C. J. (2009). Structural insight into mammalian sialyltransferases. *Nature structural & molecular biology, 16*(11), 1186-1188. doi:10.1038/nsmb.1685

Russo, D., Della Ragione, F., Rizzo, R., Sugiyama, E., Scalabrì, F., Hori, K., . . . D'Angelo, G. (2018). Glycosphingolipid metabolic reprogramming drives neural differentiation. *The EMBO Journal, 37*(7), e97674. doi:https://doi.org/10.15252/embj.201797674

Saul, R., Wilkes, G., & Stevenson, R. (1983). *Salt-And-Pepper'pigmentary changes with severe mental retardation: a new neurocutaneous syndrome.* Paper presented at the Proc. Greenwood Genet., Ctr.

Simons, K., & Toomre, D. (2000). Lipid rafts and signal transduction. *Nature Reviews Molecular Cell Biology, 1*(1), 31-39. doi:10.1038/35036052

Simpson, M. A., Cross, H., Proukakis, C., Priestman, D. A., Neville, D. C. A., Reinkensmeier, G., . . . Crosby, A. H. (2004). Infantile-onset symptomatic epilepsy syndrome caused by a

homozygous loss-of-function mutation of GM3 synthase. *Nature Genetics, 36*(11), 1225-1229. doi:10.1038/ng1460

Sipione, S., Monyror, J., Galleguillos, D., Steinberg, N., & Kadam, V. (2020). Gangliosides in the Brain: Physiology, Pathophysiology and Therapeutic Applications. *Frontiers in Neuroscience, 14*(1004). doi:10.3389/fnins.2020.572965

Takamiya, K., Yamamoto, A., Furukawa, K., Yamashiro, S., Shin, M., Okada, M., . . . Aizawa, S. (1996). Mice with disrupted GM2/GD2 synthase gene lack complex gangliosides but exhibit only subtle defects in their nervous system. *Proceedings of the National Academy of Sciences, 93*(20), 10662-10667. doi:10.1073/pnas.93.20.10662

Trainor, P. A., Sobieszczuk, D., Wilkinson, D., & Krumlauf, R. (2002). Signalling between the hindbrain and paraxial tissues dictates neural crest migration pathways. *Development, 129*(2), 433-442.

Varadkar, P., Kraman, M., Despres, D., Ma, G., Lozier, J., & McCright, B. (2008). Notch2 is required for the proliferation of cardiac neural crest-derived smooth muscle cells. *Developmental Dynamics, 237*(4), 1144-1152. doi:https://doi.org/10.1002/dvdy.21502

Wang, X.-Q., Sun, P., & Paller, A. S. (2003). Ganglioside GM3 Blocks the Activation of Epidermal Growth Factor Receptor Induced by Integrin at Specific Tyrosine Sites *. *Journal of Biological Chemistry, 278*(49), 48770-48778. doi:10.1074/jbc.M308818200

Yoshikawa, M., Go, S., Suzuki, S.-i., Suzuki, A., Katori, Y., Morlet, T., . . . Inokuchi, J.-i. (2015). Ganglioside GM3 is essential for the structural integrity and function of cochlear hair cells. *Human Molecular Genetics, 24*(10), 2796-2807. doi:10.1093/hmg/ddv041